UNIVERSITÀ DEGLI STUDI DI PADOVA

UNIVERSITA' DEGLI STUDI DI PADOVA

Dipartimento di Ingegneria Industriale DII

Corso di Laurea in Ingegneria Energetica

Simulation of a Gas Turbine – Organic Rankine Cycle Combined Power Plant with the integration of a direct Thermal Energy Storage to improve flexibility

Relatore: Prof. Anna Stoppato

Correlatori: Prof. Alberto Benato

Ing. Matteo Pecchini

Michele Zenari 2004165

Anno Accademico 2022/2023

Summary

1 Introduction

In order to reduce greenhouse emissions, the share of renewable energy production is expected to grow significantly over the next decades.

The renewable energy resources utilization has many gains including reducing the dependence on fossil fuel markets, economic convenience and environmental friendliness. However, despite renewable resources' substantial advantages, they have the deficiencies of fluctuation and uncertainty. Particularly, wind and solar energy are challenged by the variability of the resource.

These uncertainties cause large fluctuations in the power production at daily, weekly, monthly, or even annual level. However, the electric demand must be balanced instantaneously at each moment because the imbalance between supply and demand can be the source of local instabilities that, in turn, can cause local or even global grid damages, user devices fault, or, easily, blackouts.

To prevent such damaging situations, fossil fuel power stations need to be used as back-up units that will work when the energy demand is very high and the energy production is not enough to satisfy it. As solar irradiance and wind speed vary, conventional generation units are required to ramp up and down, in many cases even beyond their flexibility limits. This traditional power plants will often work at partial load with low efficiency and will be subject to large pressures and temperatures fluctuations which can cause thermo-mechanical stresses in plant components.

In this context is therefore necessary to improve fossil fuels power plants flexibility and start-up time. Flexibility is needed for generation to respond rapidly to the changing load conditions that has required short start-up and shut-down times compared to steady base-load operation.

One of the methods used to improve the flexibility of power plants is the use of Thermal Energy Storage (TES). This storage systems can control in a simple way the thermal energy used to run a power plant, storing it when low power production is needed and releasing it when the power request increases.

In this work, a Combined Power Plant made of a gas turbine and of an Organic Rankine Cycle (ORC) with the integration of a Thermal Energy Storage (TES) has been studied to improve the flexibility of the plant. Two solutions for the TES have been considered: a two-tank direct oil storage and a stratified tank direct oil storage. A preliminary economic analysis is also performed.

2 State of art

2.1 Organic Rankine Cycle

The working principle of the Organic Rankine Cycle (ORC) corresponds to that of the Clausius (steam) Rankine cycle. However, instead of water, organic working fluids are used, enabling the utilisation of lower-temperature heat sources, which cannot be effectively and economically exploited with water. Important advantages of ORC technology include its customization and optimization by tailoring the working fluid and system design to specific applications, leading to a reasonable efficiency even for the more challenging smaller-scale applications at lower temperatures.

Figure 2.1 shows the core components of a standard single-stage subcritical ORC system and a corresponding T-s diagram.

In the heat exchanger (1 → 2), the working fluid is preheated, evaporated and often slightly superheated. Afterwards, the vapour-phase working fluid is expanded to a lower pressure level (2 → 3) in an expansion device (e.g., turbine). A generator converts the mechanical shaft power of the expansion device into electricity. In the next process (3 → 4), the working fluid is desuperheated, condensed and often slightly subcooled. Finally, the pump pressurizes the working fluid to a higher pressure level (4 → 1).

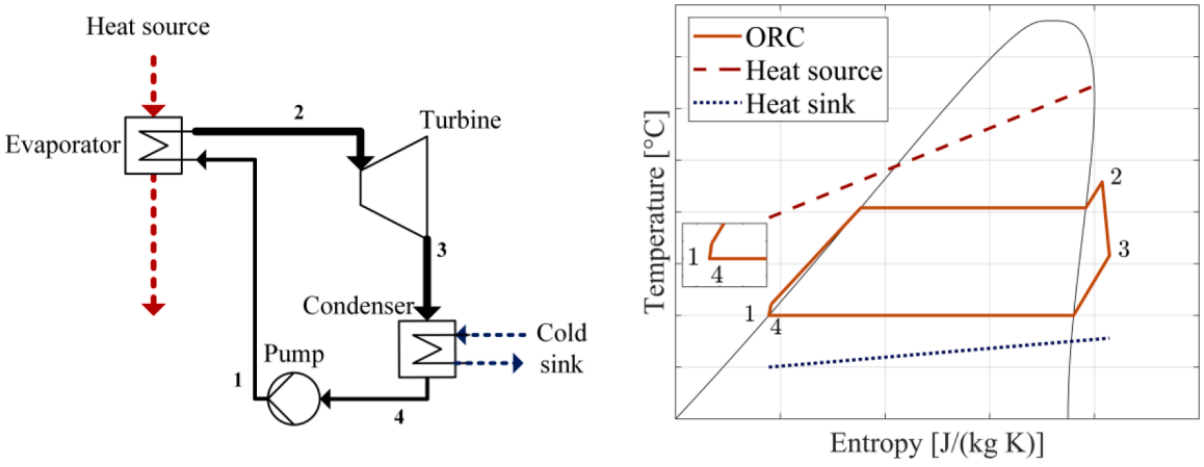

Figure 2.1: Layout scheme of an Organic Rankine Cycle and corresponding T-s diagram (1)

The generated power is given by the difference between the power produced by the generator and the power absorbed by the pump, whereas the efficiency of the cycle is given by the ratio between the generated power and the thermal power absorbed in the evaporator.

The most relevant difference between Steam Rankine Cycles and Organic Rankine Cycles is the working fluids, that can be classified based on the slope of the saturated vapor curve, that is positive for dry fluid, negative for wet fluids, as water, and infinite for isentropic fluids.

Working fluids are a very important optimisation parameter for the design and development of ORC plants. Working fluid selection, which is highly dependent on the heat source, strongly affects operating pressures and temperatures, efficiency, sizing and selection of key equipment components.

Different variants of the traditional subcritical ORC systems can be found in the literature.

In transcritical ORCs, heat input to the cycle occurs at supercritical pressure/temperature, while in supercritical ORCs, both heat input and heat rejection into/from the working fluid take place at supercritical parameters.

In recuperative ORCs, Figure 2.2, an internal heat exchanger (called recuperator) is used for utilizing the heat of the superheated vapour at the expansion outlet to preheat the working fluid before it enters the evaporator and thus reduce the external heat input to the cycle resulting in an increase of the first law efficiency, since the power output remains the same. The implementation of a recuperator is more favourable for dry working fluids, for which there is more sensible heat to recover, while the efficiency benefits are higher when more superheating is applied. Notably, the use of recuperators for waste heat recovery applications is not always beneficial, as it may result in less heat being absorbed from the heat source stream and thus reduced power output.

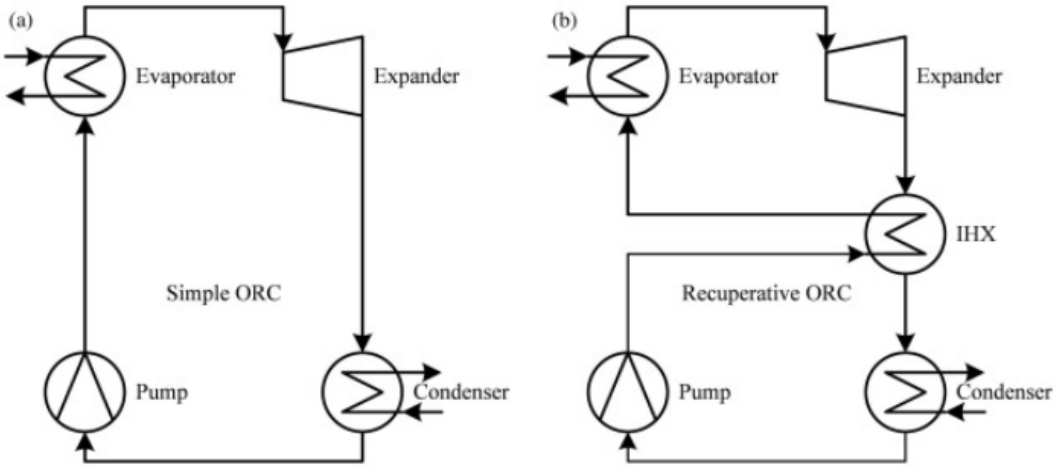

Figure 2.2: Difference between the layout scheme of a simple ORC and a recuperative ORC (2)

Similarly to the case of recuperative ORCs, in regenerative ORCs, the working fluid is preheated before entering the evaporator. However, in contrast to recuperative ORCs, heat is provided via vapour that is extracted at an intermediate expansion stage/pressure.

An exhaustive panoramic on current research trends and future perspectives on ORC can be found in (1).

2.2 Combined Cycle Power Plant

A combined cycle power plant is an assembly of heat engines that work in tandem from the same source of heat, converting it into mechanical energy. The most common type used to produce electricity is the Combined Cycle Gas Turbine (CCGT) plant. The basic idea of a CCGT consists of two power plant cycles working in cascade: the topping one is the Brayton-Joule cycle which is a gas turbine cycle and the bottoming one is the Rankine cycle which is a steam turbine cycle.

In a gas turbine, based on the Brayton cycle, the ambient air is compressed using a turbo compressor, sent into a combustion chamber where it's heated using the energy of the fuel, and then the exhaust gases expand through an axial turbine producing mechanical power. Part of the power is used to run the compressor, the other is used to produce electricity. The layout scheme of a gas turbine is shown in Figure 2.3.

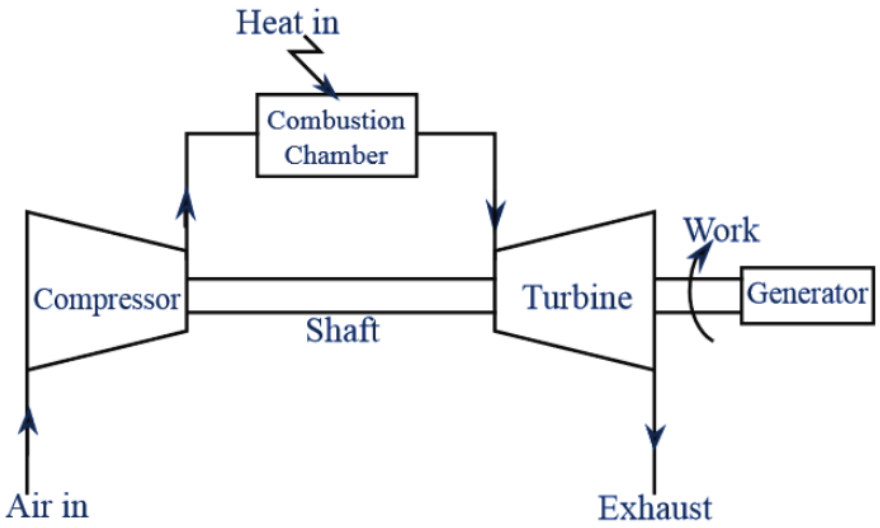

Figure 2.3: Layout scheme of a gas turbine

Usually, the exhaust gases are released into the environment, although they still have a high temperature.

The main purpose of the CCGT is to increase the overall efficiency of the system by recovering waste heat from the gas turbine to run a steam cycle. As shown in Figure 2.4, the exhaust gases are sent into a Heat Recovery Steam Generator (HRSG) that replaces the evaporator of the traditional Rankine cycle. In this way both the topping and the bottoming cycles produce electric energy without increasing the fuel consumption, thus reaching higher values of efficiency (up to 60%).

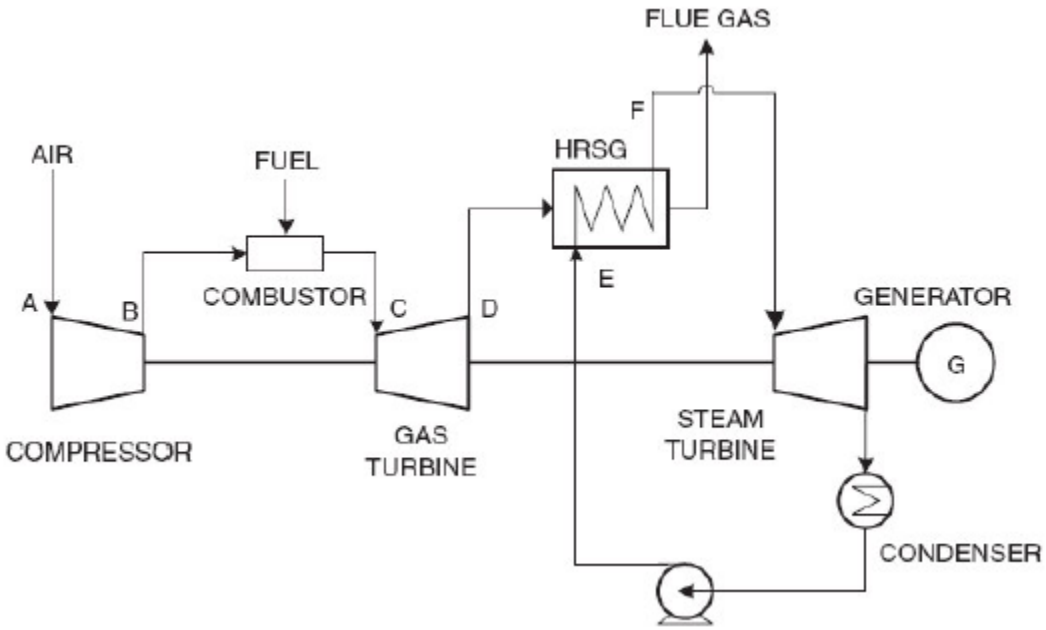

Figure 2.4: Layout of a CCGT power plant (3)

The working fluid of the bottoming cycle is chosen based on the characteristics of the exhaust gases, that are classified in high (>650°C), medium (230-650°C) and low (<230) temperature sources.

For medium-high sources, the traditional steam Rankine cycle is used, but for medium-low temperature ORC cycles are more convenient, with the opportunity to choose the working fluid that better suits the characteristics of the hot source.

2.3 Energy Storage

With the growth of electricity generation from intermittent renewable energy sources, especially wind and solar, there is the need to increase the installed storage capacity, in order to store the excess energy when the production exceeds the demand and to release it when the energy production is lower. In this way, the use of fossil fuel power plants can be further reduced.

An Energy Storage is a device or a system in which energy can be stored in some form. Subsequently, this energy can be extracted to perform some useful operation. To store some form of energy, three steps need to be done: charging, storing and discharging. Each step can occur more than once during each storage cycle, and some of the steps can take place simultaneously.

In literature, a lot of different energy storage technologies are present, both mature and in-developing. A quick overview of the most widely spread and promising storage technologies is given in the following.

- ***Pumped Hydro Storage (PHS)***

  Pumped Hydro Storage or Pumped Hydroelectric Energy Storage is the most mature, commercially available, and widely adopted largescale energy storage technology. The global capability was around 8500 GWh in 2020, accounting for over 90% of total global electricity storage (4).

  The PHS technology uses gravity to store the electrical energy and a typical plant layout consists of an upper and a lower reservoir, a waterfall, pipes and penstock, a pump, a turbine, an electric motor and an electric generator. The pump and the turbine can be separated machines or a reversible pump-turbine that supplies both the functions. The working principle of PHS is shown in Figure 2.5. Power is taken from the grid during off-peak period and used to feed the electric motor which drives the pump, pumping the water from the lower to the upper reservoir and storing it there. During high demand hours, water is released from the upper to the lower reservoir through a turbine mechanically coupled with an electric generator, which transforms the mechanical energy into the electrical ones and injects it into the electric grid.

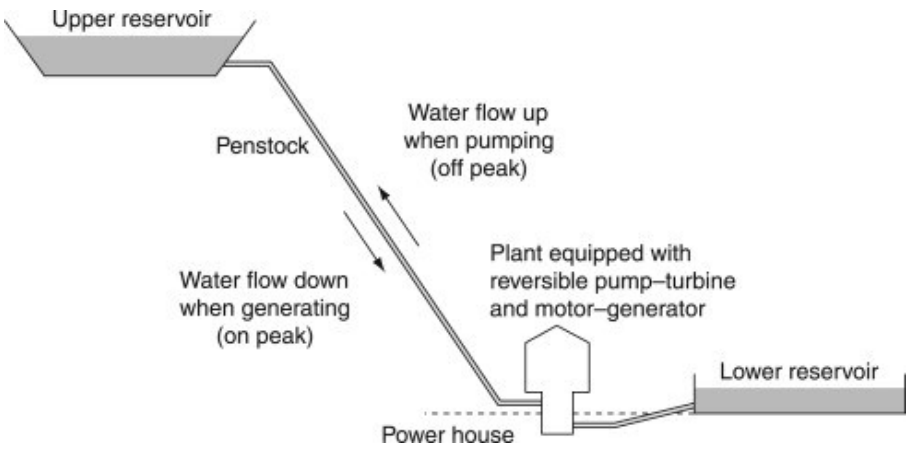

Figure 2.5: Scheme of the working principle of a PHS plant (5)

This storage technology is characterised by a very low energy density (0.5–1.5 W h/l or 0.5–1.5 W h/kg) and self-discharge (0.005–0.02 %/day), an acceptable price per stored energy unit (5 to 100 dollars / kWh) and a high round-trip efficiency (65 to 87%) (6). The major drawback of the PHS technology is related to the need of an acceptable water availability and an adequate geographical morphology. For these reasons, new PHS units can be installed only in countries with a favourable morphology or upgrading conventional hydroelectric power units.

- ***Compressed Air Energy Storage (CAES)***

  Compressed Air Energy Storage is the second commercially available large-scale energy storage technology. For this technology, the working principle is also very simple. When the power demand is low, excess generation capacity is used to compress the air and store it in an underground cavern or in man-made tanks, pipes, containers, or vessels. During high peak demand hours, the stocked and pressurised air is drawn from the storage, heated up (usually using natural gas) and expanded in an air turbine mechanically coupled with an electric generator, which converts the mechanical energy into electrical energy and injects it into the electric grid. The two CAES plants today in operation use the mentioned working principal. Based on practical experience, Diabatic CAES is characterised by a round-trip efficiency in the 40–89% range, an energy density of 3–12 Wh/l (or 30–60 Wh/kg) and a price per stored energy unit of 2–50$/kWh (6). CAES and PHS have the same drawback: they require a particular morphology of the installation site. But, until now, CAES remains the only technology able to compete with PHS for large-scale ES applications despite the actual need of a fossil fuel stream.

- ***Batteries***

  A battery is a storage technology that converts chemical energy directly into electricity. In a nutshell, it consists of two electrical terminals called cathode and anode, separated by a chemical material called electrolyte. To accept and release energy, the battery is coupled to an external circuit. Electrons move through the circuit, while simultaneously ions move through the electrolyte. When the electrons move from the cathode to the anode, they increase the chemical potential energy, thus charging the battery; when they move in the other direction, they convert this chemical potential energy to electricity in the circuit, discharging the battery. During charging or discharging, the oppositely charged ions move inside the battery through the electrolyte to balance the charge of the electrons moving through the external circuit.

  Batteries are the most widespread storage technology for low-medium capacity, due to their compactness and the possibility to be transported.

- ***Flow Batteries***

  Flow Batteries are a relatively young technology that works similarly to conventional batteries. The ions flow from the negative and the positive electrodes during charging and delivering phases, respectively, through a selective membrane. Several types of flow batteries have been developed over the years. Flow batteries offer power ranges from 0.005 to 15 MW, storage capacity from 0.010 to 10 MWh, power density in the range 0.5–25 W/l (or 45–166 W/kg), and energy density in the range 16 to 60 W h/l (or 10 to 85 W h/kg). They also have low self-discharge rate of 0.2–0.24 %/day becoming fully discharged without any damage, acceptable cycle life (2000–13000 cycles at 80% of Depth of Discharge) and satisfying round-trip efficiency (from 57 to 90%). The main drawbacks are the poor lifetime (5–15 years) and the high capital costs. (6)

- ***Gravity Energy Storage***

  Gravity Energy Storage is an in-developing energy storage technology studied with the aim of solving the main PHS drawbacks: the need of a sufficient water flow and of a particular geographical morphology of the installation site. There are different types of experimental plants, all of which share the same idea for the working principle that consists in store the energy in the form of potential energy (for example, pumping water for the Gravity Power Model or moving buckets of gravel from low to high elevation for the system proposed by Energy Cache), and then releasing it producing electricity when the power is needed. One

of the drawbacks is that many proposed systems still suffer the same topological constraints as PHS and CAES.

- ***Liquid Air Energy Storage (LAES)***

  Liquid Air Energy Storage is another in-developing large-scale storage technology which implies to store electrical energy in the form of liquefied air. In the charging phase the air is compressed, liquefied, and stoked in thermally isolated man-made vessels/tanks/containers. During discharge, the liquid air is heated up using a heat exchanger and its pressure is increased. Then, the high-pressure air is used to drive an expansion machine mechanically coupled to the electric generator. The main advantage of LAES is the high energy density, and the main drawback is the high cost.

- ***Hydrogen Energy Storage***

  Hydrogen Energy Storage is the most convenient way to store off-peak electricity when long term season-to-season storage is needed. During the charging phase, water is transformed into hydrogen using the electrolysis process. The produced hydrogen can be stored in gaseous or liquid form as well as using metal hydrides or carbon nanostructures. When power is needed, the stored hydrogen can be used in a fuel cell or directly burnt, for example, in gas turbine units. One of the advantages of this technology is that hydrogen can be easily transported and is carbon-free.

- ***Flywheel Energy Storage***

  Flywheel Energy Storage is a storage technology that works by accelerating a rotor (flywheel) to a very high speed. A typical system consists of a flywheel supported by rolling-element bearing connected to a motor–generator. The flywheel and sometimes motor–generator may be enclosed in a vacuum chamber to reduce friction and energy loss. In the charging phase, a shaft connected to the flywheel disc receives the available power to rotate at a very fast velocity, transforming the supplied electricity into inertial energy and storing it in the system as rotational power. In the discharging process, the power is taken back from the flywheel to produce power and, as a result, the rotor's velocity decreases due to energy conservation law.

  Flywheel systems are highly efficient and appropriate for short storage times and low and medium capacities, but their cost and energy density have proven to be barriers to their widespread commercialization and deployment.

- ***Thermal Energy Storage (TES)***

Thermal Energy Storage is a storage technology which stores energy in the form of heat, through the heating or cooling of a storage medium.

Thermal storage systems can be direct, where the heat transfer fluid serves also as storage medium, or indirect systems, where a second medium is used for storing the heat.

There are three types of TES systems: sensible heat storage, latent heat storage, and thermochemical storage (7).

In the case of sensible heat, the thermal energy is stored in the change of the storage medium temperature consequence of a variation in the internal energy. The most used heat transfer materials for sensible heat storage are:

- water, which is a cheap, available, and safe material, can be stored both in liquid form for temperatures below 100 °C at ambient pressure and as a vapour for higher temperatures.
- diathermic oils, which are organic fluids with good heat transfer properties, and can reach in liquid form temperatures of 250 °C at ambient pressure to temperatures of 400 °C, increasing the working pressure, depending on the type of oil used.
- molten salts, which have the advantage of reaching temperatures of 550°C, but the disadvantage of having a melting temperature of around 200-250 °C, limiting the operating temperature above these values to avoid solidification.
- natural materials such as gravel, sand, rocks, and concrete that are inexpensive and safe.

In latent heat storage, the thermal energy is stored as the phase change latent heat of some media. Usually solid-liquid phase change is used, by melting and solidification of a material. Upon melting heat is transferred to the material, storing large amounts of thermal energy at constant temperature; the heat is released when the material solidifies. Materials used for latent heat storage are called PCMs (Phase Change Materials). There are various types of PCMs such as: organic compounds (paraffin and non-paraffin compounds), inorganic compounds (salts, salt hydrate, and metallic), and eutectic which is a mixture of the previous types. Many materials have been studied as PCMs, but only few of them have been commercialized, mainly due to problems such as phase separation, subcooling, corrosion, long-term stability, and low heat conductivity, that have not yet been totally solved. Usually, PCMs are selected based on the appropriate melting enthalpy and temperature, availability and cost.

The advantage of this storage technique is that latent heat is usually much greater than specific heat, and the working temperature is kept constant.
In thermochemical energy storage, a chemical reaction with high energy involved in the reaction is used to store energy. The products of reaction should be able to be stored and the heat stored separately during the reaction should be able to be retrieved when the reverse reaction takes place. The most important challenge for this technology is to find the appropriate reversible chemical reaction for the energy source used.

Compared to CAES and PHS, TES is characterised by higher energy density, no geographical limitations and small installation footprint, and can be integrated in fossil-fuelled thermal power plant to increase flexibility and to reduce cycling operation, fast start up and overnight shutdowns.

3 Literature review

In literature, many works that studies the use of thermal storage to increase the flexibility of thermal power plants are present.

Al Kindi et al (8) presented a thermoeconomic analysis of an upgraded nuclear power plant coupled with thermal energy storage (TES) and secondary power generators. The proposed system is made of a nuclear power island that includes a PWR and a Steam Generator (SG), a Primary Steam Rankine Cycle (PSRC), five TES units, each made of two PCM tanks connected in series, and Secondary Steam Rankine Cycles (SSRC). During the nominal (full load) operation mode, the steam generated in the SG flows to the PSRC system, and no steam is directed to the TES. The TES system charging process is performed at times of low electricity demand by opening the TES system valves and allowing some amount of the generated steam to flow into the PCM tanks for heat deposition. The opening of TES valves reduces the mass flowrate of steam flowing to the PSRC due to constant steam generation in the SG. This operation method allows for operating the PSRC system at reduced power output while running the reactor at full rated thermal power output. The stored heat in the TES system is assumed to be discharged to generate extra electrical power through the operation of the SSRC systems during periods of high demand. The SSRCs are sized to fully discharge the TES in 1 hour. The use of SSRC systems is to have the ability to generate extra power during high electricity prices, and thus, higher revenues.

C. Chen et al. (9) studied a 350 MW supercritical CHP plant coupled with molten salt TES to improve flexibility. During charging, a first steam extraction passes through two pairs of storage tanks with high-temperature and low-temperature molten salt in turn for heat exchange, and then enters the low-pressure turbine. The second steam extraction enters the low-temperature storage tank for heat exchange, and then enters the low-pressure turbine. During discharging, the low-temperature storage tank replaces part of the high-pressure steam extraction to preheat the feed water, and the high-temperature storage tank preheats part of the cold reheat steam. During charging, the minimum operating load can be reduced, and the lowest stable combustion load of the boiler remains unchanged. During discharging, it can increase the maximum operating load so that more electrical energy can be obtained and keep the boiler from exceeding the maximum combustion load.

Richter et al (10) improved the flexibility of a coal-fired power plant by the integration of steam storage, that allowed an increase of the load by 4.3% for the duration of 23 minutes during discharge and a decrease of 5% during charge, keeping constant the fuel mass flow rate.

Romanos et al. (11) investigated the options of steam extraction before the reheater and/or before the low-pressure turbine of an existing 670 MW Rankine cycle nuclear power plant, to charge PCM-TES that are used to run two ORCs for the production of extra power during peak demand.

Bufi et al. (12) have analysed the implementation of a storage system made of two molten salts tanks for the recovery of waste heat from a biomass plant using an ORC.

TES is also used in combined power plants, for example Li et al (13) simulated a combined-cycle gas turbine coupled with cascaded latent heat storage for flexible operation.

In all of these studies, the integration of the TES is done in thermoelectric power plants, and the period of charge/discharge is short, in the order of an hour.

In the work proposed by Baldasso et al. (14), the charge/discharge time interests the whole day.

It investigates the technical and economic feasibility of a novel and energy-efficient way to supply zero-emission power during harbour stays for ferries. The proposed system combines the use of TES and a WHR system based on the ORC technology. The ORC unit supplies all the onboard energy demand during the harbour stays, and therefore the ship does not produce any emission while anchoring at port. During sailing, exhaust gases are used to heat up a thermal oil, which is partially stored in the TES and partially used to run the ORC unit. During port stays, the TES is discharged in order to run the ORC unit. Two types of TES were considered, the use of a stratified tank and of a two-tank system. In the two-tank system, the oil is stored in a high-temperature tank and a low-temperature tank. The oil, heated up by the exhaust gases, enters the high temperature tank, then goes to the vapour generator of the ORC exchanging heat, enters the low temperature tank, and goes back to the first heat exchanger. Therefore, the hot and the cold fluids are physically separated. The stratified tank operates according to the stratification process, which occurs due to the variation in the density of a fluid as a function of its temperature. This enables having both a hot and a cold zone in the same container. A sketch of the proposed system is shown in Figure 3.1.

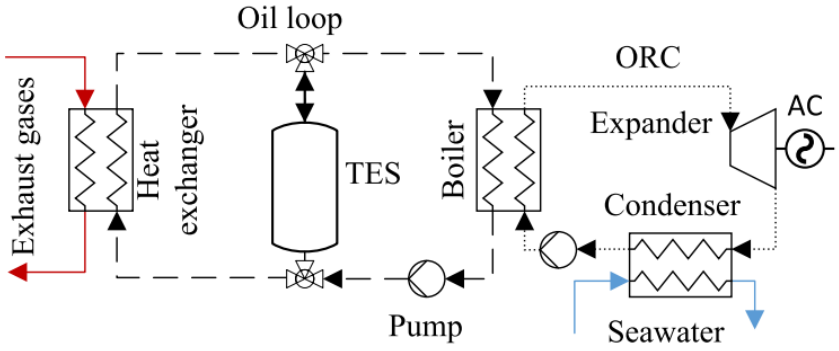

Figure 3.1: Sketch of the proposed system by Baldasso et al. The dashed line represents the oil loop, while the dotted line indicates the ORC loop. (14)

In this kind of storage, the heat transfer fluid is directly stored inside the tanks, therefore, the heat transfer fluid is also the storage medium.

This solution of directly storing the thermal oil inside the storage tanks is usually adopted in medium size Concentrating Solar Power (CSP) plants.

In (15) is compared the performance of CSP plants using an ORC power generation unit, linear Fresnel collectors, thermal oil as heat transfer fluid and two-tank direct and thermocline energy storage systems. The results of the performance assessment demonstrate that two-tank direct storage systems allow to achieve slightly higher specific energy production and that thermocline TES systems can be an interesting option to reduce energy production costs.

The study presented in (16) investigates the optimal design and operation of a solar energy driven ORC system with a parabolic trough collector (PTC) and a two-tank sensible thermal energy storage system. The power cycle system can reach a stable and continuous operation through a given day with the help of the two-tank energy storage system. A sketch of the plant configuration is shown in Figure 3.2.

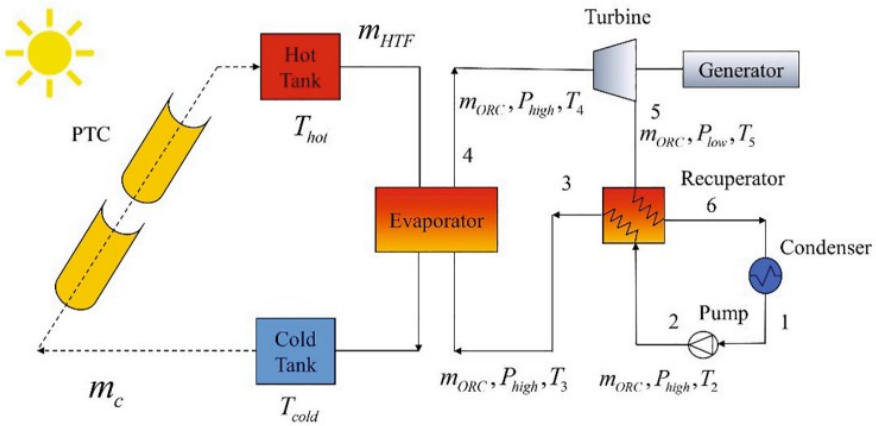

Figure 3.2: Flowsheet of the recuperative ORC system with two-tank energy storage (16)

The solid lines in the figure indicate that the flowrates of these streams are constant, while the dashed lines indicate that the flowrate of such streams varies with the insolation. By adjusting the mass flow rate of the HTF through the solar collector, it can be heated to a constant temperature even under varying solar insolation. During solar peak hours, the HTF travels through the PTC from the cold tank at a high flow rate and then is stored in the hot tank. The HTF can be released at a constant mass flowrate to the evaporator, where it delivers heat to the ORC sub-system; thus, the ORC can always operate stable at nominal design conditions. In this way, the system works under stable operation, and the drastic decrease of system efficiency during unstable operation can be avoided.

In this work, an ORC-CCGT power plant with direct thermal oil storage (two tanks and stratified tank) is studied, varying both the GT and the ORC power load, decoupling the two power productions thanks to the storage system.

4 Power Plant Models

4.1 Power Plant's Layout

The considered power plant is a combined cycle gas turbine, composed by a gas turbine and an Organic Rankine Cycle, to whom a direct thermal oil storage system has been integrated (17).

A sketch of the reference system, before the integration of the storage system, is represented in Figure 4.1.

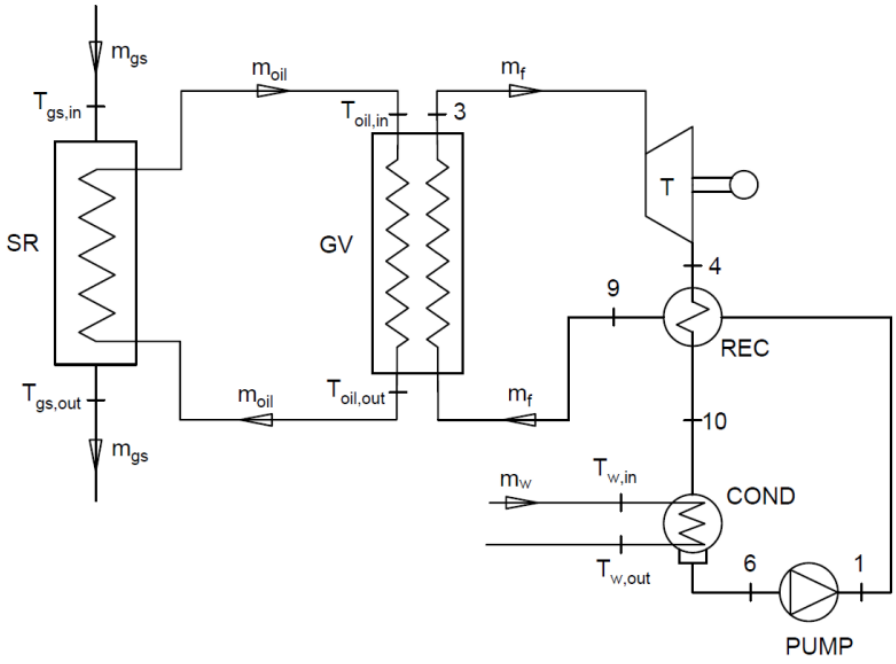

Figure 4.1: Layout of the reference plant (17)

The thermal energy of the exhaust gases $P_{th,gs}$ is extracted in the recovery heat exchanger (SR) to heat up the mass flow rate of diathermic oil $\dot{m}_{oil}$ from the temperature $T_{oil,out}$ to the temperature $T_{oil,in}$. The mass flow rate of exhaust gases $\dot{m}_{gs}$ is cooled down from the temperature $T_{gs,in}$ to the temperature $T_{gs,out}$ and released to the ambient.

The oil mass flow rate is used to feed the ORC through the vapour generator (GV), in which the mass flow rate of the organic fluid is heated up, evaporated, and eventually superheated. The generated vapour expands in the turbine, which is coupled with an electric generator that produces the additional electric power $P_{el,ORC}$. The vapour is cooled down in the recuperative heat

exchanger (REC) and then condenses in the condenser (CON) until it reaches the condition of saturated liquid. The fluid is then pressurized using a pump and sent again to the steam generator.
Without an energy storage system, the power production of the ORC is strictly linked to the thermal power extracted from the exhaust gases. If the gas turbine's load varies, the characteristics of the exhaust gases change, and the ORC follows this variation changing the output power. Also, if there is the will to vary the ORC load while the gas turbine power output remains constant, the only way is to reduce the exhaust gas mass flow rate sent to the recovery heat exchanger, thus reducing the energy recovered and wasting part of the energy that could be ideally recovered.
The integration of an energy storage system is needed to decouple the power production of the gas turbine from the power production of the ORC. In this way, it will be possible to keep constant the power production of the ORC while varying the gas cycle load, or vary the ORC load while the gas turbine power production is kept constant without losing energy, or vary both the gas turbine and the ORC power production with two different load histories.
The energy storage system is a direct thermal oil storage system, located between the recovery heat exchanger and the steam generator, as shown in Figure 4.2.

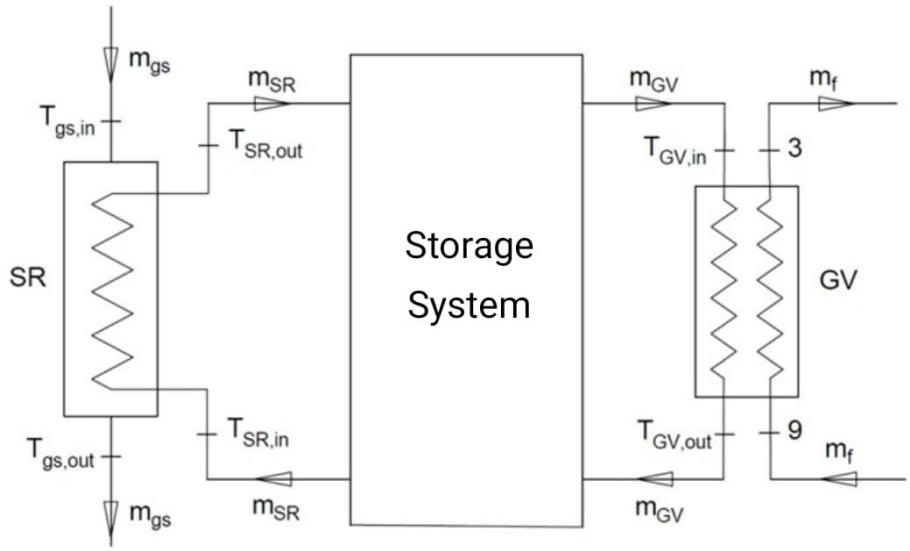

Figure 4.2: Layout of the plant with the integration of the storage system (17)

The storage system is used to decouple the power extracted from the exhaust gases and the power given to the ORC. This can be possible by regulating the mass flow rate sent to the two heat exchangers. The left side of the oil circuit, in which flows the mass flow rate m_{SR}, is responsible for the extraction of the heat from the exhaust gases, while the right part of the oil circuit, in which flows the mass flow rate m_{GV}, feeds the steam generator of the ORC. When the extracted power

from the exhaust gas is greater than the thermal power needed by the ORC, i.e. when m_{SR} is greater than m_{GV}, the storage system works in charging mode, otherwise it works in discharging mode.

In this work, two different configurations for the thermal storage are studied. In the first configuration, two separate storage tanks with different temperatures are present. The oil, heated up by the exhaust gases, enters the high temperature tank, then goes to the vapour generator of the ORC exchanging heat, enters the low temperature tank and goes back to the first heat exchanger. In the second configuration, only one tank is present, which works according to the stratification principle.

4.2 ORC Design

The optimisation of the design of the organic Rankine cycle is performed with the ORC-PD software (18).

The ORC Plant Designer is an in-house simulation tool developed in MATLAB environment able to provide the optimal fluid and plant configuration of an ORC power unit fed by different heat sources. Thermodynamic properties of the fluid are acquired from the REFPROP and COOLPROP databases.

In order to carry out the optimization the objective functions and the input variables (independent variables) must be defined. The possible objective functions that can be selected are several; in this work the optimisation is made with the objective of maximising the electric power output.

The tool input parameters are the following:

- Heat Source medium
- Inlet temperature, inlet pressure, and mass flow rate of the heat source
- Condensation temperature
- Inlet and outlet temperature and inlet pressure of the condensation medium
- Pump isentropic efficiency
- Pump mechanical efficiency
- Electric motor efficiency
- Minimum admissible temperature difference into the heat exchangers
- Mechanical efficiency of the expander
- Efficiency of the electric generator

- Recuperator Efficiency

The variables that are optimised by the ORC-PD tool are:

- The heat source outlet temperature
- The evaporation pressure of the organic medium
- The main heat exchanger outlet temperature
- Organic fluid

while the remaining variables (working fluid mass flow rate, thermodynamic state point, electric power produced by the plant, mass flow rate of the medium used into the condenser, etc.) which are 'dependent variables' are computed during the optimisation procedure.

ORC-PD allows evaluation of the convenience of superheating the organic fluid after evaporation and the convenience of using a recuperative heat exchanger. The efficiency maps of the axial and radial turbines are used in the optimisation process to choose which of the two solutions has better efficiency based on the cycle parameters and the working fluid.

The model is exposed in (18); the main equations are presented in the following.

4.2.1 Without TES

With reference to the power plant without TES, once the oil outlet temperature $T_{GV,out}$ is defined, using the value of pinch-point of the recovery heat exchanger $\Delta T_{pp,SR}$ it is possible to evaluate the exhaust gas outlet temperature $T_{gs,out}$, from 4.1.

$$T_{gs,out} = T_{GV,out} + \Delta T_{pp,SR} \qquad 4.1$$

The oil mass flow rate flowing in the recovery heat exchanger $\dot{m}_{SR}$ can be found with 4.2.

$$\dot{m}_{SR} = \dot{m}_{gs} \frac{c_{p,gs}\left(T_{gs,in} - T_{gs,out}\right)}{c_{p,oil}\left(T_{GV,out} - T_{GV,in}\right)} \qquad 4.2$$

From the oil mass flow rate, it is possible to evaluate the heat exchanged in the steam generator. Now, knowing the evaporation pressure, the condensation pressure, and the efficiency of the recuperator, the mass flow rate of the organic fluid $\dot{m}_f$ can be found, as well as all the thermodynamic points of the cycle and the water mass flow rate $\dot{m}_w$in the condenser.

The electric power produced by the cycle P_{el} is given by the difference between the electric power of the turbine P_t and the electric power absorbed by the pump P_p, equations 4.3, 4.4 and 4.5.

$$P_{el} = P_t - P_p \tag{4.3}$$

$$P_t = \dot{m}_f (h_3 - h_4) \eta_{mec,t} \eta_{gen} \tag{4.4}$$

$$P_p = \dot{m}_f \frac{h_1 - h_6}{\eta_{mec,p} \eta_{mot}} \tag{4.5}$$

4.2.2 With TES

For the power plant with TES, the optimization still consists in maximizing the power in the design condition but needs to consider the presence of TES and the operating conditions during the day. The model is therefore suitably modified. The modelling of the TES system has been simplified, considering two perfectly insulated tanks with infinite dimensions, to consider constant their temperature. The layout of the system is shown in Figure 4.3.

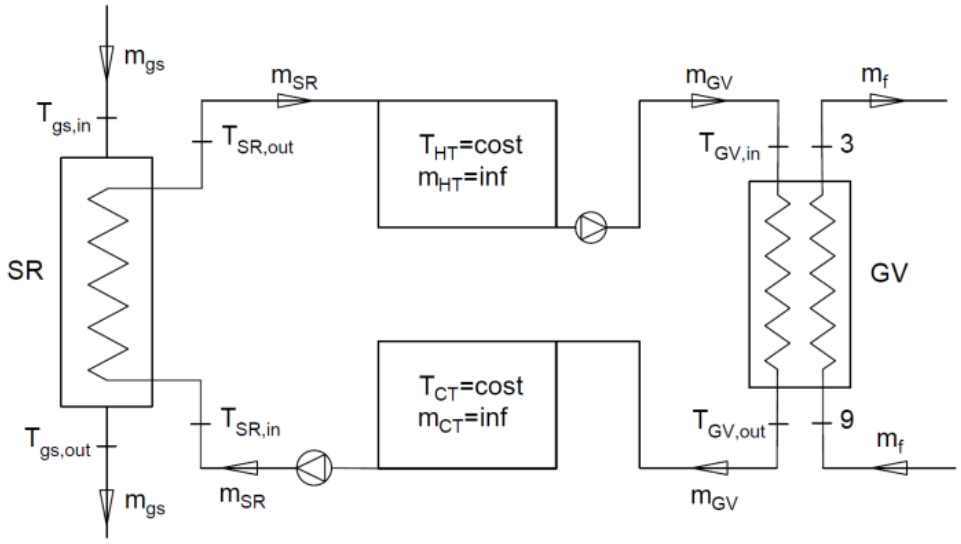

Figure 4.3: Layout of the system considered for the optimization with TES (17)

In the plant without TES, the mass flow rates were evaluated with eq. 4.2, having $\dot{m}_{SR} = \dot{m}_{GV}$. In the plant with TES, both the mass flow rate flowing in the recovery heat exchanger $\dot{m}_{SR}(t)$ and in the steam generator $\dot{m}_{GV}(t)$ are varying following the imposed load stories respectively of the gas turbine and of the ORC. The imposed condition for these mass flow rates is that the total mass entering and exiting the tanks throughout the day is equal. In this way, the level of oil inside the tanks is equal at the beginning and end of the day, and this guarantees the repeatability of the

cycle in the following days. The design value $\dot{m}_{GV,Des}$ is chosen to respect this condition and to follow the ORC load history.

The temperature of the hot tank is imposed equal to the inlet oil temperature in the steam generator $T_{HT} = T_{GV,in}$, know as an input variable. The temperature of the cold tank is imposed equal to the average oil temperature exiting the steam generator during the day, $T_{GV,out,avg}$, that can be evaluated using the prevision function $f_T(C)$, that expresses the relative oil outlet temperature as function of the ORC load $C(t)$, defined in the off-design model (see paragraph 4.3).

Knowing $T_{GV,out,Des}$, the absolute value of the steam generator oil outlet temperature during the day can be found, eq. 4.6

$$T_{GV,out}(t) = T_{GV,out,rel}(t) \cdot T_{GV,out\ Des} \qquad 4.6$$

and so, its average value $T_{GV,out,avg}$.

The temperatures of the hot and cold tanks are equal to the outlet and inlet temperature of the oil in the recovery heat exchanger, equations 4.7 and 4.8.

$$T_{SR,in} = T_{CT} \qquad 4.7$$

$$T_{SR,out} = T_{HT} \qquad 4.8$$

With these two temperatures, the oil mass flow rate flowing in the recovery heat exchanger $\dot{m}_{SR}(t)$ during the day can be evaluated with 4.9 and 4.10.

$$\dot{m}_{SR}(t) = \dot{m}_{gs}(t) \frac{c_{p,gs}\left(T_{gs,in} - T_{gs,out}\right)}{c_{p,oil}\left(T_{SR,out} - T_{SR,in}\right)} \qquad 4.9$$

$$T_{gs,out} = T_{SR,in} + \Delta T_{pp,SR} \qquad 4.10$$

The mass flow rate of the exhaust gases $\dot{m}_{gs}(t)$ varies during the day as function of the gas turbine load.

The condition of conservation of mass can be expressed by 4.11

$$\int_t \dot{m}_{SR}\,(t)dt = \int_t \dot{m}_{GV}\,(t)dt \qquad 4.11$$

The steam generator mass flow rate $\dot{m}_{GV}(t)$ can be expressed as the product between its design value and its relative value $\dot{m}_{GV,rel}(t)$, calculated through the prevision function $f_{\dot{m}}(C)$ defined in

the off-design model (see paragraph 4.3), that express the relative value of the oil mass flow rate in the steam generator $\dot{m}_{GV,rel}(t)$ as function of the ORC load $C(t)$, eq. 4.12

$$\dot{m}_{GV,rel}(t) = f_{\dot{m}}\big(C(t)\big) \tag{4.12}$$

The conservation of mass becomes eq. 4.13

$$\int_t \dot{m}_{SR}\,(t)dt = \int_t \dot{m}_{GV,rel}(t)\,\dot{m}_{GV,Des}\,dt \tag{4.13}$$

This allows to find the design oil mass flow rate at the steam generator, eq. 4.14

$$\dot{m}_{GV,Des} = \frac{\int_t \dot{m}_{SR}\,(t)dt}{\int_t \dot{m}_{GV,rel}(t)\,dt} \tag{4.14}$$

4.3 Off-Design ORC

The ORC in off-design will operate in sliding pressure mode. Sliding pressure operation is the method that controls the power output by varying the steam pressure using boiler load control while maintaining the turbine control valve in a fully open state.

To build the off-design model it is necessary to define the equations that describe the behaviour of all the components of the cycle in off-design operation.

The heat transfer coefficient UA of the heat exchangers (recovery heat exchanger, steam generator, recuperator, and condenser) is obtained with 4.15 and 4.16

$$UA = UA_{Des}\left(\frac{\dot{m}}{\dot{m}_{Des}}\right)^n \tag{4.15}$$

$$UA = \frac{Q_{Des}}{\Delta T_{ml,Des}} \tag{4.16}$$

This equation assumes that one of the two sides of the heat exchanger is dominant with respect to the other. UA_{Des} is the heat transfer coefficient in design condition, $\dot{m}_{Des}$ is the mass flow rate of the dominant fluid in design condition, $\dot{m}$ is the mass flow rate of the dominant fluid in off-design, and n is a parameter that depends on the position of the dominant fluid in the heat exchanger. The values that have been used are reported in Table 4.1.

Table 4.1: Values of the n coefficient for the heat exchangers (17)

Heat Exchanger	Dominant Fluid	n
Recovery Heat Exchanger	Exhaust gases	0.6
Steam Generator (superheater)	Organic fluid	0.8
Steam Generator (evaporator)	Diathermic oil	0.6
Steam Generator (economizer)	Diathermic oil	0.6
Condenser	Water	0.8
Recuperator	Organic fluid	0.6

The off-design conditions of the turbine are described by 4.17

$$C_t = \frac{\dot{m}_f \sqrt{T_{in}}}{\sqrt{p_{in}^2 + p_{out}^2}} \qquad 4.17$$

where C_t is a parameter that can be calculated in design condition and is constant also in off-design, T_{in} is the turbine inlet temperature and p_{in} and p_{out} the turbine inlet and outlet pressure.
Turbine's efficiency in off-design is given by 4.18

$$\frac{\eta_{exp,is}}{\eta_{exp,is,Des}} = 2\sqrt{\frac{\Delta h_{exp,is,Des}}{\Delta h_{exp,is}}} - \frac{\Delta h_{exp,is,Des}}{\Delta h_{exp,is}} \qquad 4.18$$

where $\eta_{exp,is}$ and $\eta_{exp,is,Des}$ are the off-design and design isentropic efficiencies of the turbine, and $\Delta h_{exp,is}$ and $\Delta h_{exp,is,Des}$ are the enthalpy differences in off-design and design conditions.
The efficiency of the pump can be evaluated using equations 4.19 and 4.20.

$$\frac{\eta_{p,is}}{\eta_{p,is,Des}} = 0.86387 + 0.3096F - 0.14086F^2 - 0.029265F^2 \qquad 4.19$$

$$F = \frac{\frac{\dot{V}}{N}}{\left(\frac{\dot{V}}{N}\right)_{Des}} \qquad 4.20$$

$\eta_{p,is}$ and $\eta_{p,is,Des}$ are the off-design and design isentropic efficiencies of the pump, $\dot{V}$ is the volumetric flow rate of the organic fluid and N is the number of rounds per minute of the pump.
It is possible to determine the off-design working conditions by knowing the mass flow rate $\dot{m}_{oil}$ and the temperature $T_{oil,in}$ of the hot source, solving in an iterative way the equations of the model. In this way, the mass flow rate of the organic fluid $\dot{m}_f$, the turbine inlet temperature $T_{in,t}$,

the oil outlet temperature $T_{oil,out}$, all the thermodynamic points of the cycle, the electrical power output P_{el} and the efficiency η_{ORC} can be determined.

The off-design model will be used both for the plant with and without TES.

The study of the off-design condition of the ORC without TES is needed to obtain a prediction of the behaviour of the cycle, necessary for the optimization of the ORC with TES. Given a specific load C and fixed the inlet temperature of the oil, two prevision functions are defined to determine the mass flow rate of the organic fluid needed to produce the desired power and the corresponding oil outlet temperature. The prevision functions are defined by equations 4.21 and 4.22, where the quantities are expressed in relation to their design value.

$$f_{\dot{m}}(C) = \dot{m}_{GV,rel}(C) = \frac{\dot{m}_{GV}(C)}{\dot{m}_{GV_{Des}}} \qquad 4.21$$

$$f_T(C) = T_{GV,out,rel}(C) = \frac{T_{GV,out}(C)}{T_{GV,out,Des}} \qquad 4.22$$

The same off-design model will be used after the design optimisation process of the ORC with TES in order to:

- See if the prediction functions obtained with the off-design model of the plant without TES and used for the optimisation of the design of the plant with TES were correct.
- Create off-design maps that can relate the oil conditions at the inlet of the steam generator and the off-design conditions. With these maps, knowing the temperature and the mass flow rate of the oil, the output power and the oil outlet temperature can be determined. In addition, knowing one property between the mass flow rate or the inlet temperature of the oil and the power output, the value of the unknown property can be evaluated.

  These maps will be useful to treat the ORC in a simplified way during the sizing of the storage system and the simulations of the overall system.

4.4 Two Tanks

The two tanks TES configuration is integrated in the system as in Figure 4.4.

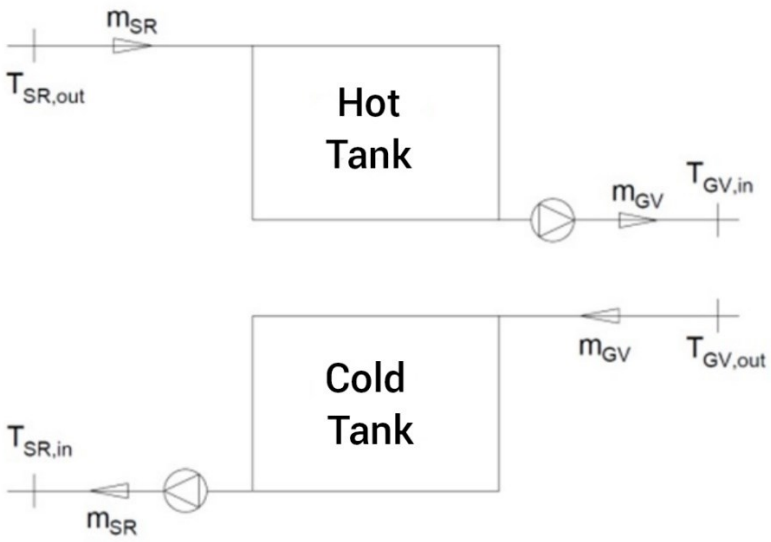

Figure 4.4: Integration of the two-tank TES into the system (17)

The oil mass flow rate $\dot{m}_{SR}$ is heated up by the exhaust gases in the recovery heat exchanger, exits at temperature $T_{SR,out}$ and enters the hot tank, where it mixes with the oil already present inside. The oil mass flow rate $\dot{m}_{GV}$ is then extracted from the hot tank and sent to the steam generator. In the steam generator, the oil cools down from temperature $T_{GV,in}$ to temperature $T_{GV,out}$, heating to the organic fluid. The oil at the exit of the steam generator is sent to the cold tank, where it mixes with the oil already present inside. The oil mass flow rate $\dot{m}_{SR}$ is taken from the cold tank and sent back to the recovery heat exchangers, entering at temperature $T_{SR,in}$.

The mass flow rates $\dot{m}_{SR}$ and $\dot{m}_{GV}$ are controlled respectively by the characteristics of the heat source i.e., the operating conditions of the gas turbine, and by the requested load by the ORC.

When $\dot{m}_{SR} > \dot{m}_{GV}$, the storage system works in charging mode, with an increase of the oil mass stored in the hot tank and a decrease of oil in the cold tank. The system works in discharging mode when $\dot{m}_{SR} < \dot{m}_{GV}$, with an opposite trend of the level of oil inside the tanks with respect to the charging phase.

The two tanks are modelled with the hypothesis of complete mixing; this means that the oil inside the tanks is considered to have the same temperature at each point and that the oil exits the tanks with the same temperature of the oil inside it, $T_{out} = T$.

The equations used for the model are listed below, equations 4.23, 4.24, 4.25 and 4.26, with reference to Figure 4.5

$$\frac{dm}{dt} = \dot{m}_{in} - \dot{m}_{out} \qquad 4.23$$

$$\frac{d(mh)}{dt} = \dot{m}_{in}h_{in} - \dot{m}_{out}h_{out} - UA(T - T_{amb}) \qquad 4.24$$

$$m\frac{dh}{dt} + h\frac{dm}{dt} = \dot{m}_{in}h_{in} - \dot{m}_{out}h_{out} - UA(T - T_{amb}) \quad 4.25$$

$$\frac{dh}{dt} = \frac{1}{m}\left[\dot{m}_{in}h_{in} - \dot{m}_{out}h_{out} - UA(T - T_{amb}) - h\frac{dm}{dt}\right] \quad 4.26$$

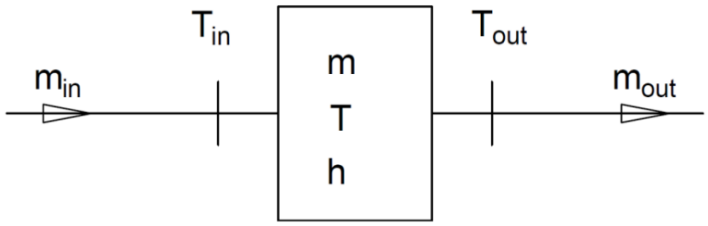

Figure 4.5: Model of the perfectly mixed tank (17)

The sizing of the two tanks TES consists of an iterative procedure in which the temperature profile of the hot tank, the maximum electric power, and the initial state of the two tanks are defined at the beginning and then progressively updated to respect the imposed conditions.

The level of oil inside the tanks needs to be the same at the beginning and at the end of the day to guarantee the repeatability of the cycle in the following days, and the produced power needs to follow the imposed load history as close as possible.

The iterative procedure is exposed in the following and reported in the flux diagram of Figure 4.6.

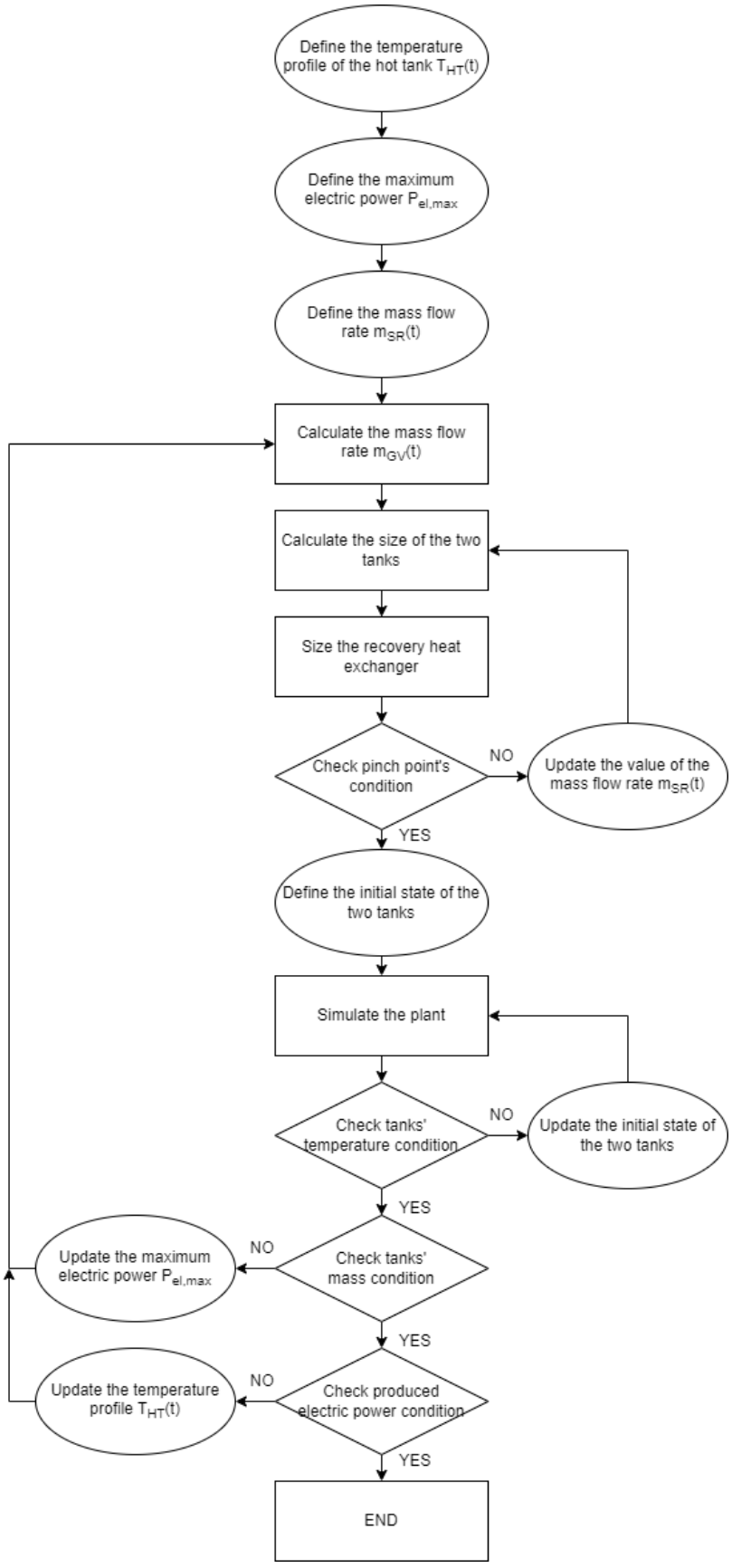

Figure 4.6: Flux diagram of the storage system design for the two-tanks configuration

The first step consists of defining the temperature profile of the hot tank during the day $T_{HT}(t)$. As a starting value, $T_{HT}(t)$ is imposed to be constant and equal to the oil inlet temperature of the steam generator in design condition, $T_{HT}(t) = T_{GV,in} = const$. Then, the initial value of the maximum produced power is defined and imposed equal to the nominal power of the ORC, $P_{el,max} = P_{el,Des}$. From the maximum power $P_{el,max}$ and the load history of the ORC $C(t)$, the trend of the produced power during the day $P(t)$ can be determined.

The next step consists of defining the oil mass flow rates $\dot{m}_{SR}(t)$ to be sent to the recovery heat exchanger. The latter depends on the working conditions of the gas turbine during the day, and is evaluated through eq. 4.27

$$\dot{m}_{SR}(t) = \dot{m}_{gs}(t)\frac{c_{p,gs}(T_{gs,in} - T_{gs,out})}{c_{p,oil}(T_{SR,out} - T_{SR,in})} \quad 4.27$$

where $\dot{m}_{gs}(t)$ is the mass flow rate of the exhaust gases during the day, that is function of the gas turbine load, and the temperatures values are taken considering the design conditions.

Then, the oil mass flow rate flowing inside the steam generator $\dot{m}_{GV}(t)$ is evaluated using the maps built in the off-design model, knowing the steam generator inlet temperature $T_{GV,in}(t) = T_{HT}(t)$ and the electric power output imposed by the load history $P(t)$ during the day.

From the mass flow rates, it is possible to find the mass of oil M_{oil} that needs to be stored. This value is increased by 10% to ensure that the tanks are never completely full or empty. From M_{oil}, the volumes of the tanks are found with equations 4.28 and 4.29

$$V_{HT} = \frac{M_{oil}}{\rho_{HT}} \quad 4.28$$

$$V_{CT} = \frac{M_{oil}}{\rho_{CT}} \quad 4.29$$

The values of density ρ_{HT} and ρ_{CT} are taken considering the maximum temperature reached in the respective tank.

The dimensions of the tanks are evaluated as a function of the defined aspect ratio $R = \frac{h}{D}$, with the following equations, 4.30, 4.31 and 4.32

$$d = \sqrt[3]{\frac{4V}{\pi R}} \quad 4.30$$

$$h = R \cdot d \quad 4.31$$

$$A = 2\frac{\pi d^2}{4} + \pi d h \quad 4.32$$

The following step of the iterative process is the sizing of the recovery heat exchanger. The design value of the oil mass flow rate inside the heat exchanger is chosen as the maximum value of $\dot{m}_{SR}(t)$, $\dot{m}_{SR,Des} = max(\dot{m}_{SR}(t))$. The recovery heat exchanger must be able to heat the design mass flow rate $\dot{m}_{SR,Des}$ from the inlet temperature $T_{SR,in,Des}$ to the outlet temperature $T_{SR,out,Des}$. These temperatures are considered to be equal to the average oil temperature inside the tanks, taking into account the heat losses to the environment, equations 4.33 and 4.34

$$T_{SR,in,Des} = T_{CT,avg} - \frac{UA_{CT}(T_{CT,avg} - T_{amb})}{\dot{m}_{SR,Des} \cdot c_p} \quad 4.33$$

$$T_{SR,out,Des} = T_{HT,avg} - \frac{UA_{HT}(T_{HT,avg} - T_{amb})}{\dot{m}_{SR,Des} \cdot c_p} \quad 4.34$$

where the term $UA\Delta T$ considers the losses to the environment.

From the energy balance of the recovery heat exchanger, the design outlet temperature of the exhaust gases can be found with the eq. 4.35

$$T_{gs,out,Des} = T_{gs,in,Des} - \frac{\dot{m}_{SR,Des} \cdot c_{p,oil}}{\dot{m}_{gs} \cdot c_{p,gs}} (T_{SR,out,Des} - T_{SR,in,Des}) \quad 4.35$$

as well as the value of the pinch point, eq. 4.36

$$\Delta T_{pp,SR} = T_{gs,out,Des} - T_{SR,in,Des} \quad 4.36$$

Now, the first check is done, regarding the pinch point of the recovery heat exchanger. If the obtained value is close to the chosen optimal value $\Delta T_{pp,SR,opt}$, the procedure can continue; if not, the value of the oil mass flow rate $\dot{m}_{SR}(t)$ is updated in order to have the desired pinch point and the procedure starts again from the sizing of the two tanks.

Now, the initial state of the tanks needs to be defined. The mass is chosen for the tanks to be with a level of oil between 5% and 95% during the day, while the temperatures are imposed equal to the average temperatures defined before.

The next step consists in simulating the overall system. In the simulation of the system, the time is discretised in intervals Δt. For each time interval, knowing the initial state and the values of $\dot{m}_{GV}(t)$ and $\dot{m}_{SR}(t)$, the value of the thermodynamic state, the exchanged thermal power, the produced electric power, and the new state of the tanks are found.

At the end of the simulation, a first check is done on the condition of the initial state of the tanks. To guarantee the repeatability of the cycle, the initial temperatures must be equal to the temperatures at the end of the day. If the check fails, the initial temperatures are updated with the temperatures at the end of the previous simulation and the simulation is run again until the condition is respected.

A second check is then made to guarantee that the levels of oil inside the tanks are the same at the beginning and at the end of the day. To do so, the energy inside the tanks is evaluated at the beginning and end of the day. If the values are different, it means that there is an energy difference between the energy absorbed from the exhaust gases and the energy given to the ORC; in particular, if the variation is positive it means that the system has stored more energy that can be used and the maximum load $P_{el,max}$ can be increased, vice versa if the variation is negative the value needs to be reduced. In this way, the load is updated, and the procedure is repeated considering the updated load until the condition is respected.

The last check on the produced power $P_{el}(t)$ is needed because the mass flow rate $\dot{m}_{GV}(t)$ was calculated to obtain the desired power $P(t)$ following an imposed temperature profile of the hot tank $T_{HT}(t)$, initially considered constant, but the real generated power $P_{el}(t)$ will be different because the effective trend of the temperature inside the hot tank is different. So, the procedure is repeated updating the temperature profile $T_{HT}(t)$ with the profile obtained with the last simulation, until the condition is respected.

Once all the conditions are satisfied, the procedure is concluded, and the performance of the overall system can be analysed.

4.5 Stratified Tank

The stratified tank is integrated in the system as shown in Figure 4.7.

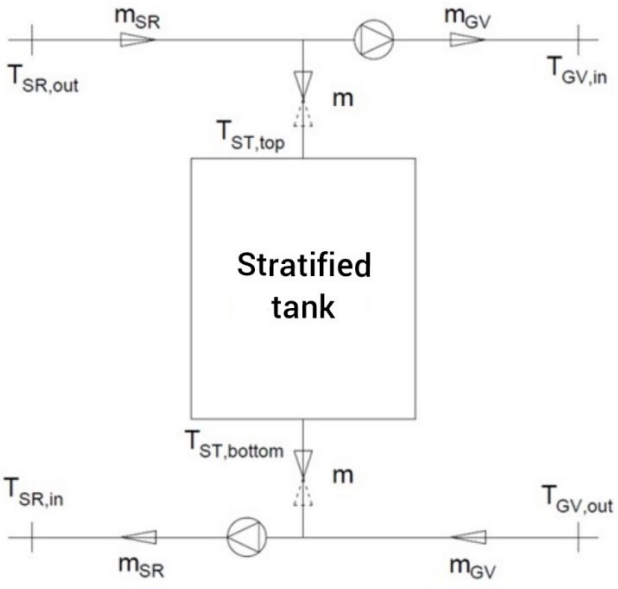

Figure 4.7: Integration of the stratified tank TES into the system (17)

When $\dot{m}_{SR} > \dot{m}_{GV}$ the tank works in charging mode; the mass flow rate $\dot{m}_{SR}$ exiting the recovery heat exchanger at the temperature $T_{SR,out}$ is divided into the mass flow rate $\dot{m}_{GV}$ that is sent to the steam generator and the mass flow rate $\dot{m}$ that enters the tank from the top. The same mass flow rate $\dot{m}$ is extracted from the bottom of the tank at a lower temperature and mixed with the mass flow rate exiting the steam generator and feeds the recovery steam generator.

When $\dot{m}_{SR} < \dot{m}_{GV}$ the tank works in discharging mode; the mass flow rate $\dot{m}$ is extracted from the top of the tank and is mixed with the mass flow rate exiting the recovery heat exchanger $\dot{m}_{SR}$, in order for $\dot{m}_{GV}$ to be enough to feed the ORC requested power load. When $\dot{m}_{GV}$ exits the steam generator at the temperature $T_{GV,out}$, it is divided into $\dot{m}$ that enters the tank from the bottom and $\dot{m}_{SR}$ that is sent to the recovery steam generator.

Stratified tanks operate according to the stratification process, which occurs due to the variation in the density of a fluid as a function of its temperature. In these tanks, the energy is stored keeping a thermal gradient inside the tanks, called thermocline, that separates the hot liquid that tends to go in the upper zone because of its lower density, and the cold liquid that tends to go down. The level of charge is given by the quantity of hot fluid with respect to the cold fluid, and so to the position of the thermocline. When the tank is fully charged, the thermocline is in the lower part of the tank that is full of hot fluid; vice versa, a fully discharged tank presents the thermocline in its upper zone and is full of cold working fluid.

With this configuration, all the necessary fluid is stored in a single tank that is always full, allowing to reduce the volumes and the costs relative to the storage with respect to the two tank solution.

In the monodimensional model of the stratified tank used, the latter is discretized in N nodes that represent N equal slices of equal height, each behaving as a fully mixed tank. This N nodes interact with each other and with the external environment through mass and heat fluxes that determine its thermodynamic state. The model is represented in Figure 4.8.

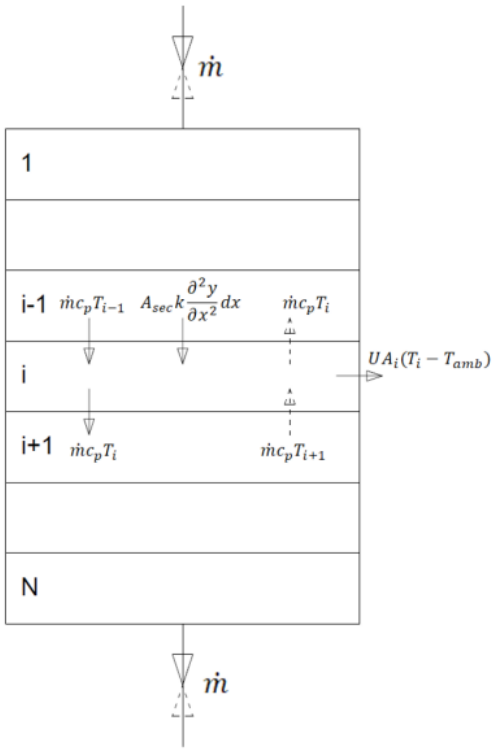

Figure 4.8: Model of the stratified tank (17)

The balance of energy for each node N is given by eq. 4.37, which shows that the variation of temperature $\frac{dT_i}{dt}$ for the node i depends on several terms.

$$\frac{dT_i}{dt} = -\frac{\dot{m}}{\rho A_{sec}}\frac{dT}{dx} + \frac{k}{\rho c_p}\frac{d^2T}{dx^2} - \frac{U}{\rho c_p}\frac{P}{A_{sec}}(T_i - T_{amb}) \qquad 4.37$$

The first term represents the thermal flux of the mass flow rate $\dot{m}$ flowing inside the layer, where ρ is the density of the fluid, $A_{sec} = \frac{\pi d^2}{4}$ is the area of the transversal section of the tank and $\frac{dT}{dx}$ is the temperature variation through the longitudinal axis of the tank, negative due to stratification.

If the mass flow rate $\dot{m}$ is positive (from top to bottom), the stratified tank is in charging mode; if $\dot{m}$ is negative (from bottom to top), the tank is in discharging mode.

The second term represents the thermal flux due to conduction, where k is the thermal conductivity of the fluid, c_p is the specific heat and $\frac{d^2T}{dx^2}$ the gradient of temperature.

The third term represents the losses to the environment; U is the global heat transfer coefficient of the tank, $P = \pi d$ is the perimeter of the transversal section of the tank, $(T_i - T_{amb})$ the difference between the temperature of the oil inside the node and the ambient temperature.

Discretising the time in intervals Δt, knowing the state of the tank in instant t_j and the boundary conditions, the state of the various layers can be determined at instant $t_{j+1} = t_j + \Delta t$, solving eq. 4.38

$$T_i^{j+1} = T_i^j + \left(\frac{|\dot{m}|}{\rho A_{sec}} \frac{T_{in,i}^j - T_i^j}{\Delta x} + \frac{k}{\rho c_p} \frac{T_{i-1}^j - 2T_i^j + T_{i+1}^j}{\Delta x^2} - \frac{U}{\rho c_p} \frac{P}{A_{sec}} \left(T_i^j - T_{amb}\right) \right) \Delta t \qquad 4.38$$

where the index i represents the node and the apex j the instant of time, and $T_{in,i}^j$ is the input fluid temperature in node i, with $T_{in,i}^j = T_{i-1}^j$ during charging phase and $T_{in,i}^j = T_{i+1}^j$ during discharging phase.

A limit is imposed for the discretization interval Δt, that must be lower than a maximum value given by eq. 4.39

$$\Delta t_{max} = \frac{m_i}{\dot{m}} \qquad 4.39$$

that represents the time for which the mass that enters and exits node i is equal to the total mass inside the node.

For the first and last nodes, the equation must be modified to take into account that the losses to the environment occur also through the upper and lower surfaces of the tank. The term $\frac{P}{A_{sec}}$ is therefore substituted with $\left(\frac{P}{A_{sec}} - \frac{1}{\Delta x}\right)$ for these two nodes.

This model also considers the turbulence generated by the fluid entering the tank, with the hypothesis that the mass flow rate $\dot{m}$ is mixed in equal parts with the first n_{mix} nodes of the tank. The value of this parameter is evaluated through the mixing factor γ_{mix}, that represent the percentage of fluid inside the tank with which happens the mixing process, having $n_{mix} = N \cdot \gamma_{mix}$.

A conservative hypothesis is made for the density of the oil inside the tank that should vary with temperature but is considered constant and equal to the density correspondent to the maximum reached temperature. In this way, the effective volume occupied by the oil inside the tank will always be lower than the volume of the tank, creating an empty zone inside it.

After the balances are solved for each node, a check is made to find if there are areas with inversion of temperature that must be eliminated because the hot fluid will always be in a higher position with respect to a colder fluid. The iterative procedure to erase these inversions of temperature starts from node N, going up until an inversion of temperature is found between two nodes. Then, a mixing process between the two nodes is made and, if in the next node the

inversion is still present, another mixing process is made, until no more inversions of temperature are present inside the tank.

The performances of TES made of a stratified tank are directly influenced by the amount of oil stored inside. As already said, the thermocline moves along the tank depending on the level of charge. When the tank is fully charged, the thermocline is in the upper zone of the tank; when the tank is fully discharged, it is in the lower zone. If the stored mass is not enough, at the end of the charging phase, the oil exiting the tank will decrease its temperature because of the near presence of the thermocline, influencing the temperature of the mass flow rate that feeds the ORC and so its performances. Similarly, at the end of the discharging phase, if the thermocline is too close to the lower outlet of the tank, the extracted mass flow rate will increase its temperature, increasing all successive temperatures, and thus influencing the performance of the cycle. These problems can be avoided by increasing the stored mass because the thermocline occupies a lower portion of the overall dimension of the tank, keeping it far from the upper and lower outlet during the maximum discharge and charge.

To choose the correct amount of mass that need to be stored, limits are therefore imposed for the operating conditions of the ORC and for the minimum and maximum temperatures that can be reached in the upper and lower edges of the tank during operation.

These limits are reported in Table 4.2.

Table 4.2: Limits on the operating conditions of the ORC

	Lower Limit	**Upper Limit**
Oil inlet temperature $T_{GV,in}$	$T_{GV,in,Des} - 20°C$	$T_{GV,in,Des} + 5°C$
Oil mass flow rate $\dot{m}_{GV}$	$40\%\ \dot{m}_{GV,Des}$	$110\%\ \dot{m}_{GV,Des}$
Oil temperature tank's upper edge	$T_{GV,in,Des} - 50°C$	-
Oil temperature tank's lower edge	-	$T_{GV,out,Des} + 50°C$

The sizing of the stratified tank is an iterative procedure in which the maximum produced power, the size of the tank, the initial state and the oil mass flow rates are determined, respecting the imposed conditions and the repeatability of the cycle. The sizing of the recovery heat exchanger is not done because the one obtained with the two tanks simulation is considered.

The iterative procedure is exposed in the following and reported in the flux diagram of Figure 4.9.

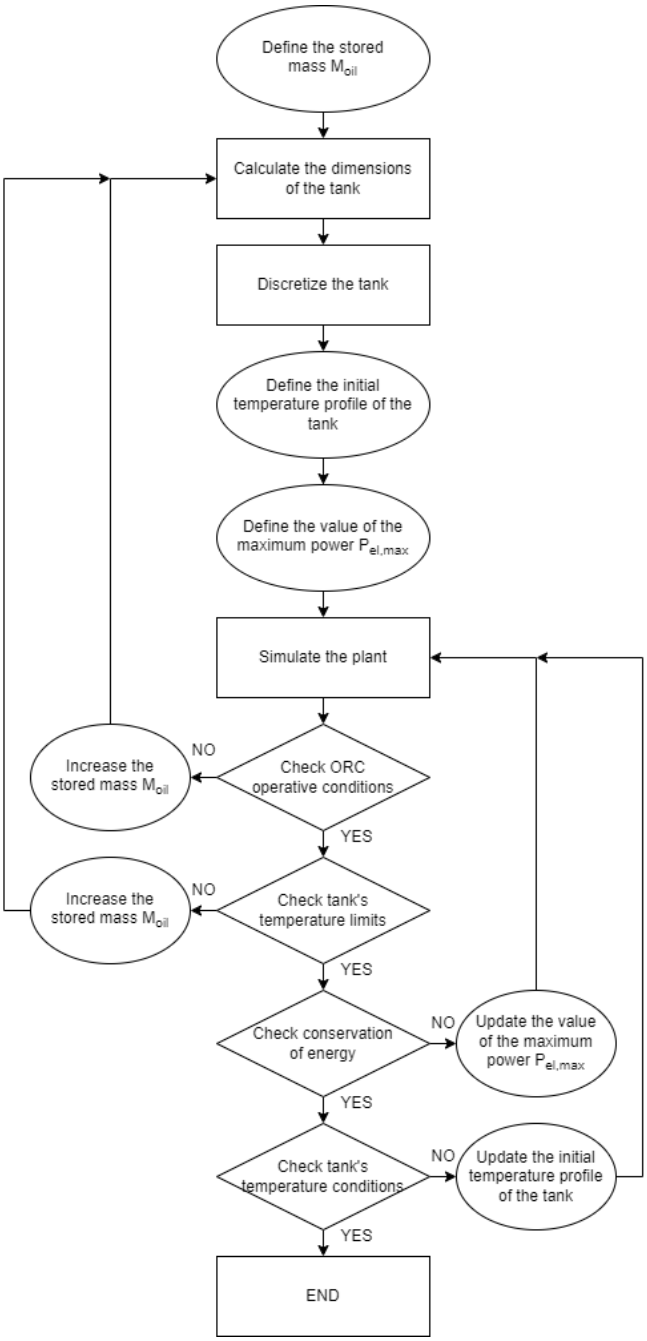

Figure 4.9: Flux diagram of the storage system design for the stratified tank configuration

The first step consists of defining the stored mass of oil M_{oil}. A good starting value can be the one obtained with the two tanks configuration. Then, the dimensions of the tank can be evaluated through equations 4.30, 4.31 and 4.32.

The discretization of the tank is done considering layers that are characterized by the same mass m_i. In this way, with the increase of the total mass M_{oil}, the simulations will always have the same level of accuracy. The value of m_i is chosen with eq. 4.40, as the ratio between the mass of oil obtained with the two tanks' configuration and a reference number of divisions N_{ref}.

$$m_i = \frac{M_{oil}}{N_{ref}} \tag{4.40}$$

The first volume analysed will be discretized with N_{ref} nodes, the following with an increasing value N given by eq. 4.41

$$N = \frac{M_{oil}}{m_i} \tag{4.41}$$

The height of the nodes is calculated with eq. 4.42

$$\Delta x = \frac{H_{ST}}{N} \tag{4.42}$$

The next step consists in defining the initial temperature profile of the tank. As a first attempt, the thermocline is considered null, with hot and cold masses of oil equal to the corresponding initial values obtained with the two tanks' configuration and temperature equal to the average temperatures $T_{HT,avg}$ and $T_{CT,avg}$. During the simulation, the real thermocline will be determined.

The maximum power value $P_{el,max}$ and the relative load history $P(t)$ is defined, starting with the values obtained with the two tanks' configuration.

The next step is the simulation of the system.

The oil mass flow rate flowing inside the recovery heat exchanger $\dot{m}_{SR}(t)$ depends on the working conditions of the gas turbine during the day, and is evaluated through eq. 4.43

$$\dot{m}_{SR}(t) = \dot{m}_{gs}(t) \frac{c_{p,gs}(T_{gs,in} - T_{gs,out})}{c_{p,oil}(T_{SR,out} - T_{SR,in})} \tag{4.43}$$

where $\dot{m}_{gs}(t)$ is the mass flow rate of the exhaust gases during the day, that is function of the gas turbine load, and the temperatures values are taken considering the design conditions.

The mass flow rate $\dot{m}_{GV}(t)$ is determined, for each time interval, to obtain the desired power output $P(t)$. Then, all the thermodynamic points and the exchanged powers, as well as the status of the stratified tank are determined for each interval.

During the simulations, the operative limits imposed for the ORC regarding the temperature and the mass flow rate are verified, and if they are not respected, it means that the mass stored inside the tank is not enough, so this value is increased, and the iterative procedure starts again from the sizing of the tank.

After the simulation, the imposed conditions for the minimum and maximum temperatures that can be reached at the upper and lower edges of the tank during operation are checked and, if the values exceed the limits, the stored mass is increased, and the iterative procedure starts again from the tank sizing.

Once these conditions are verified, the repeatability of the cycle need to be guaranteed, both in terms of temperature and energy.

If the total energy contained inside the tank in the initial state is different from the one in the ending state, it means that there is an energy difference between the energy absorbed from the exhaust gases and the energy given to the ORC; in particular, if the variation is positive it means that the system has stored more energy that can be used and the maximum load $P_{el,max}$ can be increased, vice versa if the variation is negative the value needs to be reduced. In this way, the load is updated, and the procedure starts again from the simulation of the plant considering the updated load.

The last condition regards the temperature profile; during the simulation, the thermocline that initially was imposed equal to zero starts to increase in dimensions. The simulations are then repeated, updating the initial temperature profile with the one obtained in the last simulations, until the two profiles coincide. Once this condition is also respected, the continuity of the cycle is guaranteed, so the procedure in concluded and the performance of the overall system can be analysed.

5 Simulation

The gas turbine used for the design of the system is the GE10-1 by General Electric. The main characteristics of this turbine are reported in Table 5.1.

Table 5.1: Main characteristics of the gas turbine in design condition

Electrical Output [MW]	Electrical Efficiency	Exhaust Flow [kg/sec]	Exhaust Temperature [°C]
11.25	31.4 %	47.5	482

The off-design performances of the gas turbine are based on the description made by Lozza (19), in which the regulation of the power production of a gas turbine is done as follow:

- From 50 to 100% of the power the regulation is made with the variable guide vanes, which determine the linear reduction of the air mass flow rate. The turbine outlet temperature is kept constant by the fuel mass flow rate. The compression ratio decreases because the maximum pressure of the cycle follows the reduction of the mass flow rate. With a constant turbine's outlet temperature and a reduction of the compression ratio, the turbine's inlet temperature decreases.
- From 0 to 50%, the gas turbine operates at constant air mass flow rate, with the variable guide vanes as close as possible, varying the fuel mass flow rate and therefore the inlet and outlet temperature of the turbine. The compression ratio slightly decreases due to the reduction of the turbine's inlet temperature.

Figure 5.1 shows the trend of the mass flow rate of exhaust gases and their outlet temperature as a function of the gas turbine load.

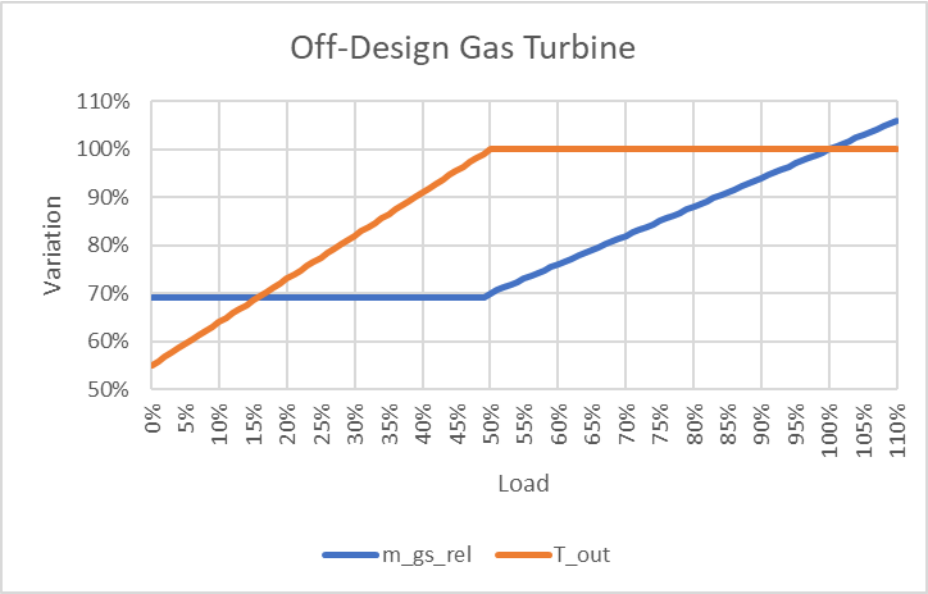

Figure 5.1: Trend of the mass flow rate of exhaust gases and their temperature as function of the gas turbine load

The chosen diathermic oil is Therminol-66 (20), characterised by a high working temperature (up to 357 °C), without the need to be pressurised.

The aspect ratio of the tanks $R = \frac{h}{D}$ is imposed equal to 2.

For the choice of the ORC's organic fluid, the design optimization of the reference plant without TES has been done for different fluids. Given the type of heat source, and its relatively high temperature compared to those for which the ORC cycles are usually used, the most suitable fluids are Toluene, Benzene, Cyclopentane, and Cyclohexane, as demonstrated by Carcasci et al. (21) and Chacartegui et al. (22).

The input variables used for the design optimization are reported in Table 5.2.

Table 5.2: Input variables used for the design optimization

Gas	Oil	Condenser	Efficiencies
$T_{gs} = T_{gs,avg} = 482°C$	$T_{oil,in} = 340°C$	$T_{w,in} = 15°C$	$\eta_{is,p} = 0.8$
$\dot{m}_{gs} = \dot{m}_{gs,avg} = 47.5\ \frac{kg}{s}$	$p_{oil} = 101.3\ kPa$	$T_{w,out} = 25°C$	$\eta_{mec,p} = 0.92$
$p_{gs} = 101.3\ kPa$	$\Delta T_{pp,SR} = 15°C$	$p_w = 101.3\ kPa$	$\eta_{mec,t} = 0.9$
			$\eta_{mot} = 0.9$
			$\eta_{gen} = 0.92$

For the design of the ORC, the characteristics of the heat source are taken as the mean values during the day. The oil inlet temperature $T_{oil,in}$ chosen for the design is 340°, taking a safety margin from the maximum temperature of the oil that is $T_{oil,max} = 357°C$, considering that

during the operation of the plant the temperature could increase, especially with the introduction of the TES.

The limits imposed on the optimisation variables are reported in Table 5.3.

Table 5.3: Limits imposed on the optimization variables

	Lower limit	**Upper limit**
$\boldsymbol{T_{GV\_out}}$ $[°\boldsymbol{C}]$	90	$T_{oil,in}$
$\boldsymbol{p_{ev}}$ $[\boldsymbol{bar}]$	$p_{cond,max}$	$p_{ev,max} = 35\ bar$
$\boldsymbol{T_3}$ $[°\boldsymbol{C}]$	$T_{cond,max} + 10°C$	$T_{oil,in}$
$\boldsymbol{T_{cond}}$ $[°\boldsymbol{C}]$	$T_{cond,min}$	$T_{cond,max}$
$\boldsymbol{\Delta T_{pp,GV}}$ $[°\boldsymbol{C}]$	25	100
$\boldsymbol{\Delta T_{pp,REC}}$ $[°\boldsymbol{C}]$	20	100
$\boldsymbol{\Delta T_{pp,COND}}$ $[°\boldsymbol{C}]$	10	100
$\boldsymbol{E}$	0	0.8

The maximum evaporation temperature $p_{ev,max}$ is chosen considering technical limitations. The condensation temperature values $T_{cond,min}$ and $T_{cond,max}$ are defined considering the respective pressure limits $p_{cond,min} = 0.8\ bar$, to avoid to keep an excessively pushed vacuum inside the condenser, and $p_{cond,man} = 1.1\ bar$, to avoid to keep a pressure to high with respect to atmospheric pressure.

Results of the optimisation for the different fluids are reported in Table 5.4

Table 5.4: Main parameters and performances of the optimised cycle without TES for different organic fluids

	Toluene	Benzene	Cyclopentane	CycloHexane
$\boldsymbol{T_{oil,out}}$ $[°\boldsymbol{C}]$	192	182	118	162
$\boldsymbol{p_{ev}}$ $[\boldsymbol{bar}]$	4.4	20.4	31.9	23.1
$\boldsymbol{T_3}$ $[°\boldsymbol{C}]$	237	257	250	241
$\boldsymbol{T_{cond}}$ $[°\boldsymbol{C}]$	110	75	45	78
$\boldsymbol{\Delta T_{pp,GV}}$ $[°\boldsymbol{C}]$	38	27	33	40
$\boldsymbol{\Delta T_{pp,REC}}$ $[°\boldsymbol{C}]$	34	32	28	39
$\boldsymbol{\Delta T_{pp,cond}}$ $[°\boldsymbol{C}]$	79	25	18	43
$\boldsymbol{E}$	0.39	0.56	0.44	0.28
$\boldsymbol{P_{th,ORC}}$ $[\boldsymbol{MW}]$	14.5	15.0	18.3	16.1
$\boldsymbol{P_{el}}$ $[\boldsymbol{MW}]$	1.35	2.76	3.64	2.60
$\boldsymbol{\eta_{ORC}}$	0.093	0.184	0.199	0.162

T_{ev} [°C]	172	223	213	237
ΔT_{surr} [°C]	65	34	37	4
p_{cond} [bar]	0.992	0.860	0.875	0.928
m_{oil} [kg/s]	40.2	39.3	35.7	37.8
m_f [kg/s]	28.5	25.9	29.1	28.3
m_w [kg/s]	308	279	331	308
$\eta_{is,t}$	0.914	0.903	0.898	0.900

Cyclopentane is the fluid that shows better performances with respect to the other fluids, with higher electric power P_{el} and cycle efficiency η_{ORC}, therefore this fluid will be used for the following simulations.

The simulation and the sizing of the overall system consists of various steps, summarised in the following and schematized in the flow chart of Figure 5.2.

First of all, the gas turbine power plant needs to be chosen, and the load history of the gas turbine needs to be defined.

The following step consists in the optimization of the design condition of the ORC without TES. Then, the off-design model will be used with the ORC without TES for defining some prevision functions that will be needed for the optimisation of the design of the ORC with TES.

When these prevision functions are obtained, the load history of the ORC is defined, and the optimisation of the design of the ORC with TES can be done, based on the load history of the gas turbine and of the ORC. After that, the off-design model is used with the ORC with TES to assess the correctness of the previously used prediction functions and to build off-design maps of the plant, that will be used in the simulation of the plant to describe in a simple way the behaviour of the ORC in off-design. The last step consists in sizing the TES (both two tanks and stratified tank) and the simulation of the overall system.

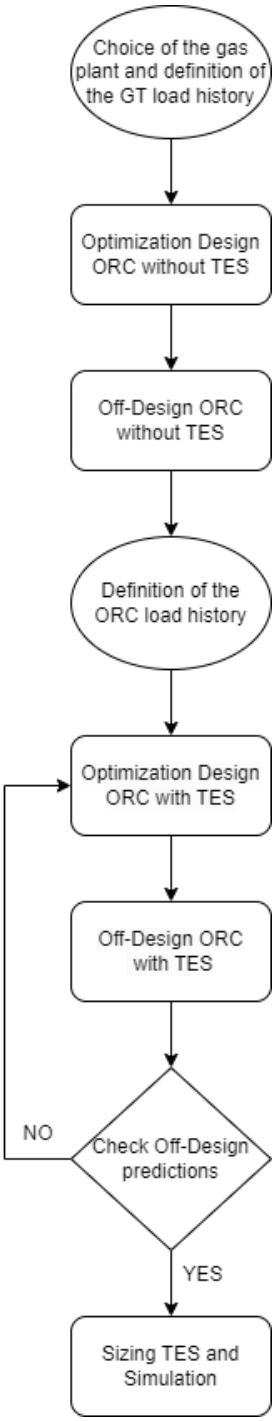

Figure 5.2: Flow chart of the simulation and sizing of the overall plant

5.1 Load History 1

The first load history analysed is shown in Figure 5.3, with the gas turbine working at nominal power for the entire day and the ORC that works at 100% of the load from 7 a.m. to 10 p.m. and at 50% for the rest of the time.

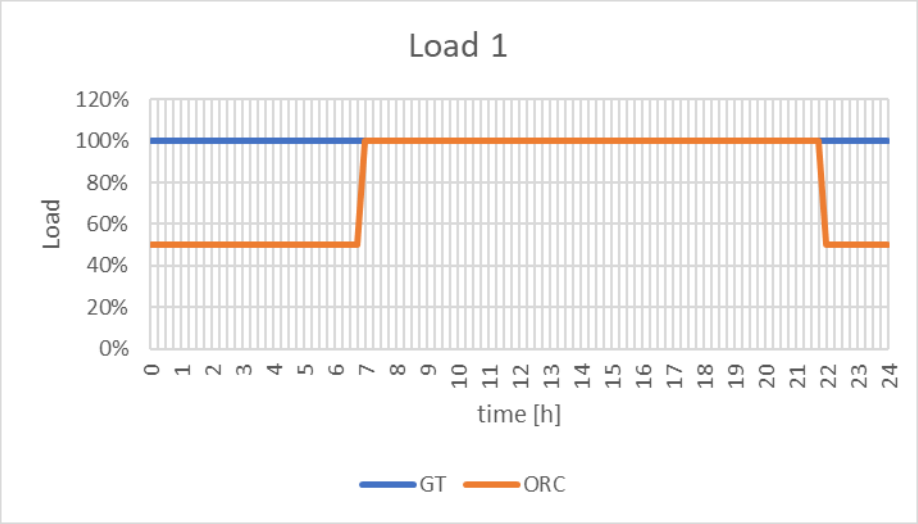

Figure 5.3: Load History 1

The simulation procedure is the one schematized in the diagram flux of Figure 5.2; for brevity, only the optimisation results regarding the design of the ORC with TES are reported here.

The input variable used for the optimization design of the ORC are reported in Table 5.2, while limits imposed on optimisation variables are reported in Table 5.3.

Table 5.5 shows the main parameters and performances of the cycle.

Table 5.5: Main parameters and performances of the optimised cycle with TES

$T_{oil,out}$ [°C]	105.85
p_{ev} [bar]	34.85
T_3 [°C]	255.85
T_{cond} [°C]	42.85
$\Delta T_{pp,GV}$ [°C]	29.31
$\Delta T_{pp,REC}$ [°C]	65.94
$\Delta T_{pp,cond}$ [°C]	19.96
E	0.35
$P_{th,ORC}$ [MW]	22.98
P_{el} [MW]	4.59
η_{ORC}	0.20
T_{ev} [°C]	218.96
ΔT_{surr} [°C]	36.89
p_{cond} [bar]	0.82

$\boldsymbol{m_{oil}\ [kg/s]}$	42.99
$\boldsymbol{m_f\ [kg/s]}$	35.20
$\boldsymbol{m_w\ [kg/s]}$	414.51
$\boldsymbol{\eta_{is,t}}$	0.90

The T-s diagram of the cycle is reported in Figure 5.4.

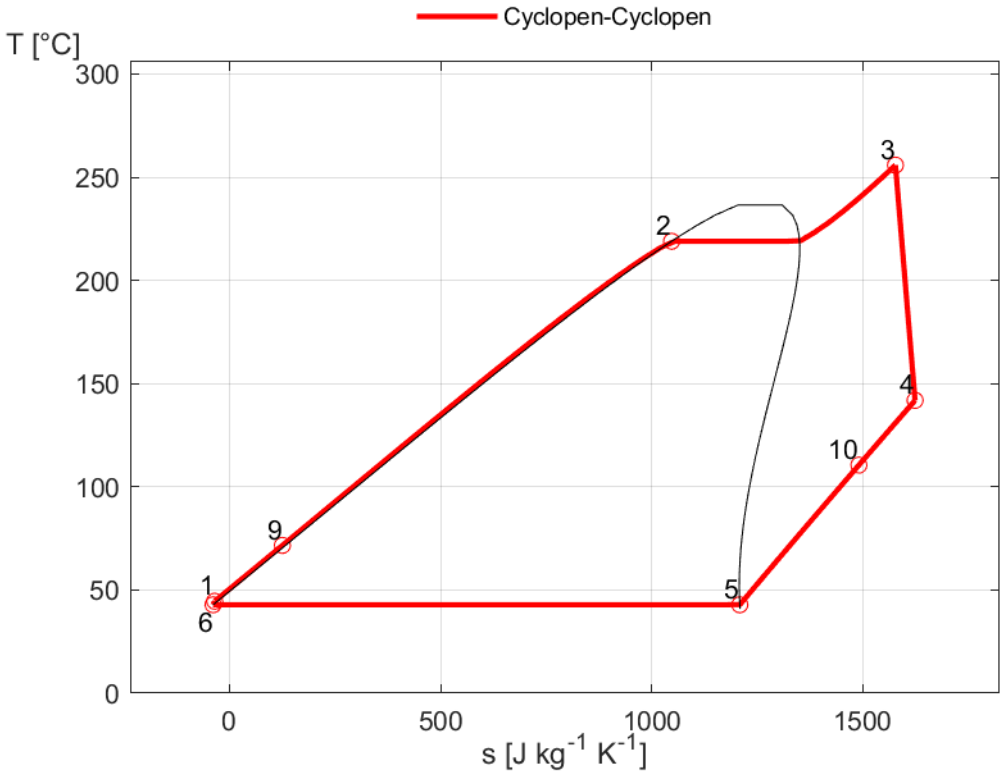

Figure 5.4: T-s diagram of the cycle

The graphs of the heat exchangers are reported in Figure 5.5, Figure 5.6 and Figure 5.7.

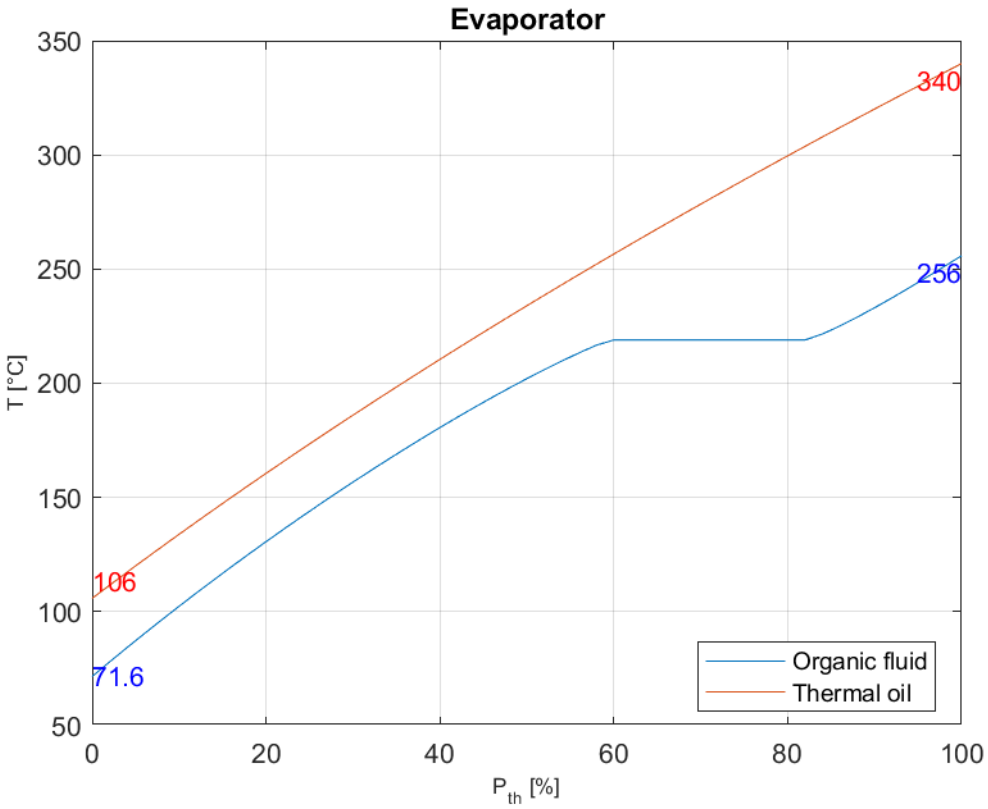

Figure 5.5: Heat transfer diagram of the evaporator

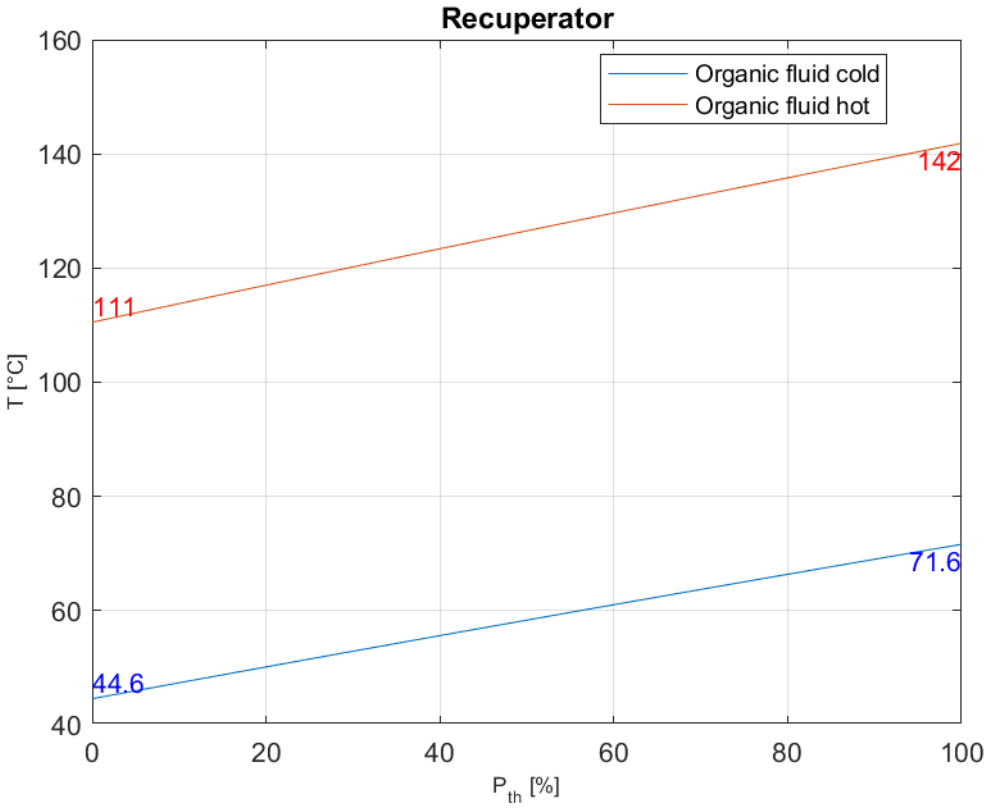

Figure 5.6: Heat transfer diagram of the recuperator

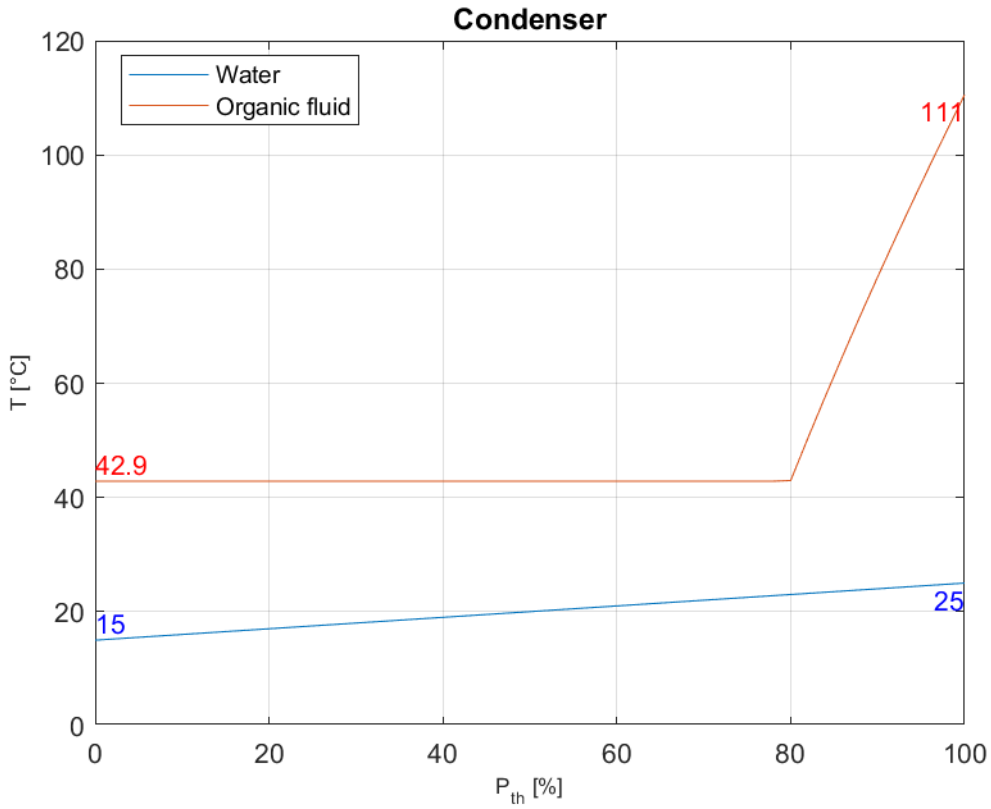

Figure 5.7: Heat transfer diagram of the condenser

The next step consists in the sizing of the tanks and the simulation of the system for both the TES configurations.

The main results are reported in Table 5.6.

Table 5.6: TES sizing and simulation of the system main results

	Load History 1	
	Two Tanks	**Stratified Tank**
	TES Sizing	
$V_{HT}\ [m^3]$	585.767	
$V_{CT}\ [m^3]$	476.634	
$M\ [kg]$	453218.691	543862.429
$V_{tot}\ [m^3]$	1062.401	702.131
$d_{HT}\ [m]$	7.198	7.646
$d_{CT}\ [m]$	6.720	
$T_{HT,avg}\ [°C]$	340.254	
$T_{CT,avg}\ [°C]$	102.020	
$T_{HT,iniz}\ [°C]$	340.303	
$T_{CT,iniz}\ [°C]$	100.132	
$m_{HT,in}\ [kg]$	118715.880	
$m_{CT,in}\ [kg]$	334502.811	
	Recovery Heat Exchanger	
$m_{SR,Des}\ [kg/s\ ]$	35.136	
$T_{SR,in,Des}\ [°C]$	100.130	

$T_{SR,out,Des}$ [°C]	340.408	
$T_{gs,out,Des}$ [°C]	115.057	
$\Delta T_{pp,SR}$ [°C]	14.927	
	Plant's Performances	
$P_{el,max}$ [MW]	4.582	4.574
C_{max}	0.998	0.996
$E_{th,gs}$ [MWh]	458.467	457.770
$E_{th,loss}$ [MWh]	1.148	0.673
$E_{th,ORC}$ [MWh]	457.318	456.793
$e_{el,ORC}$ [MWh]	89.381	89.264
eta_{TES}	0.997	0.998
eta_{ORC}	0.195	0.195
eta_{tot}	0.195	0.195

The total volume of storage is, as expected, greater for the two tank configuration with respect to the stratified tank, due to the presence of two tanks that fill and empty during their operation instead of one that remains always full.

The total mass of oil stored is greater for the stratified tank configuration, due to the presence of the thermocline. The energy stored in the thermocline is characterized by the fact that it cannot be reused because made of oil with a range of temperature not suitable for the operating conditions of the plant.

The power plant's performances are almost the same for the two configurations. The thermal losses to the environment $E_{th,loss}$ are greater for the two tanks configuration due to its greater volume.

For the two tanks configuration, the power trends are reported in Figure 5.8, while the trends of the oil mass flow rates, the fill level of the tanks and the temperatures in the hot and the cold tanks are reported in Figure 5.9.

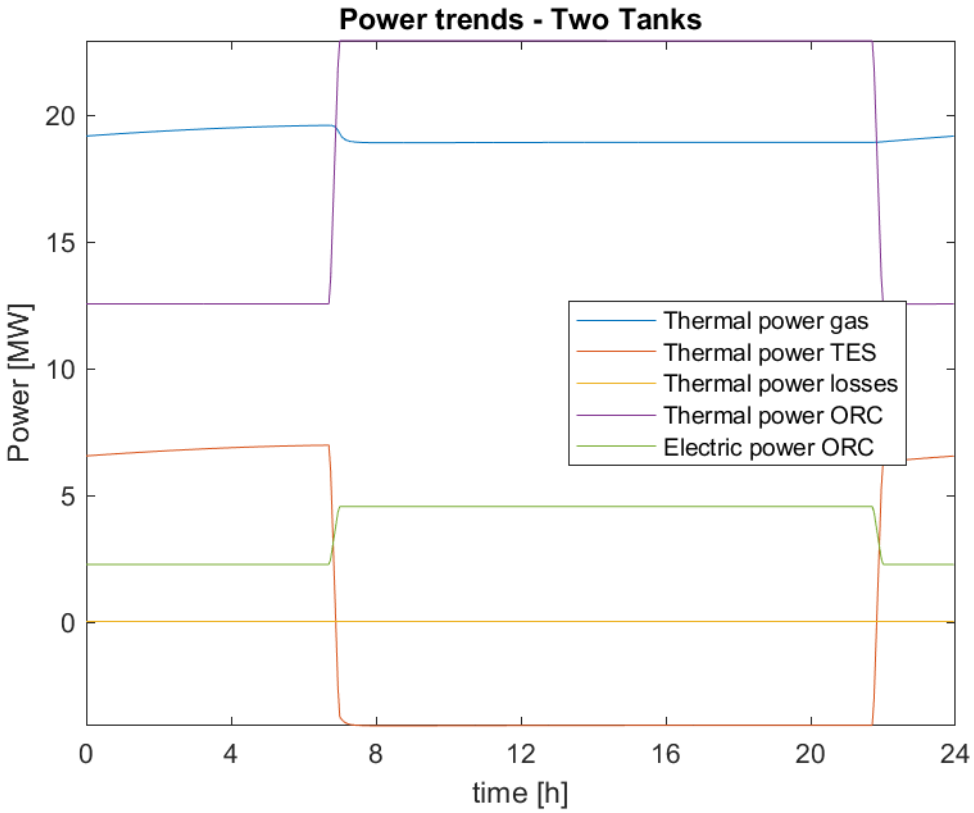

Figure 5.8: Power trends for the two-tanks configuration

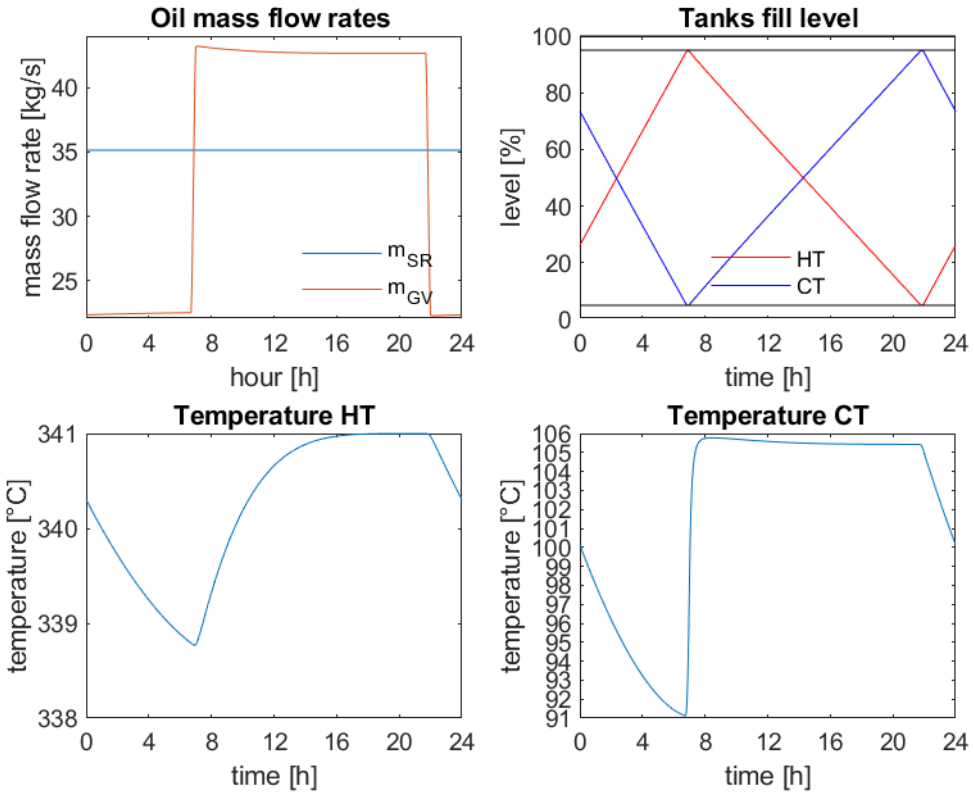

Figure 5.9: Trends of the oil mass flow rates, the fill level of the tanks and the temperatures in the hot and the cold tanks

The TES is in discharging phase from 7 a.m. to 10 p.m. and in charging phase the rest of the time. During the discharging phase, $\dot{m}_{GV} > \dot{m}_{SR}$, the fill level of the cold tank increases while the level of the hot tank decreases; the opposite during charging phase.

The temperature inside the hot tank is almost constant during the day, with a fluctuation of 2°C, while in the cold tank the temperature fluctuation is of 15°C. These temperature variations are due to the different adaptation of the oil outlet temperature from the steam generator in partial working condition of the ORC and are considered acceptable because don't affect the performances of the system.

As shown in Figure 5.8, the thermal power extracted from the exhaust gasses is almost constant during the operation, but with a slightly increase during the charging phase. The expression of the extracted thermal power is given by equation 5.1

$$P_{th,gs}(t) = \dot{m}_{SR}(t)\, c_{p,oil}(T_{SR,out} - T_{SR,in}) \qquad 5.1$$

Being $\dot{m}_{SR}(t)$ fixed (equation 4.43), this little variation is due to the variation in the difference between the inlet and outlet oil temperature from the recovery heat exchanger, i.e. the temperature variations of the oil inside the two tanks.

The electric power trend produced by the ORC follows the imposed load history.

For the stratified tank configuration, the power trends are reported in Figure 5.10, the trend of the mass flow rates in Figure 5.11 and the trends in temperature on the hot and cold side of the tank in Figure 5.12.

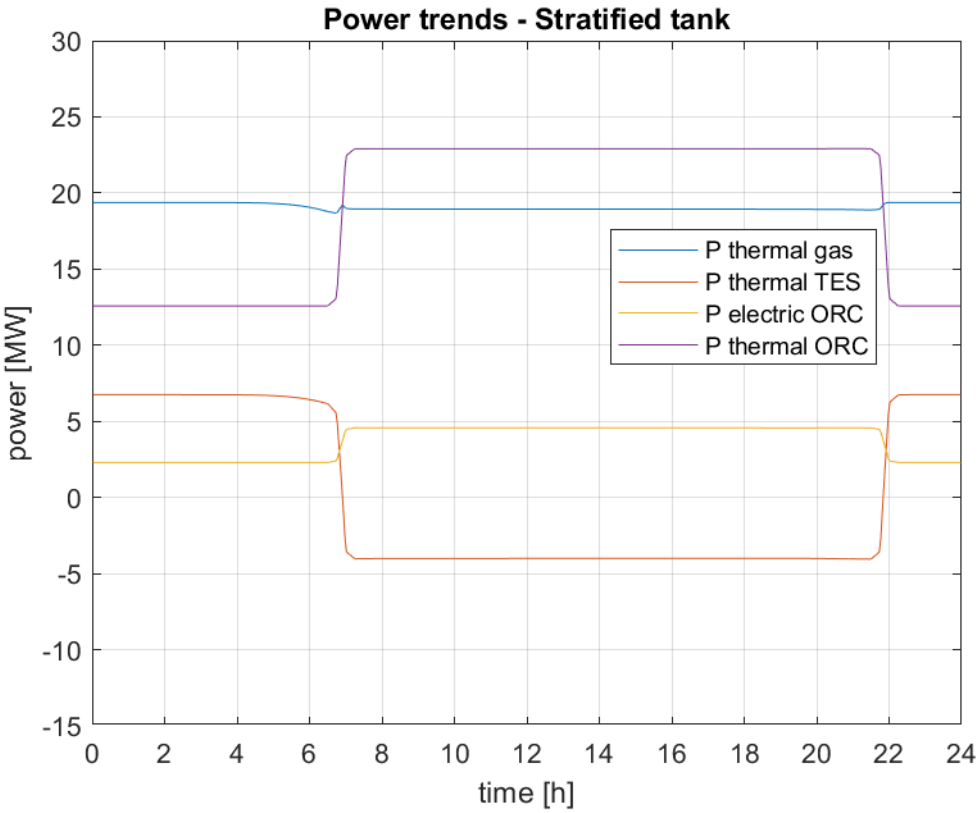

Figure 5.10: Power trends for the stratified tank configuration

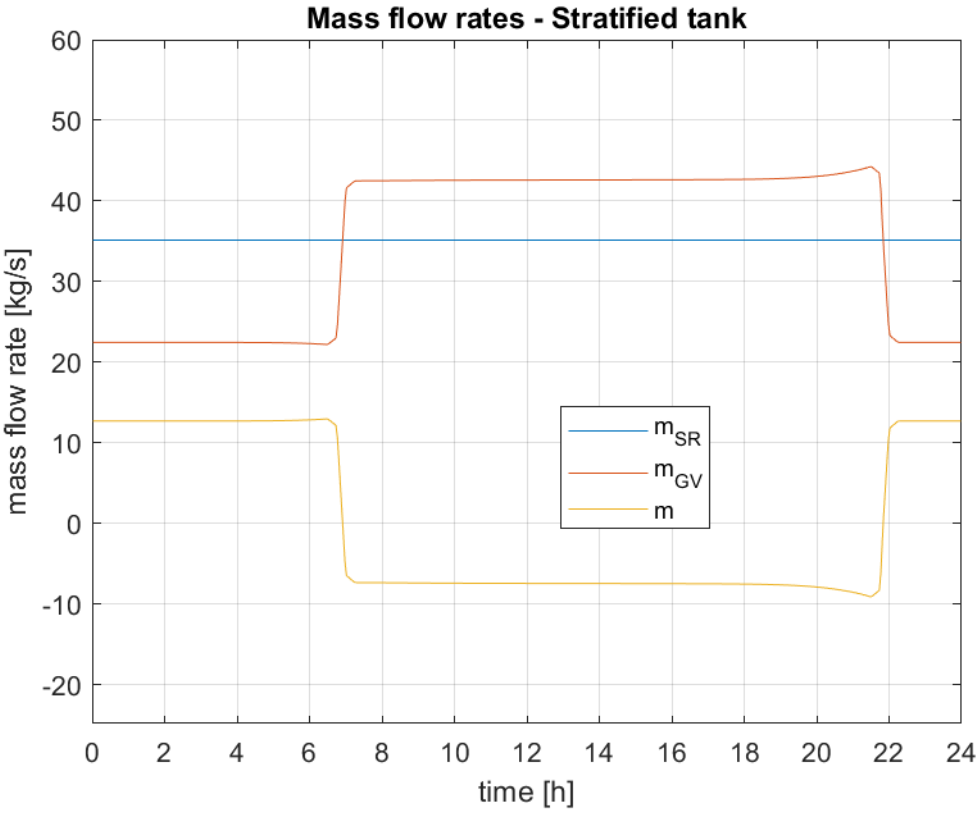

Figure 5.11: Mass flow rate trends for the stratified tank configuration

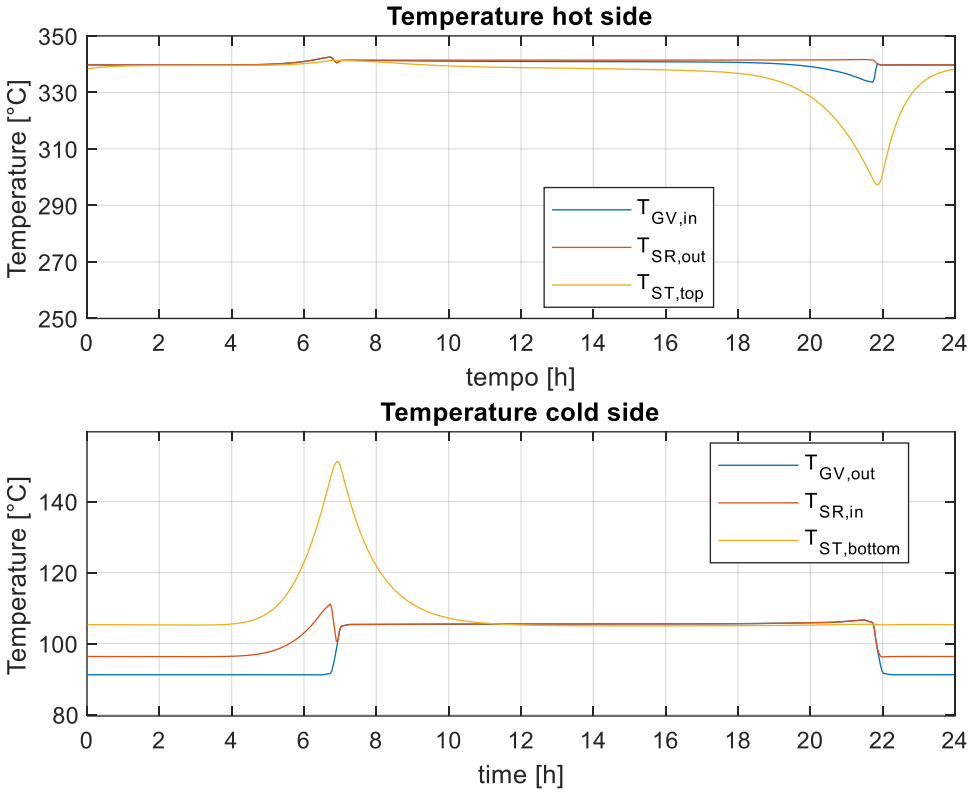

Figure 5.12: Temperature trends on the hot and cold side of the stratified tank

At the end of the discharge phase (10 p.m.), the oil temperature on the hot side of the stratified tank starts to decrease due to the proximity of the thermocline, and consequently also the temperature $T_{GV,in}$ of the mass flow rate $\dot{m}_{GV}$ at the inlet of the steam generator. Therefore, to maintain constant the output power of the ORC, the mass flow rate $\dot{m}_{GV}$ slightly increases while the output mass flow rate $\dot{m}$ of the stratified tank decreases.

At the end of the charging phase (7 a.m.), the thermocline is close to the bottom of the stratified tank, leading to an increase in the stratified tank oil output temperature and therefore of the temperature $T_{SR,in}$.

The temperature profiles inside the tank, and therefore the position of the thermocline, are shown in Figure 5.13 for the initial state and the instants of maximum charge and discharge.

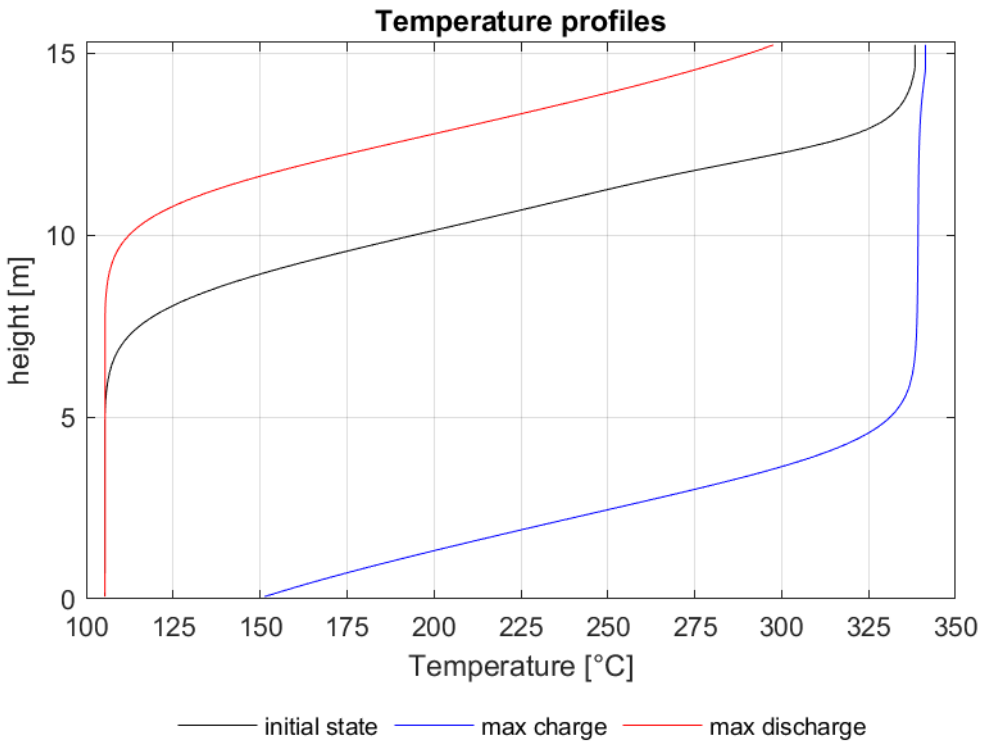

Figure 5.13: Temperature profiles inside the stratified tank

As already said, during the instant of maximum discharge the thermocline is located in the upper part of the tank, that is full of oil at low temperature, while during the instant of maximum charge the thermocline is in proximity of the bottom of the tank, that is full of high temperature oil.

Variations in oil temperature in the hot and cold areas of the tank remain within the imposed limits and do not affect the performance of the cycle in a significant way.

All the quantities are equal at the beginning and at the end of the day, therefore the repeatability of the cycle is guaranteed for both the TES configurations.

5.2 Load History 2

The load history is reported in Figure 5.14, with the gas turbine working at nominal power for the whole day, while the ORC operates at 100% load from 7 a.m. to 12 p.m. and from 5 p.m. to 10 p.m., and at 50% load for the rest of the day.

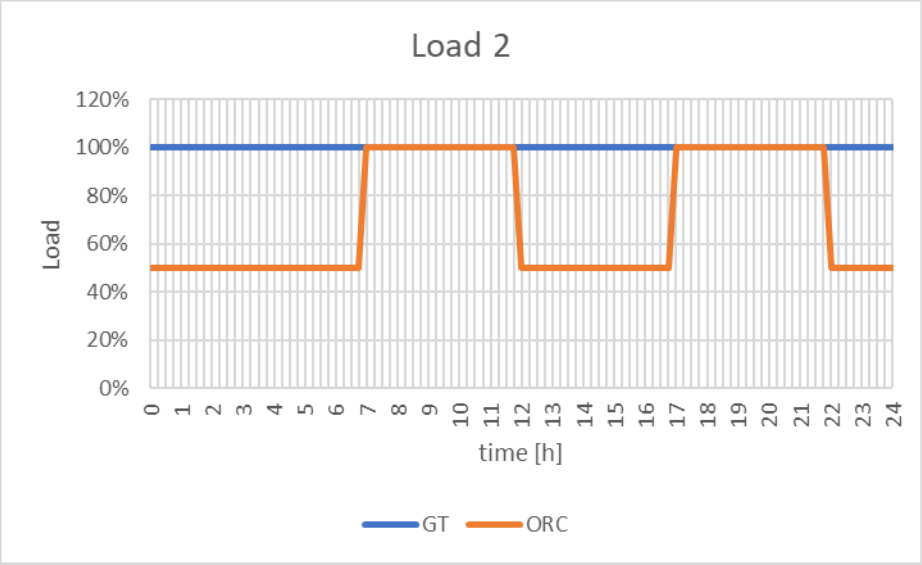

Figure 5.14: Load History 2

A new optimization design of the ORC is done considering the current load history, with the same input variables and limits imposed on the optimisation variables reported in Table 5.2 and Table 5.3.

Table 5.7 shows the main parameters and performances of the optimised cycle with TES.

Table 5.7: Main parameters and performances of the optimised cycle with TES

$T_{oil,out}$ [°C]	104.85
p_{ev} [bar]	29.26
T_3 [°C]	241.85
T_{cond} [°C]	42.85
$\Delta T_{pp,GV}$ [°C]	31.46
$\Delta T_{pp,REC}$ [°C]	58.28
$\Delta T_{pp,cond}$ [°C]	19.65
E	0.38
$P_{th,ORC}$ [MW]	26.19
P_{el} [MW]	5.13
η_{ORC}	0.20
T_{ev} [°C]	206.48
ΔT_{surr} [°C]	35.37
p_{cond} [bar]	0.82

m_{oil} $[kg/s]$	48.82
m_f $[kg/s]$	41.46
m_w $[kg/s]$	475.59
$\eta_{is,t}$	0.90

With respect to the previous optimization, the nominal electric power of the cycle P_{el} is increased from 4.59 MW to 5.13 MW. From equation 4.14, a decrease in the integral of the relative oil mass flow rate in the steam generator due to the change in ORC load history leads to an increase in the design mass flow rate $\dot{m}_{GV,Des}$, and thus to the nominal power of the ORC P_{el}.

The main results on the tank sizing and system simulation for both TES configurations are reported in Table 5.8.

Table 5.8: TES sizing and simulation of the system main results

	Load History 2	
	Two Tanks	**Stratified Tank**
	TES Sizing	
V_{HT} $[m^3]$	430.216	
V_{CT} $[m^3]$	349.538	
M $[kg]$	332657.440	432454.672
V_{tot} $[m^3]$	779.755	558.303
d_{HT} $[m]$	6.494	7.084
d_{CT} $[m]$	6.060	
$T_{HT,avg}$ $[°C]$	340.332	
$T_{CT,avg}$ $[°C]$	97.858	
$T_{HT,iniz}$ $[°C]$	340.475	
$T_{CT,iniz}$ $[°C]$	96.566	
$m_{HT,in}$ $[kg]$	87165.426	
$m_{CT,in}$ $[kg]$	245492.014	
	Recovery Heat Exchanger	
$m_{SR,Des}$ $[kg/s]$	35.037	
$T_{SR,in,Des}$ $[°C]$	95.614	
$T_{SR,out,Des}$ $[°C]$	340.333	
$T_{gs,out,Des}$ $[°C]$	110.514	
$\Delta T_{pp,SR}$ $[°C]$	14.900	
	Plant's Performances	
$P_{el,max}$ $[MW]$	5.093	5.082
C_{max}	0.992	0.990
$E_{th,gs}$ $[MWh]$	463.559	463.079
$E_{th,loss}$ $[MWh]$	0.926	0.575
$E_{th,ORC}$ $[MWh]$	462.635	462.255
$e_{el,ORC}$ $[MWh]$	86.855	86.769
eta_{TES}	0.998	0.998
eta_{ORC}	0.188	0.188
eta_{tot}	0.187	0.187

The size of the storage is reduced with respect to Load History 1, from 1062.401 m^2 to 779.755 m^2 for the two tanks configuration and from 702.131 m^2 to 558.303 m^2 for the stratified tank configuration, and the produced electricity is slightly decreased despite the bigger size of the plant, because it works at partial load for more time.

For the two tanks configuration, the power trends are reported in Figure 5.15, while the trends of the oil mass flow rates, the fill level of the tanks and the temperatures in the hot and the cold tanks are reported in Figure 5.16.

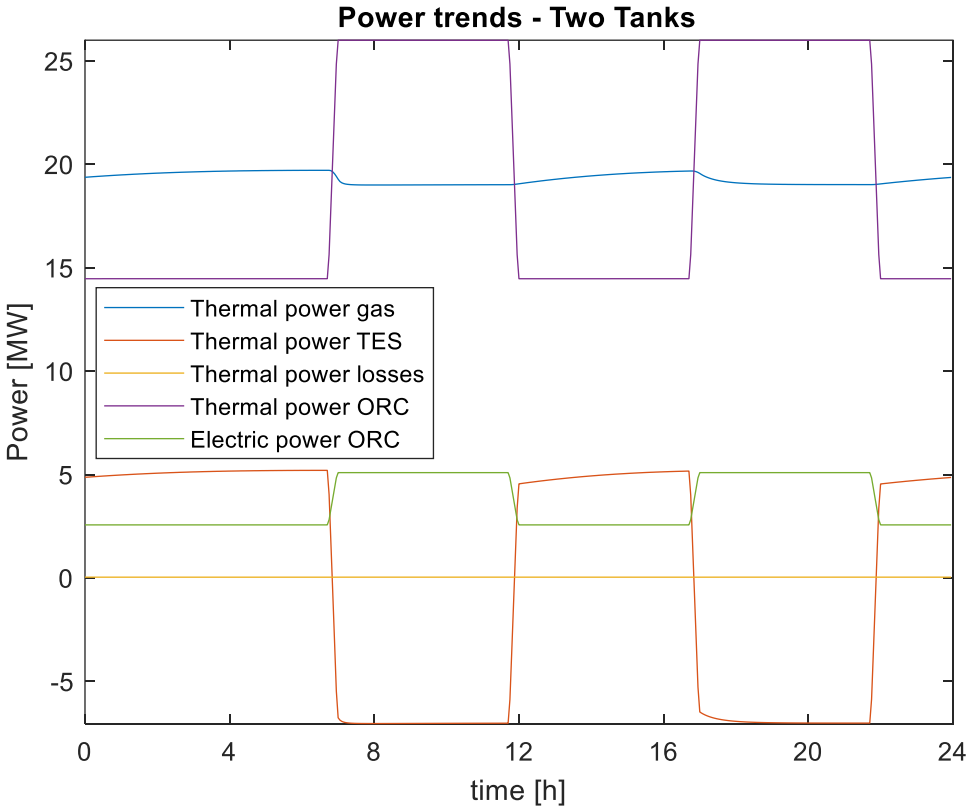

Figure 5.15: Power trends for the two-tanks configuration

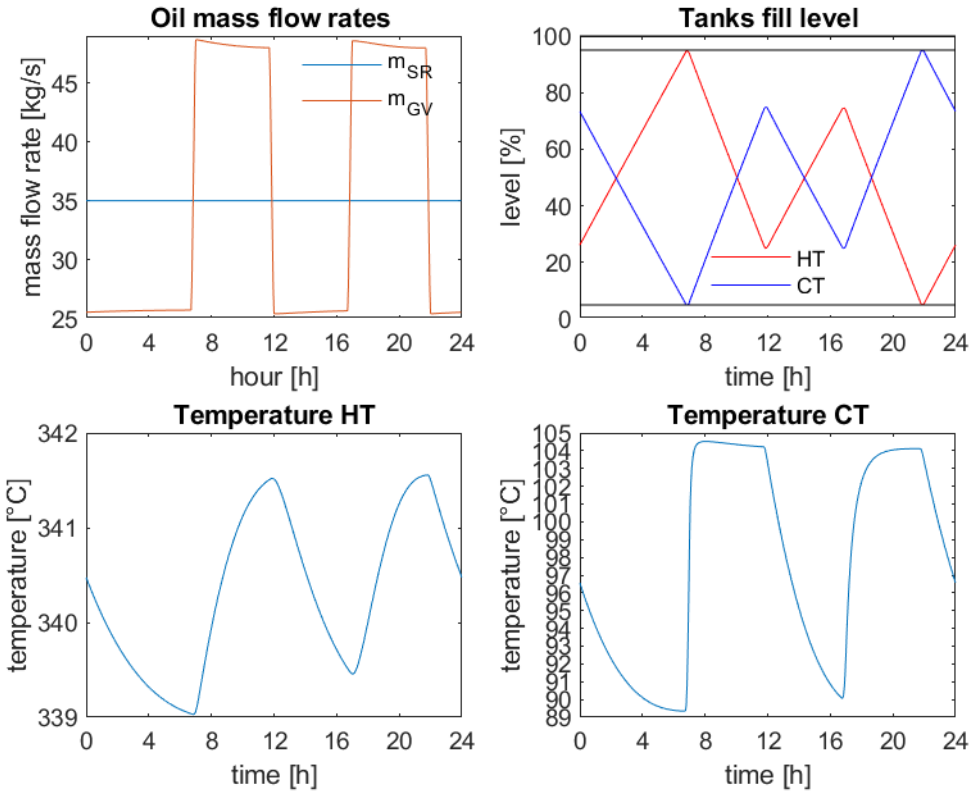

Figure 5.16: Trends of the oil mass flow rates, the fill level of the tanks and the temperatures in the hot and the cold tanks

The TES is in discharging phase from 7 a.m. to 12 p.m. and from 5 p.m. to 10 p.m., and in charging phase the rest of the time.

As for the previous case, the temperature fluctuation in the hot tank is more restricted than in the cold tank.

The oil mass flow rate $\dot{m}_{SR}(t)$ is constant as the gas turbine's load, while $\dot{m}_{GV}(t)$ follows the trend of the ORC load.

For the stratified tank configuration, the power trends are reported in Figure 5.17, the trend of mass flow rates in Figure 5.18 and the temperature trends in the hot and cold side of the tank in Figure 5.19.

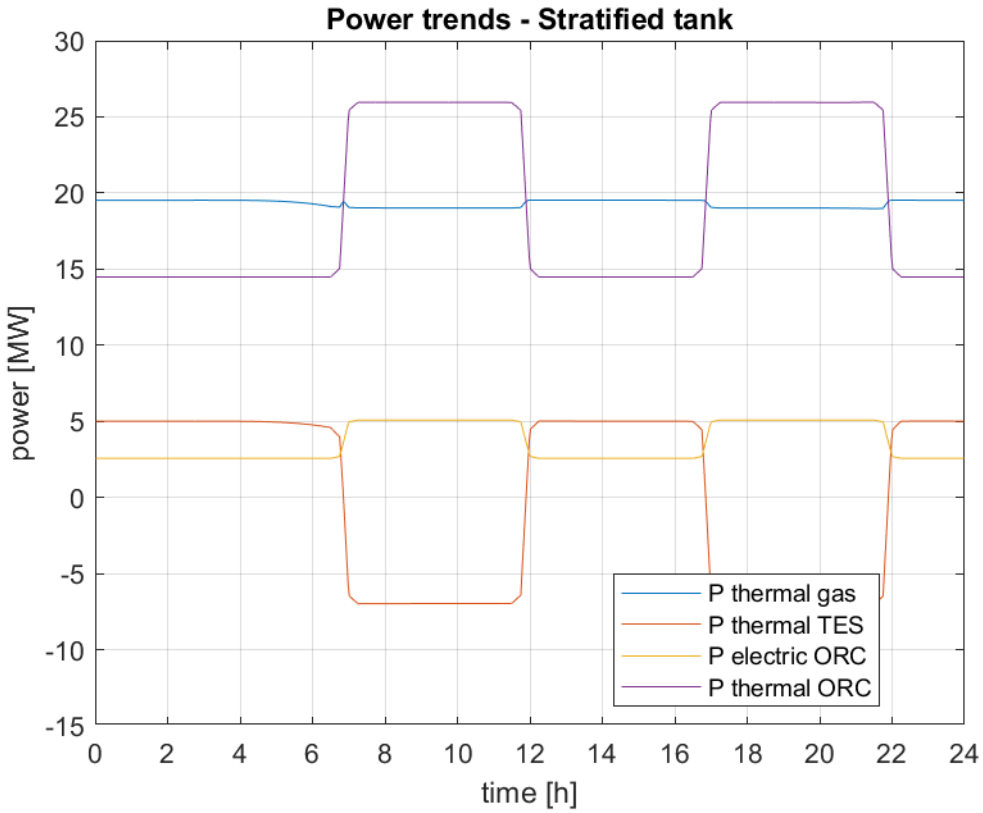

Figure 5.17: Power trends for the stratified tank configuration

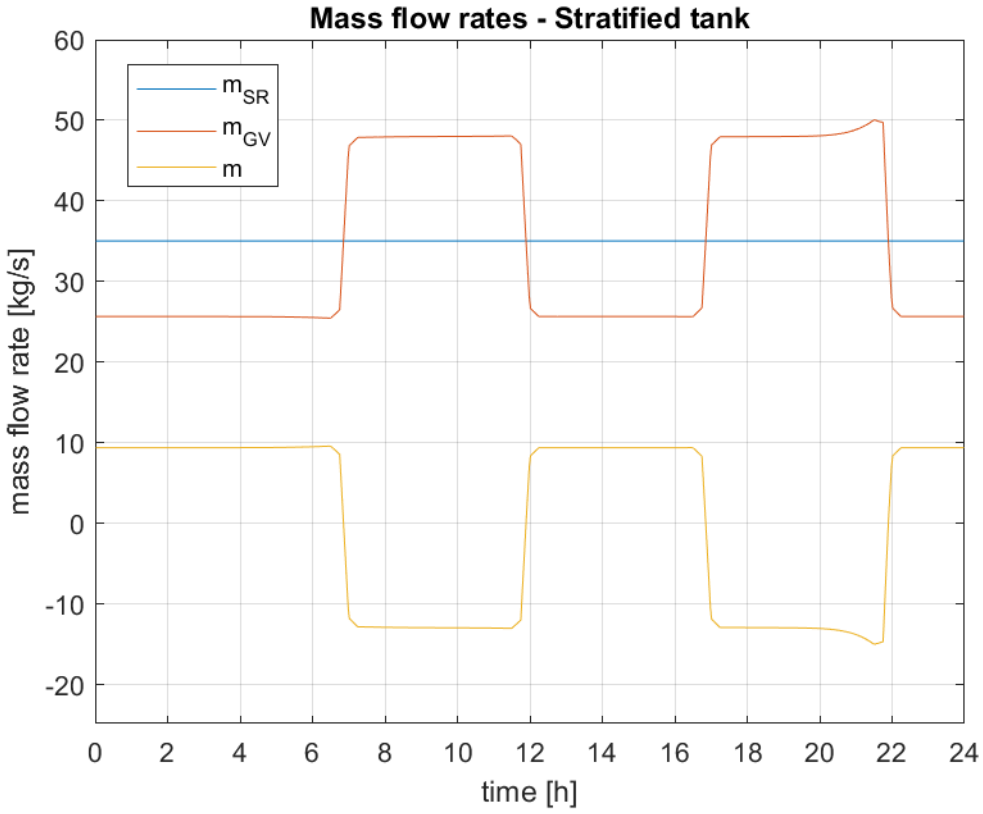

Figure 5.18: Mass flow rate trends for the stratified tank configuration

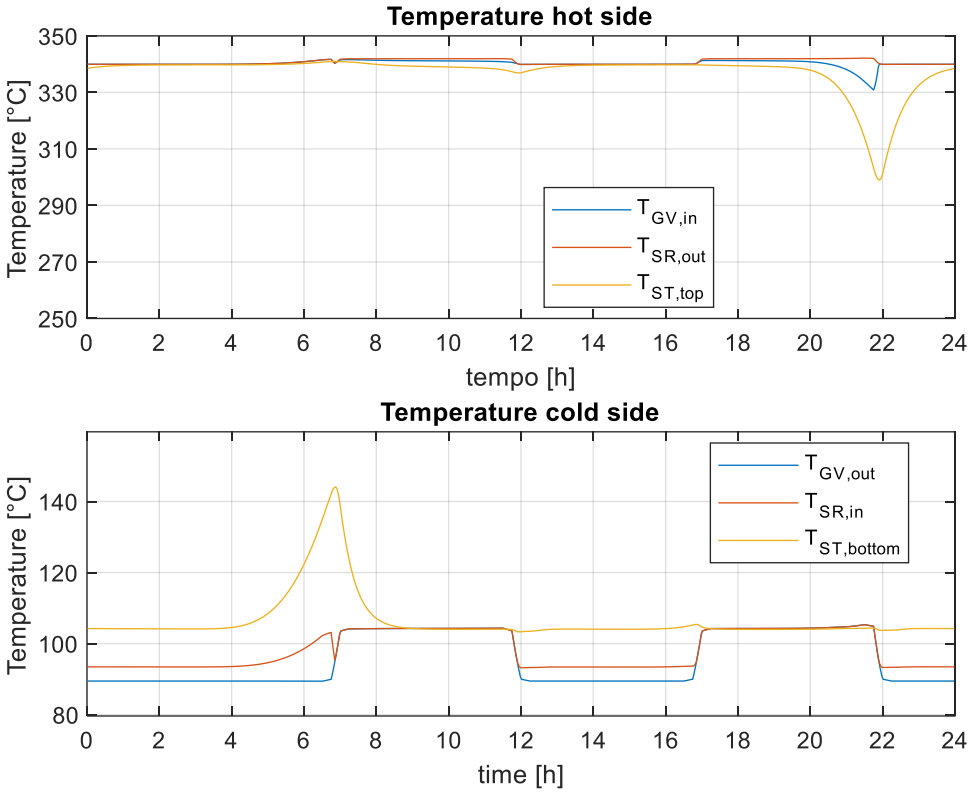

Figure 5.19: Temperature trends on the hot and cold side of the stratified tank

From the graph of the temperature trends, it can be seen that the period of charge from 12 p.m. to 5 p.m. does not influence in a significant way the temperature trends on the hot and cold sides of the tank, while at 7 a.m. and at 10 p.m. the transitions from charge to discharge or vice versa influence these temperatures. The explanation of this behaviour is given by the position of the thermocline. At 7 a.m., the TES is at the end of its charging phase and the thermocline is close to the bottom of the tank, increasing the temperature of the oil in this region. Then, from 7 a.m. to 12 p.m., the TES works in discharging mode and the thermocline raises its position inside the tank, but not enough to influence the oil temperature on the top of the tank. From 12 to 5 p.m. the TES works in charging phase and the thermocline lowers its position inside the tank, but also in this case not enough to influence the oil temperature on the bottom of the tank. From 5 to 10 p.m. the TES is in discharging mode, and this time the thermocline has enough time to approach the top of the tank, reducing the oil temperature on the hot side.

5.3 Load History 3

The load history is reported in Figure 5.20, with the gas turbine operating at 100% load from 7 a.m. to 10 p.m., while the ORC power output is kept constant.

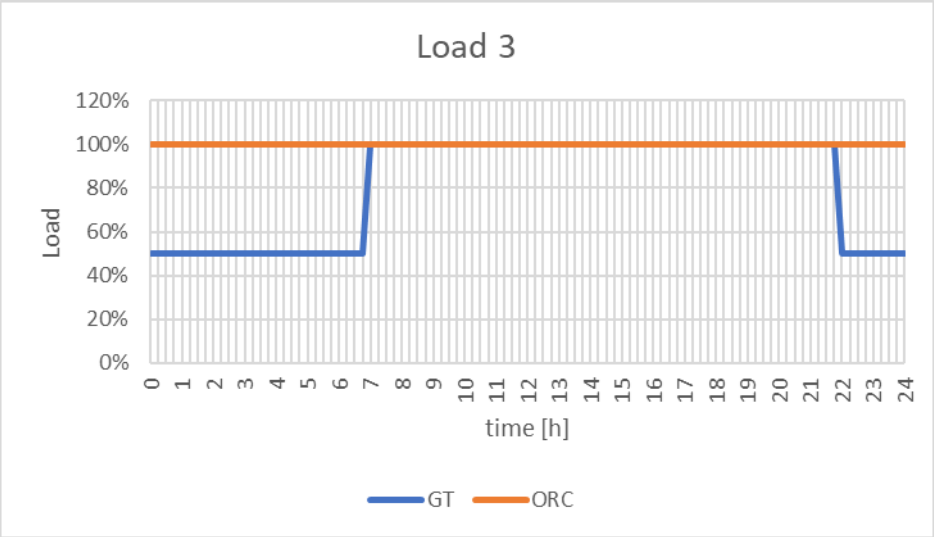

Figure 5.20: Load History 3

This time, the characteristic of the heat source of the ORC varies because the gas turbine works also in off-design conditions. As already said, for the design of the ORC the characteristics of the heat source are taken as the mean values during the day. For this reason, the input variable used in the new optimization design of the ORC are the those reported in Table 5.2, with the difference that now the mean value of the exhaust gases mass flow rate $\dot{m}_{gs}(t)$ during the day is $\dot{m}_{gs,avg} = 42.156\ kg/s$.

Limits imposed on optimisation variables are reported in Table 5.3.

Table 5.9 shows the main parameters and performances of the optimised cycle with TES.

Table 5.9: Main parameters and performances of the optimised cycle with TES

$T_{oil,out}\ [°C]$	113.85
$p_{ev}\ [bar]$	34.29
$T_3\ [°C]$	244.85
$T_{cond}\ [°C]$	42.85
$\Delta T_{pp,GV}\ [°C]$	25.36
$\Delta T_{pp,REC}\ [°C]$	28.70
$\Delta T_{pp,cond}\ [°C]$	18.85
E	0.68
$P_{th,ORC}\ [MW]$	16.42
$P_{el}\ [MW]$	3.48
η_{ORC}	0.21

T_{ev} [°C]	217.78
ΔT_{surr} [°C]	27.07
p_{cond} [bar]	0.82
m_{oil} [kg/s]	31.60
m_f [kg/s]	27.88
m_w [kg/s]	290.27
$\eta_{is,t}$	0.90

The size of the plant is 3.48 MW, lower with respect to the previous two cases because according to equation 4.14 a decrease in the integral during the day of the oil mass flow rate sent to the recovery heat exchanger due to the change in the gas turbine load leads to a decrease in the design mass flow rate $\dot{m}_{GV,Des}$, and thus to the nominal power of the ORC P_{el}.

The main results on the tank size and system simulation for both TES configurations are reported in Table 5.10.

Table 5.10: TES sizing and simulation of the system main results

	Load History 3	
	Two Tanks	**Stratified Tank**
	TES Sizing	
V_{HT} [m^3]	307.012	
V_{CT} [m^3]	251.510	
M [kg]	237808.131	309150.571
V_{tot} [m^3]	558.522	399.116
d_{HT} [m]	5.803	6.334
d_{CT} [m]	5.430	
$T_{HT,avg}$ [°C]	339.964	
$T_{CT,avg}$ [°C]	113.729	
$T_{HT,iniz}$ [°C]	339.928	
$T_{CT,iniz}$ [°C]	113.731	
$m_{HT,in}$ [kg]	176046.265	
$m_{CT,in}$ [kg]	61761.866	
	Recovery Heat Exchanger	
$m_{SR,Des}$ [kg/s]	35.549	
$T_{SR,in,Des}$ [°C]	113.740	
$T_{SR,out,Des}$ [°C]	340.262	
$T_{gs,out,Des}$ [°C]	128.729	
$\Delta T_{pp,SR}$ [°C]	14.989	
	Plant's Performances	
$P_{el,max}$ [MW]	3.469	3.469
C_{max}	0.998	0.998
$E_{th,gs}$ [MWh]	394.114	393.758
$E_{th,loss}$ [MWh]	0.766	0.477

$E_{th,ORC}$ $[MWh]$	393.351	393.167
$e_{el,ORC}$ $[MWh]$	83.265	83.225
eta_{TES}	0.998	0.999
eta_{ORC}	0.212	0.212
eta_{tot}	0.211	0.211

Being the plant size smaller than before, the size of the TES is smaller as well, with the two tank configuration that still occupies more volume but in which less thermal oil is stored with respect to the stratified configuration, and the produced energy is less, even though now the ORC works always at 100% of its load.

For the two tanks configuration, the power trends are reported in Figure 5.21, while the trends of the oil mass flow rates, the fill level of the tanks and the temperatures in the hot and the cold tanks are reported in Figure 5.22.

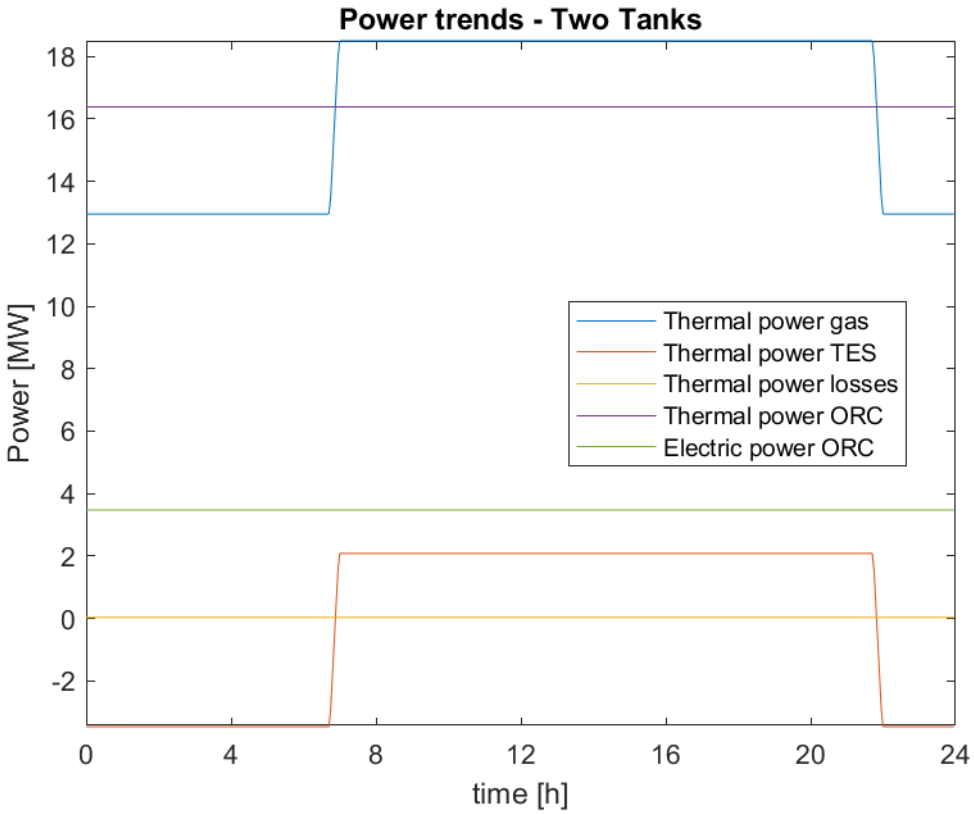

Figure 5.21: Power trends for the two-tanks configuration

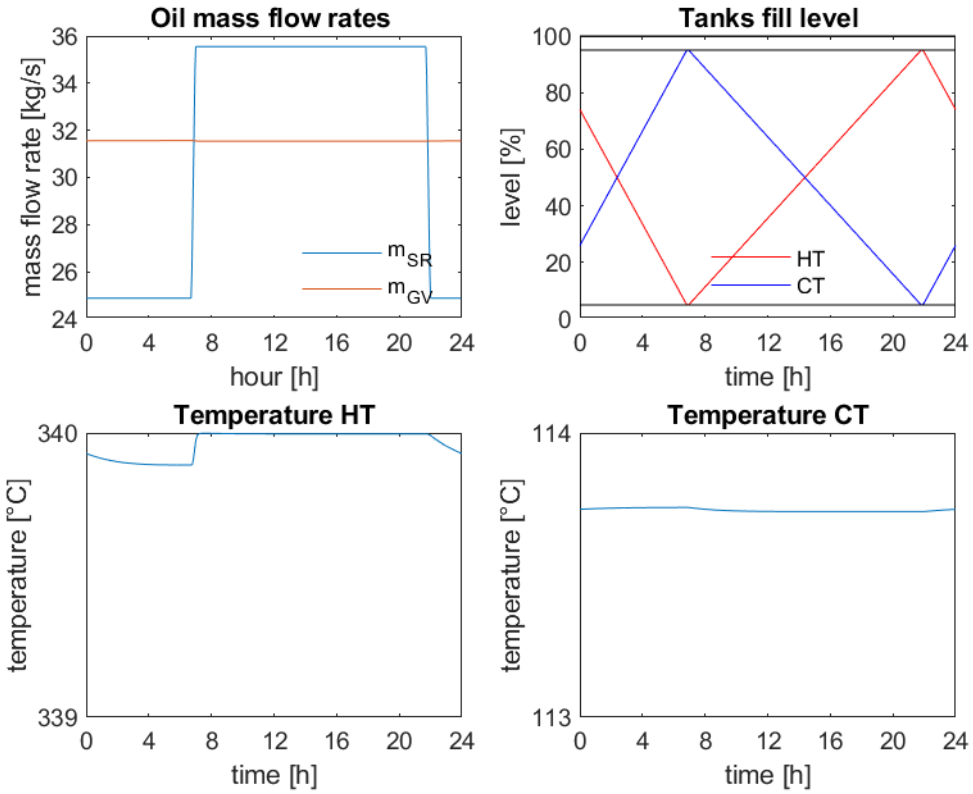

Figure 5.22: Trends of the oil mass flow rates, the fill level of the tanks and the temperatures in the hot and the cold tanks

The TES is in charging phase from 7 a.m. to 10 p.m. and in discharging phase the rest of the time. During the discharging phase, $\dot{m}_{GV} > \dot{m}_{SR}$, the fill level of the cold tank increases while the level of the hot tank decreases; the opposite during charging phase. The oil mass flow rate $\dot{m}_{SR}(t)$ follows the trend of the gas turbine's load, while $\dot{m}_{GV}(t)$ follows the trend of the ORC load. The oil temperatures inside the tanks are almost constant during the day.

For the stratified tank configuration, the power trends are reported in Figure 5.23, the trend of mass flow rates in Figure 5.24 and the temperature trends in the hot and cold side of the tank in Figure 5.25.

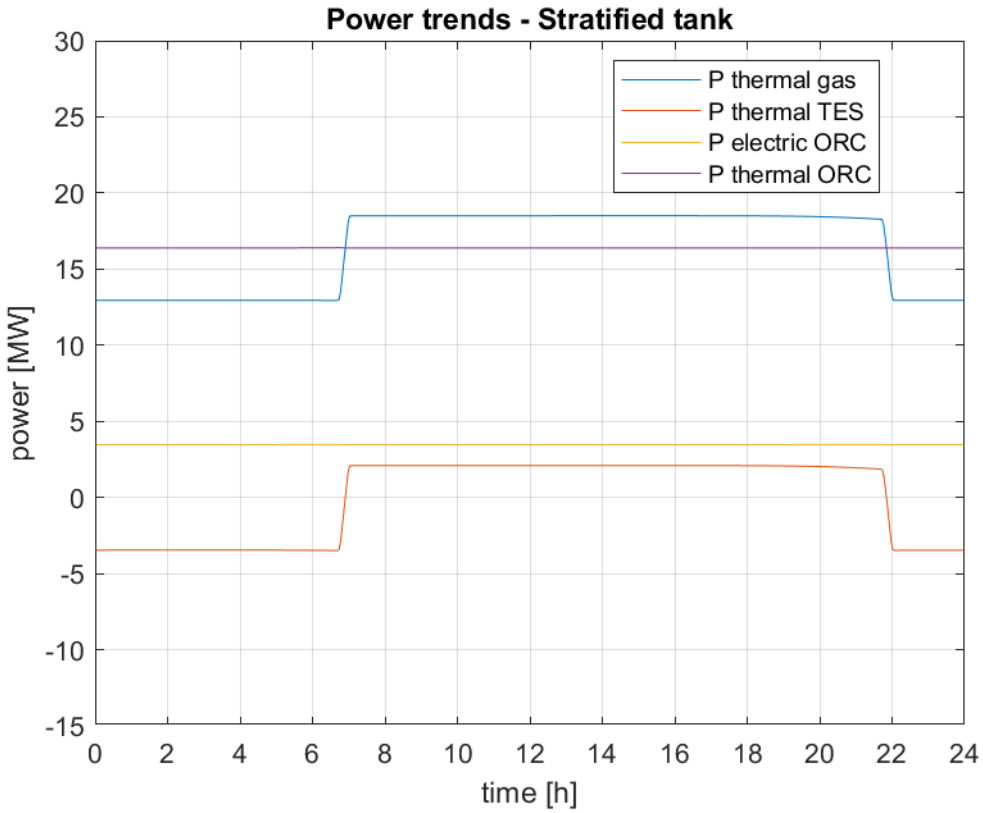

Figure 5.23: Power trends for the stratified tank configuration

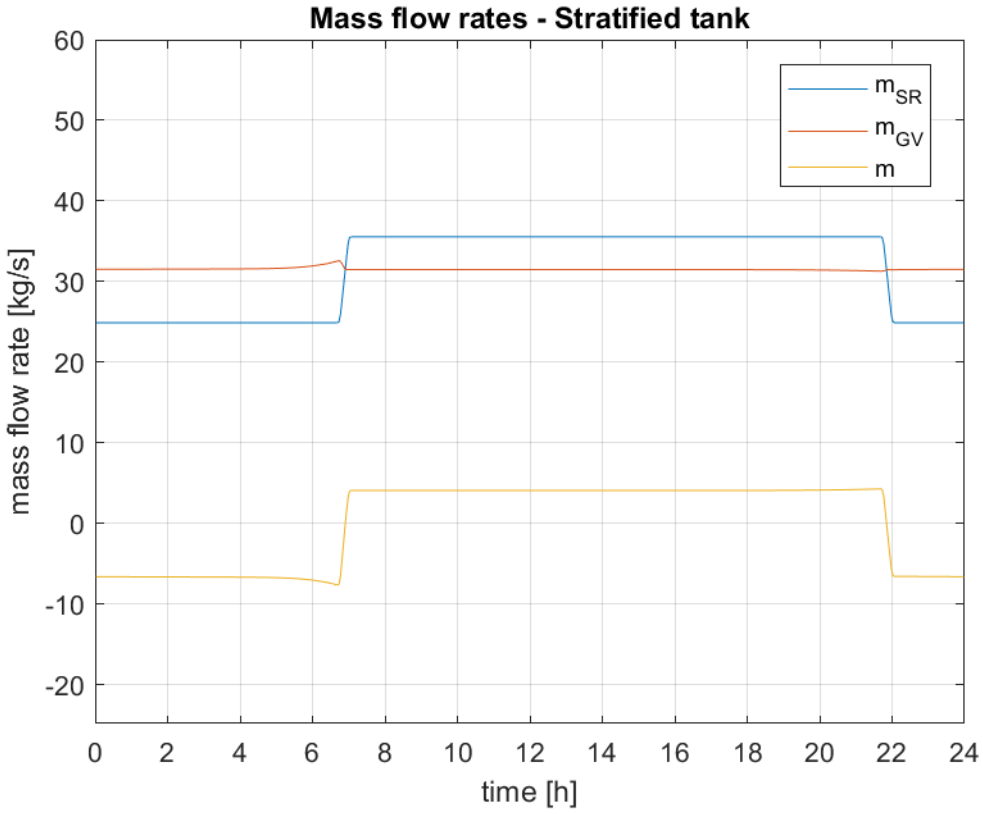

Figure 5.24: Mass flow rate trends for the stratified tank configuration

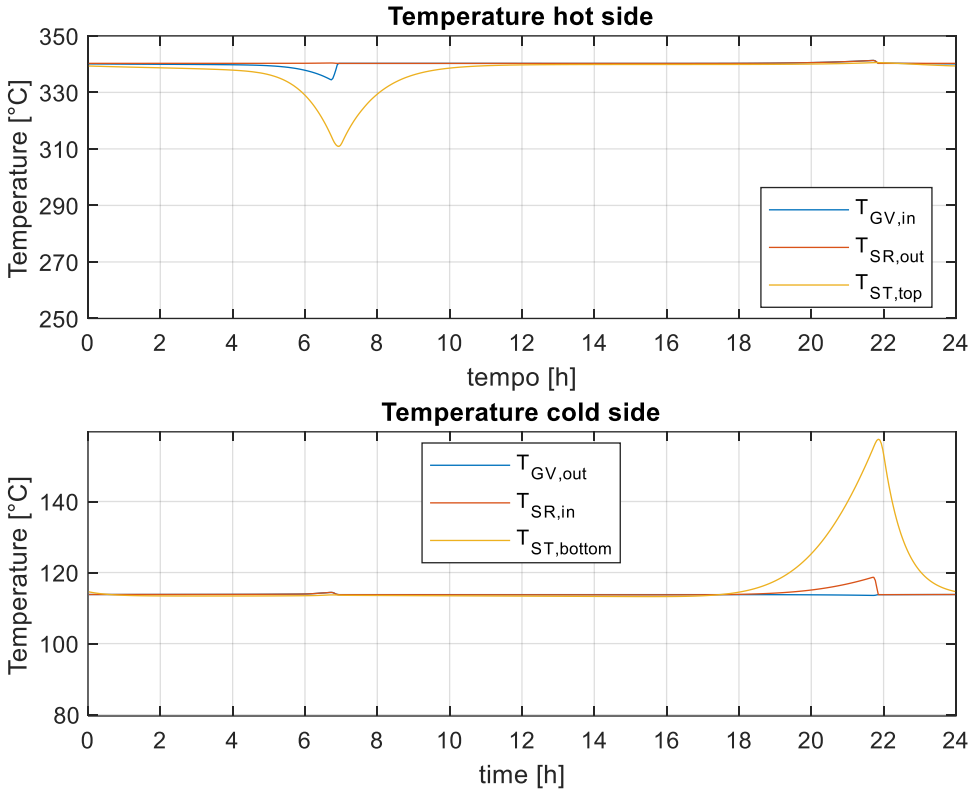

Figure 5.25: Temperature trends on the hot and cold side of the stratified tank

At the end of the discharge phase (7 a.m.), the oil temperature on the hot side of the stratified tank starts to decrease due to the proximity of the thermocline, and consequently also the temperature $T_{GV,in}$ of the mass flow rate $\dot{m}_{GV}$ at the inlet of the steam generator. Therefore, to maintain constant the output power of the ORC, the mass flow rate $\dot{m}_{GV}$ slightly increases while the output mass flow rate $\dot{m}$ of the stratified tank decreases.

At the end of the charging phase (10 p.m.), the thermocline is close to the bottom of the stratified tank, leading to an increase in the stratified tank oil output temperature and therefore of the temperature $T_{SR,in}$.

Variations in oil temperature in the hot and cold areas of the tank remain within the imposed limits and do not affect the performance of the cycle in a significant way.

All the quantities are equal at the beginning and at the end of the day, therefore the repeatability of the cycle is guaranteed for both the TES configurations.

5.4 Load History 4

The load history is reported in Figure 5.26, with the gas turbine operating at 100% load from 7 a.m. to 12 p.m. and from 5 p.m. to 10 p.m., while the ORC power output is kept constant.

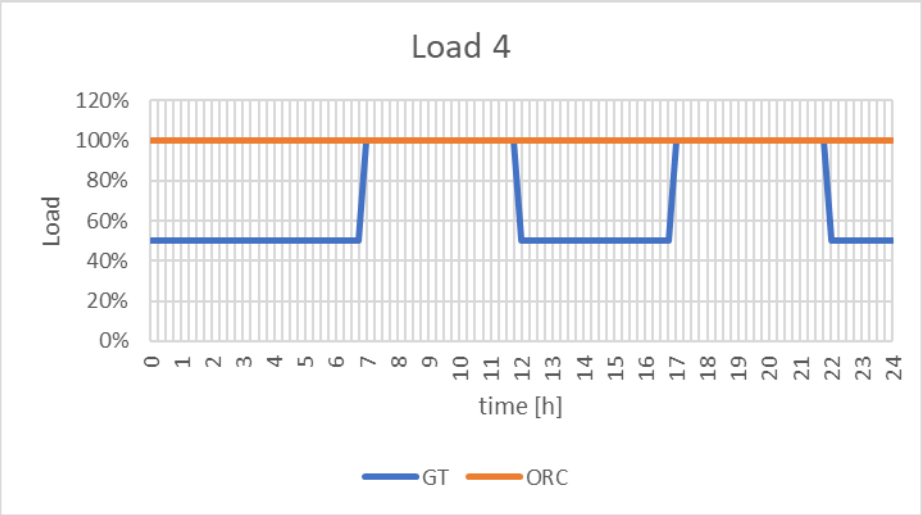

Figure 5.26: Load History 4

The input variable used for the optimization design of the ORC are reported in Table 5.2, with the difference that now the mean value of the exhaust gases mass flow rate $\dot{m}_{gs}(t)$ during the day is $\dot{m}_{gs,avg} = 39.187\ kg/s$.

Limits imposed on optimisation variables are reported in Table 5.3.

Table 5.11 shows the main parameters and performances of the optimised cycle with TES.

Table 5.11: Main parameters and performances of the optimised cycle with TES

$T_{oil,out}\ [°C]$	108.85
$p_{ev}\ [bar]$	32.80
$T_3\ [°C]$	252.85
$T_{cond}\ [°C]$	42.85
$\Delta T_{pp,GV}\ [°C]$	30.35
$\Delta T_{pp,REC}\ [°C]$	63.23
$\Delta T_{pp,cond}\ [°C]$	19.85
E	0.38
$P_{th,ORC}\ [MW]$	15.47
$P_{el}\ [MW]$	3.08
η_{ORC}	0.20
$T_{ev}\ [°C]$	214.57
$\Delta T_{surr}\ [°C]$	38.28
$p_{cond}\ [bar]$	0.82
$m_{oil}\ [kg/s]$	29.24

$m_f\ [kg/s]$	23.95
$m_w\ [kg/s]$	279.41
$\eta_{is,t}$	0.90

The size of the plant is further reduced with respect to the previous cases.

The main results on the tank sizing and system simulation for both TES configurations are reported in Table 5.12.

Table 5.12: TES sizing and simulation of the system main results

	Load History 4	
	Two Tanks	**Stratified Tank**
	TES Sizing	
$V_{HT}\ [m^3]$	202.598	
$V_{CT}\ [m^3]$	165.377	
$M\ [kg]$	156930.266	219702.373
$V_{tot}\ [m^3]$	367.975	283.638
$d_{HT}\ [m]$	5.052	5.652
$d_{CT}\ [m]$	4.722	
$T_{HT,avg}\ [°C]$	339.955	
$T_{CT,avg}\ [°C]$	108.743	
$T_{HT,iniz}\ [°C]$	339.931	
$T_{CT,iniz}\ [°C]$	108.746	
$m_{HT,in}\ [kg]$	116390.115	
$m_{CT,in}\ [kg]$	40540.151	
	Recovery Heat Exchanger	
$m_{SR,Des}\ [kg/s\ ]$	35.408	
$T_{SR,in,Des}\ [°C]$	108.757	
$T_{SR,out,Des}\ [°C]$	340.199	
$T_{gs,out,Des}\ [°C]$	123.745	
$\Delta T_{pp,SR}\ [°C]$	14.988	
	Plant's Performances	
$P_{el,max}\ [MW]$	3.073	3.073
C_{max}	0.998	0.998
$E_{th,gs}\ [MWh]$	371.340	371.091
$E_{th,loss}\ [MWh]$	0.574	0.375
$E_{th,ORC}\ [MWh]$	370.766	370.628
$e_{el,ORC}\ [MWh]$	73.754	73.723
eta_{TES}	0.998	0.999
eta_{ORC}	0.199	0.199
eta_{tot}	0.199	0.199

The size of the TES, as well as the produced energy, are reduced with respect to the previous cases.

For the two tanks configuration, the power trends are reported in Figure 5.27, while the trends of the oil mass flow rates, the fill level of the tanks and the temperatures in the hot and the cold tanks are reported in Figure 5.28.

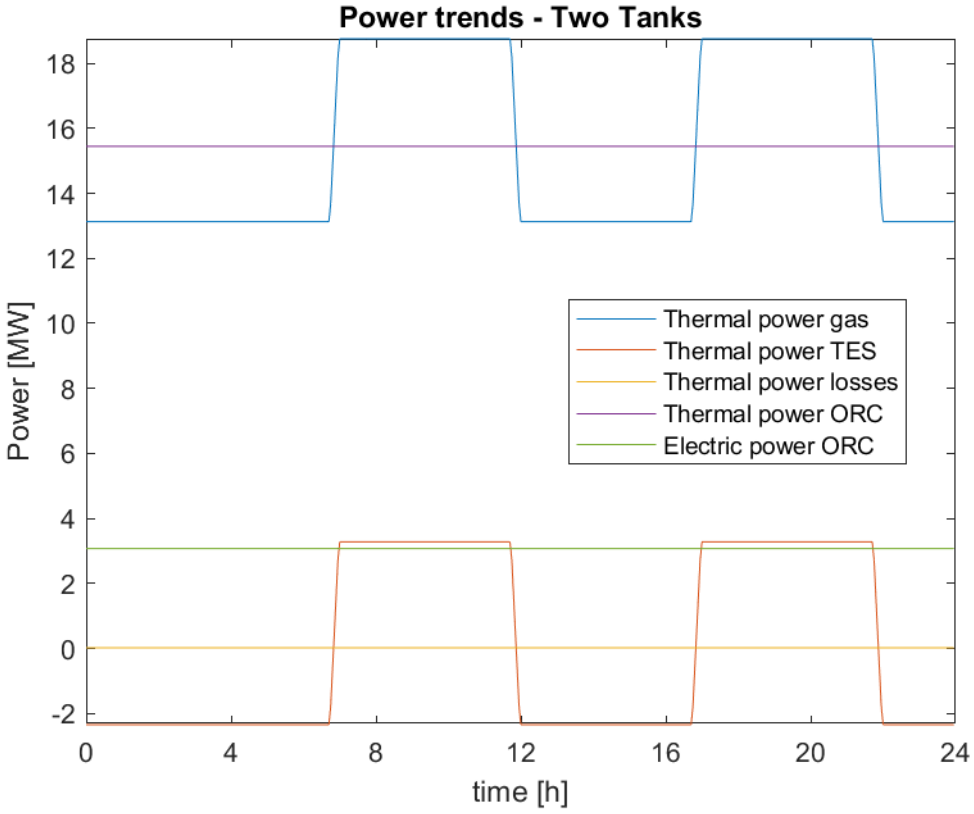

Figure 5.27: Power trends for the two-tanks configuration

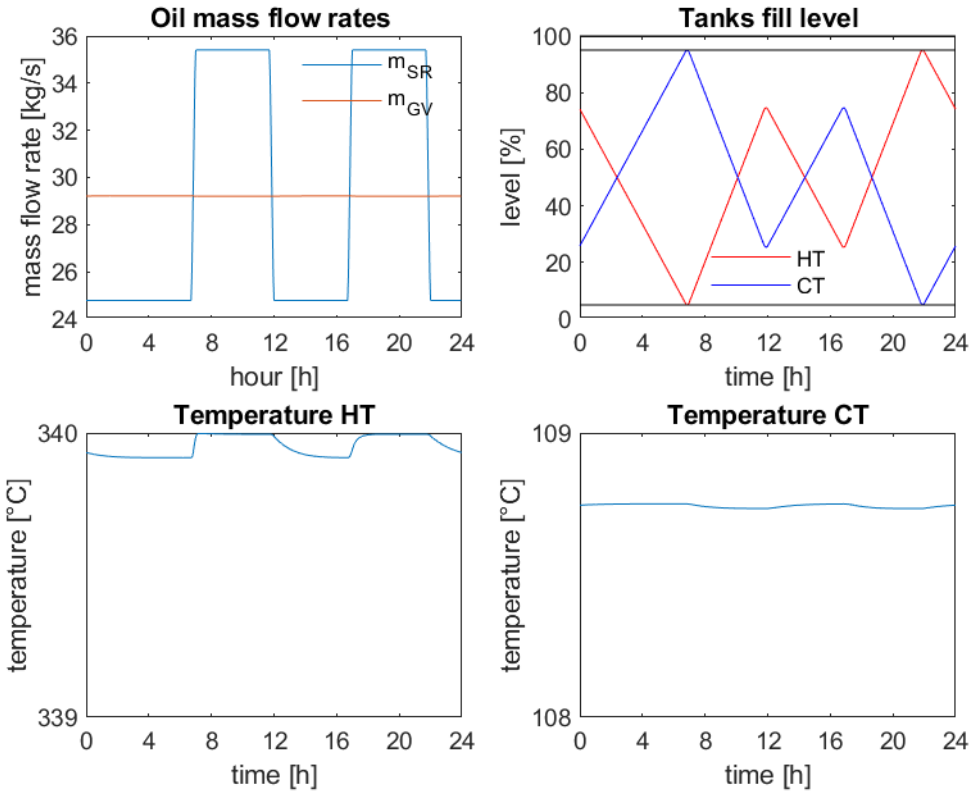

Figure 5.28: Trends of the oil mass flow rates, the fill level of the tanks and the temperatures in the hot and the cold tanks

In comparison to the previous case, the TES enters in discharge mode also from 12 to 5 p.m., due to the decrease in the load of the gas turbine in the corresponding period. As can be seen from the tank fill level graph, during this period of discharge, the hot tank empties and the cold tank fills up a bit, without being completely filled or emptied.

As in the previous load history, the oil mass flow rate $\dot{m}_{SR}(t)$ follows the trend of the gas turbine's load, while $\dot{m}_{GV}(t)$ follows the trend of the ORC load, and the oil temperatures inside the tanks are almost constant during the day.

For the stratified tank configuration, the power trends are reported in Figure 5.29, the trend of mass flow rates in Figure 5.30 and the temperature trends on the hot and cold side of the tank in Figure 5.31.

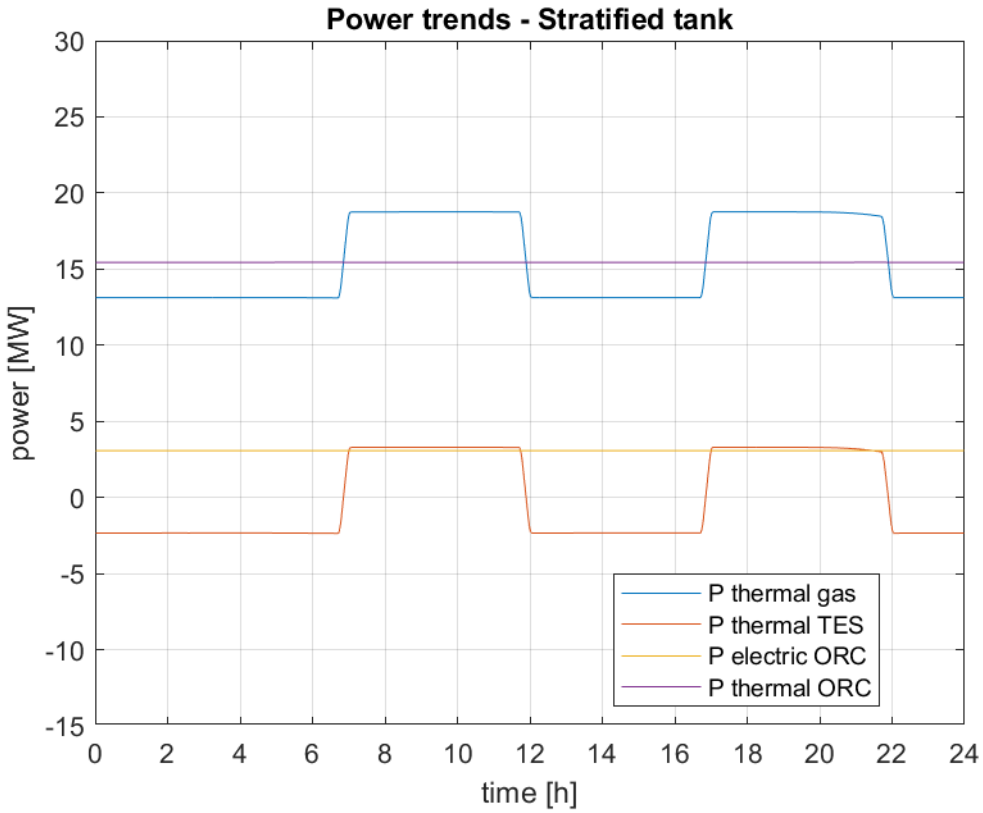

Figure 5.29: Power trends for the stratified tank configuration

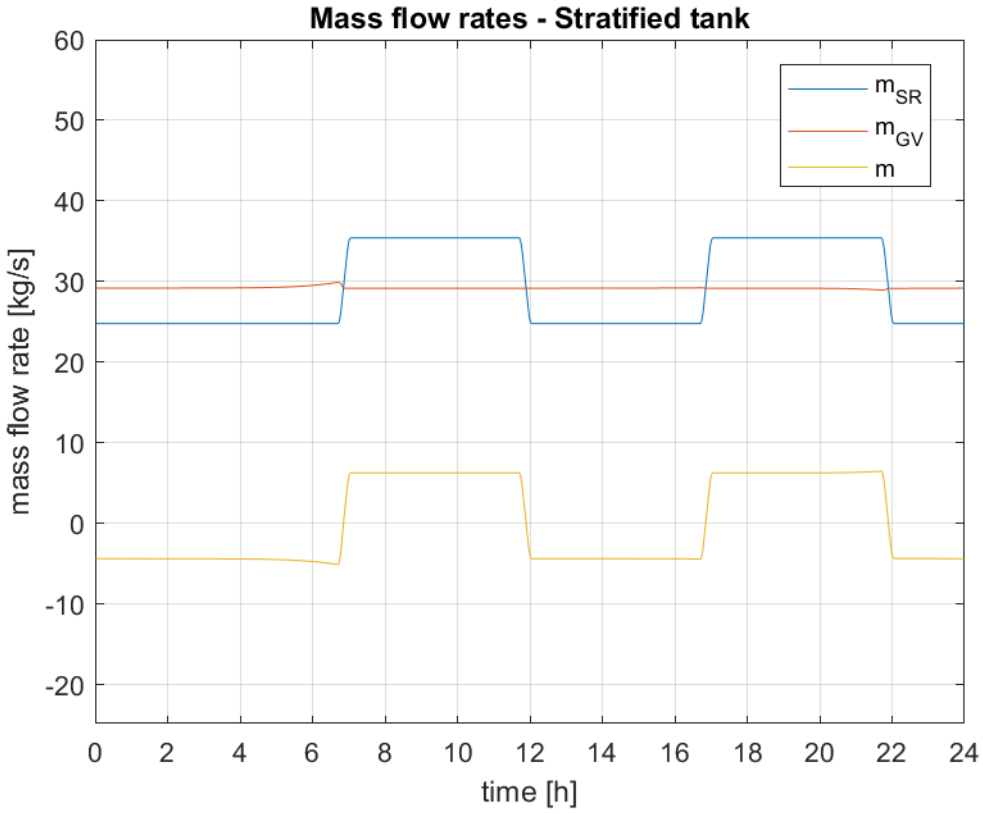

Figure 5.30: Mass flow rate trends for the stratified tank configuration

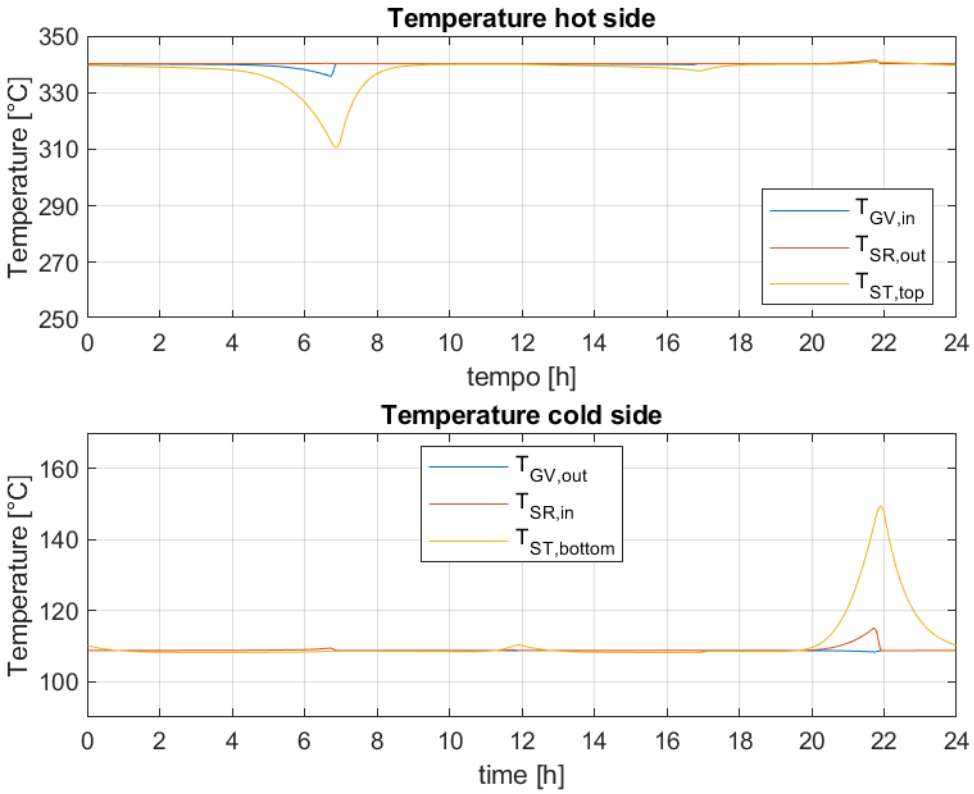

Figure 5.31: Temperature trends on the hot and cold side of the stratified tank

As explained for Load History 2, the period of discharge from 12 to 5 p.m. (charge for Load History 2) does not influence the temperature trends on the hot and cold sides of the tank, because the thermocline doesn't reach the edges of the tank in this period, while at 7 a.m. the thermocline is close to the top of the tank decreasing the local oil temperature and at 10 p.m. the thermocline is close to the bottom of the tank increasing the oil temperature in this area.

5.5 Load History 5

In the following load histories, both the gas turbine and the ORC load will vary.

Gas turbine and ORC loads are reported in Figure 5.32.

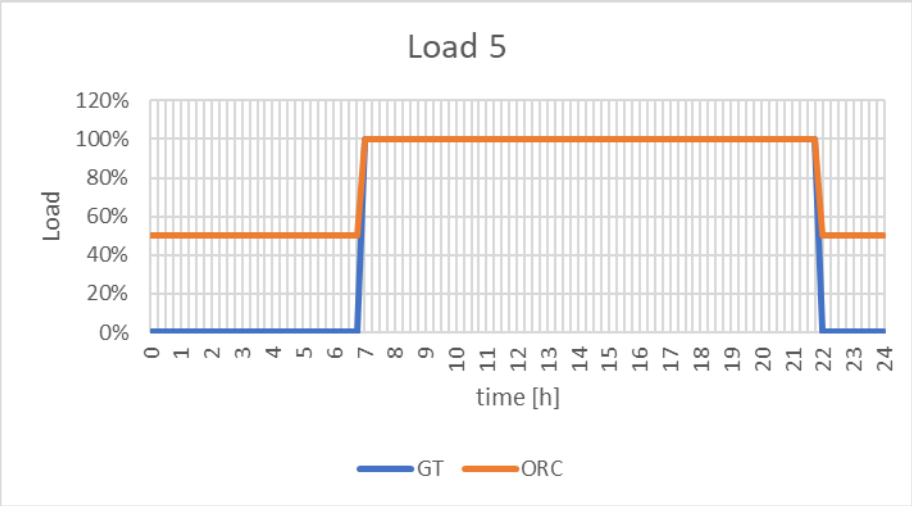

Figure 5.32: Load History 5

The gas turbine works 100% of its load from 7 a.m. to 10 p.m. and is turned off the rest of the time. When the gas turbine is off, the ORC works at 50%, else at 100% of the load.

The input variable used for the optimization design of the ORC are reported in Table 5.2, with the difference that now the mean value of the exhaust gases mass flow rate $\dot{m}_{gs}(t)$ during the day is $\dot{m}_{gs,avg} = 29.687\ kg/s$.

The limits imposed on the optimisation variables are reported in Table 5.3.

Table 5.13 shows the main parameters and performances of the optimised cycle with TES.

Table 5.13: Main parameters and performances of the optimised cycle with TES

$T_{oil,out}\ [°C]$	105.85
$p_{ev}\ [bar]$	33.11
$T_3\ [°C]$	245.85
$T_{cond}\ [°C]$	42.85
$\Delta T_{pp,GV}\ [°C]$	29.62
$\Delta T_{pp,REC}\ [°C]$	51.87
$\Delta T_{pp,cond}\ [°C]$	19.65
E	0.44
$P_{th,ORC}\ [MW]$	14.38
$P_{el}\ [MW]$	2.88
η_{ORC}	0.20
$T_{ev}\ [°C]$	215.24
$\Delta T_{surr}\ [°C]$	30.61

p_{cond} [bar]	0.82
m_{oil} [kg/s]	26.90
m_f [kg/s]	23.05
m_w [kg/s]	259.01
$\eta_{is,t}$	0.89

The size of the ORC is further reduced to the previous cases, with a nominal power of 2.88 MW. The main results on the tank sizing and the system simulation for both TES configurations are reported in Table 5.14.

Table 5.14: TES sizing and simulation of the system main results

	Load History 5	
	Two Tanks	**Stratified Tank**
	TES Sizing	
V_{HT} [m^3]	646.228	
V_{CT} [m^3]	525.898	
M [kg]	500082.749	750124.124
V_{tot} [m^3]	1172.126	968.417
d_{HT} [m]	7.437	8.511
d_{CT} [m]	6.944	
$T_{HT,avg}$ [°C]	340.044	
$T_{CT,avg}$ [°C]	98.979	
$T_{HT,iniz}$ [°C]	340.567	
$T_{CT,iniz}$ [°C]	93.933	
$m_{HT,in}$ [kg]	370550.873	
$m_{CT,in}$ [kg]	129531.876	
	Recovery Heat Exchanger	
$m_{SR,Des}$ [kg/s]	35.135	
$T_{SR,in,Des}$ [°C]	100.462	
$T_{SR,out,Des}$ [°C]	340.435	
$T_{gs,out,Des}$ [°C]	115.435	
$\Delta T_{pp,SR}$ [°C]	14.973	
	Plant's Performances	
$P_{el,max}$ [MW]	2.865	2.861
C_{max}	0.994	0.992
$E_{th,gs}$ [MWh]	286.392	285.882
$E_{th,loss}$ [MWh]	1.216	0.825
$E_{th,ORC}$ [MWh]	285.176	284.850
$e_{el,ORC}$ [MWh]	55.946	55.876
eta_{TES}	0.996	0.996
eta_{ORC}	0.196	0.196
eta_{tot}	0.195	0.195

Although the ORC is smaller in size than the previous load histories, the stored mass flow rates and total storage volumes are greater for this case. The reason is because, being the gas turbine off for a part of the day, the available thermal energy of the exhaust gases is less, therefore a greater amount of mass needs to be stored to guarantee the continuous operation of the ORC also while the gas turbine is off.

For the two tanks configuration, the power trends are reported in Figure 5.33, while the trends of the oil mass flow rates, the fill level of the tanks and the temperatures in the hot and the cold tanks are reported in Figure 5.34.

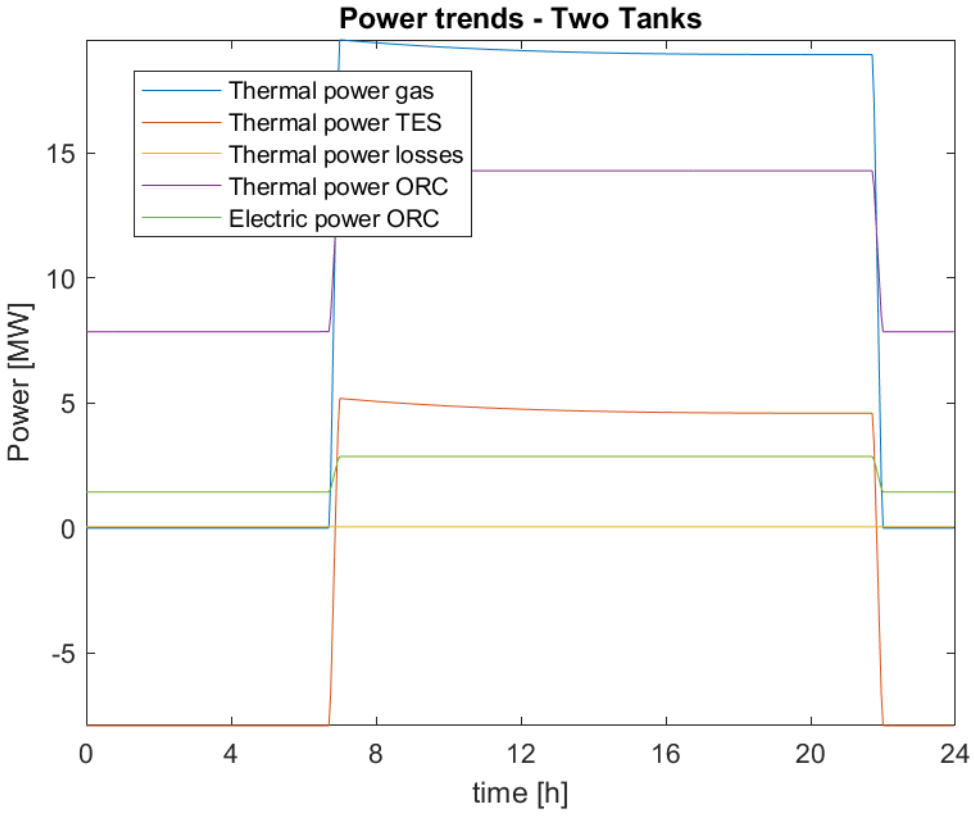

Figure 5.33: Power trends for the two-tanks configuration

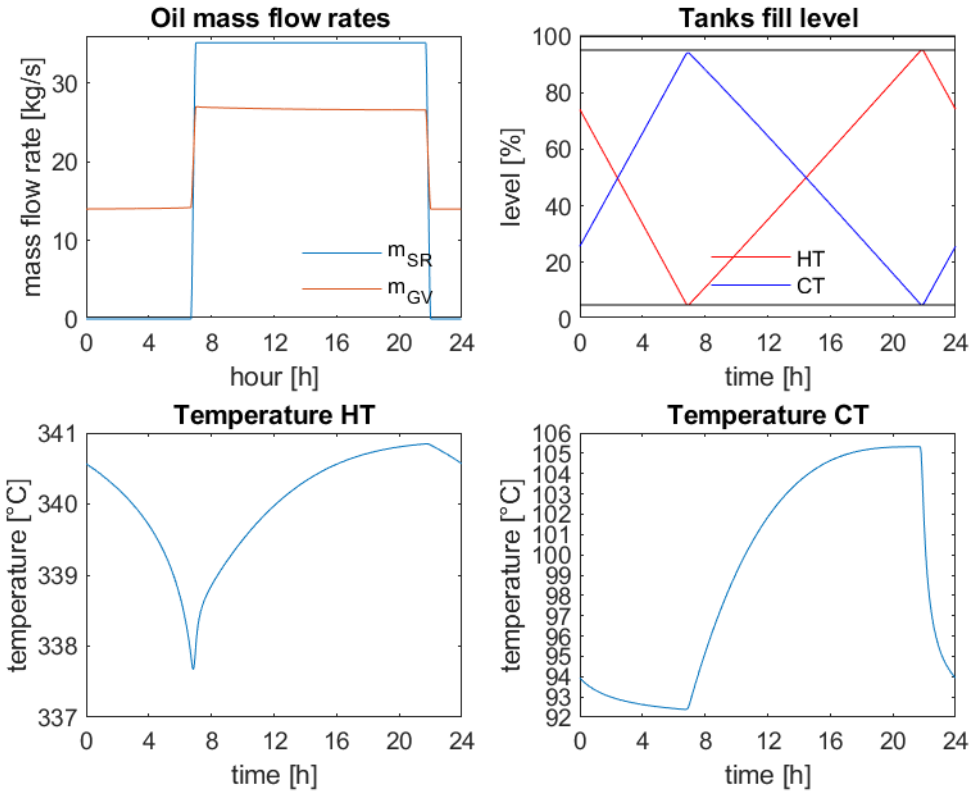

Figure 5.34: Trends of the oil mass flow rates, the fill level of the tanks and the temperatures in the hot and the cold tanks

The TES is in charging phase from 7 a.m. to 10 p.m., else is in discharging phase.

When the gas turbine is off, $\dot{m}_{SR}$ is zero and the recovery heat exchanger doesn't work.

During the discharging phase, the temperatures of the oil inside the hot and the cold tanks decrease because, being the gas turbine off and so the recovery heat exchanger, the heat source of the ORC is only the thermal energy of the oil stored inside the tanks, which gives its energy to the ORC and lowers its temperature with the depth in discharge level. During the charging phase, the gas turbine is on, and the recovery heat exchanger is working, recovering the thermal energy of the exhaust gases, and thus increasing the temperature inside the tanks. These temperature variations are in a range that does not affect the operation of the ORC and are therefore considered acceptable.

For the stratified tank configuration, the power trends are reported in Figure 5.35, the trend of the mass flow rates in Figure 5.36 and the trends of the temperature in the hot and cold side of the tank in Figure 5.37.

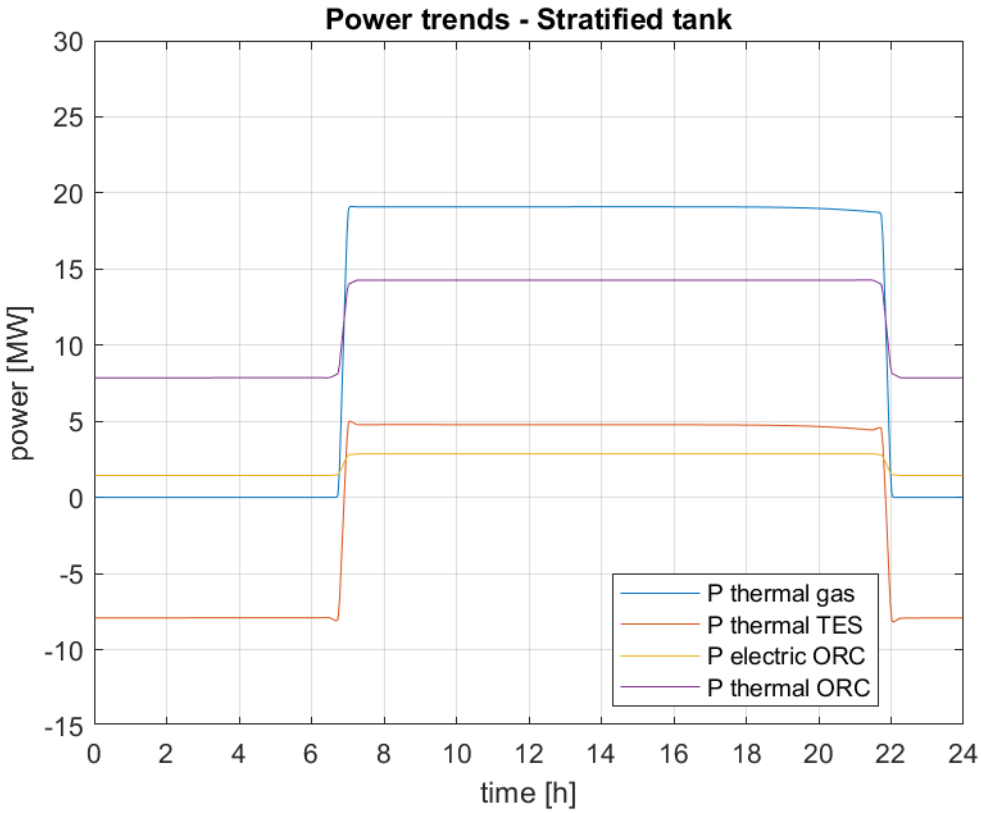

Figure 5.35: Power trends for the stratified tank configuration

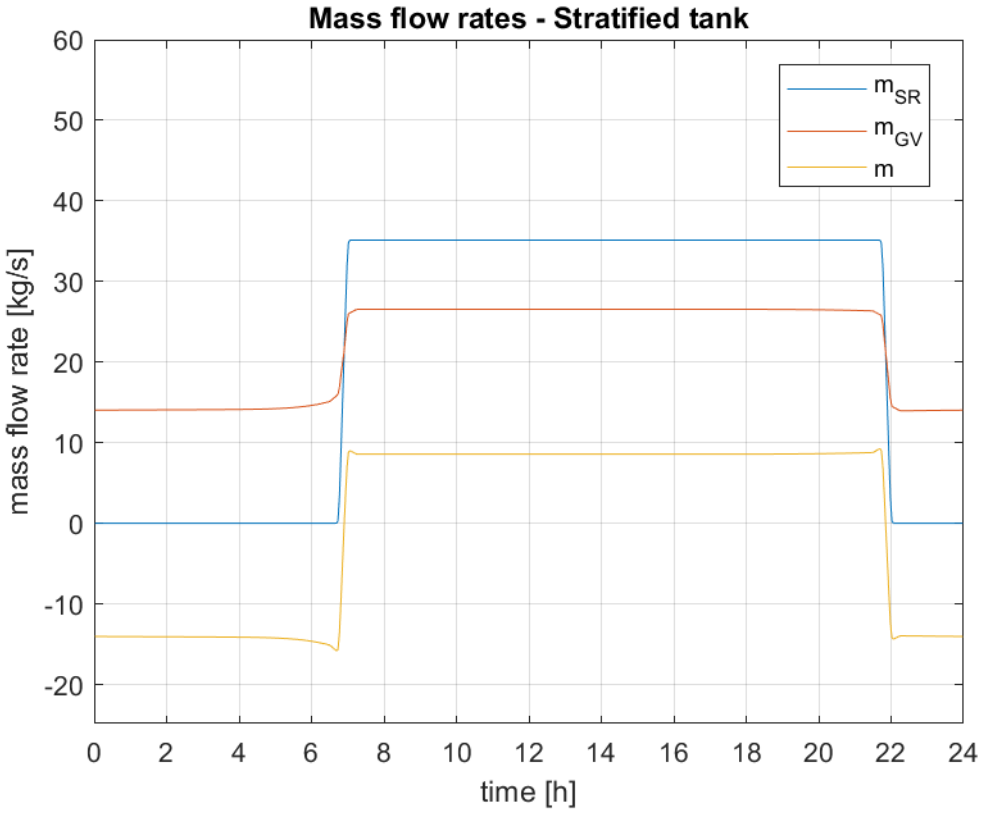

Figure 5.36: Mass flow rate trends for the stratified tank configuration

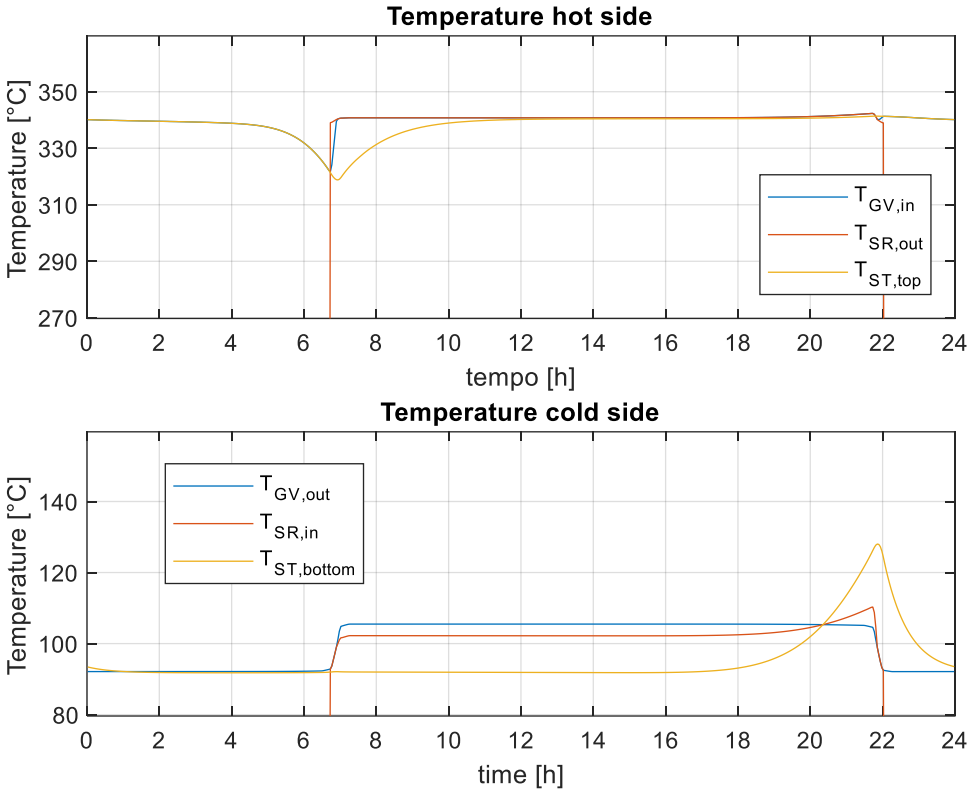

Figure 5.37: Temperature trends on the hot and cold side of the stratified tank

As for the two tanks' configuration, when the gas turbine is off, the mass flow rate $\dot{m}_{SR}$ is zero and the recovery heat exchanger doesn't work. The oil temperatures at the inlet and outlet of the recovery heat exchanger $T_{SR,in}$ and $T_{SR,out}$ are not considered because meaningless during this period, because there is no oil that enters or exits the recovery heat exchanger. Therefore, during discharge phase $|\dot{m}| = \dot{m}_{GV}$ (in absolute value because the mass flow rate $\dot{m}$ is considered positive when enters from the top and exits from the bottom of the stratified tank), so $T_{GV,in} = T_{ST,top}$ and $T_{GV,out} = T_{ST,bottom}$.

5.6 Load History 6

Gas turbine and ORC loads are reported in Figure 5.38.

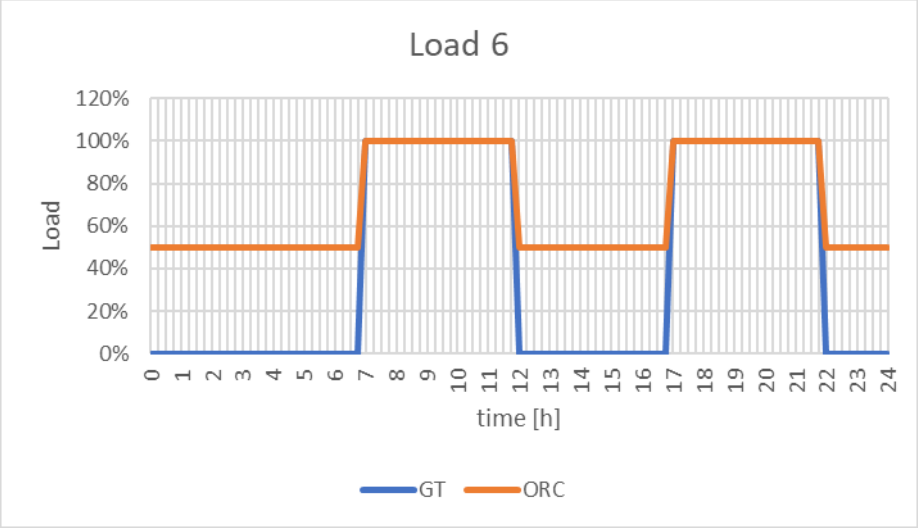

Figure 5.38: Load History 6

The gas turbine works at 100% of its load from 7 a.m. to 12 p.m. and from 5 p.m. to 10 p.m., and is turned off the rest of the time.

When the gas turbine is off, the ORC works at 50%, else at 100% of the load.

The input variable used for the optimization design of the ORC are reported in Table 5.2, with the difference that the mean value of the exhaust gases mass flow rate $\dot{m}_{gs}(t)$ during the day that is $\dot{m}_{gs,avg} = 19.791\ kg/s$.

The limits imposed on the optimisation variables are reported in Table 5.3.

Table 5.15 shows the main parameters and performances of the optimised cycle with TES.

Table 5.15: Main parameters and performances of the optimised cycle with TES

$T_{oil,out}\ [°C]$	108.85
$p_{ev}\ [bar]$	34.77
$T_3\ [°C]$	253.85
$T_{cond}\ [°C]$	42.85
$\Delta T_{pp,GV}\ [°C]$	31.59
$\Delta T_{pp,REC}\ [°C]$	63.91
$\Delta T_{pp,cond}\ [°C]$	19.85
E	0.36
$P_{th,ORC}\ [MW]$	10.80
$P_{el}\ [MW]$	2.14
η_{ORC}	0.20
$T_{ev}\ [°C]$	218.79

ΔT_{surr} [°C]	35.06
p_{cond} [bar]	0.82
m_{oil} [kg/s]	20.42
m_f [kg/s]	16.69
m_w [kg/s]	195.23
$\eta_{is,t}$	0.89

The main results on the tank sizing and the system simulation for both TES configurations are reported in Table 5.16.

Table 5.16: TES sizing and simulation of the system main results

	Load History 6	
	Two Tanks	**Stratified Tank**
	TES Sizing	
V_{HT} [m^3]	482.961	
V_{CT} [m^3]	393.831	
M [kg]	373686.577	635267.181
V_{tot} [m^3]	876.792	820.136
d_{HT} [m]	6.749	8.052
d_{CT} [m]	6.306	
$T_{HT,avg}$ [°C]	339.973	
$T_{CT,avg}$ [°C]	98.338	
$T_{HT,iniz}$ [°C]	340.673	
$T_{CT,iniz}$ [°C]	94.420	
$m_{HT,in}$ [kg]	277427.424	
$m_{CT,in}$ [kg]	96259.153	
	Recovery Heat Exchanger	
$m_{SR,Des}$ [kg/s]	35.110	
$T_{SR,in,Des}$ [°C]	99.084	
$T_{SR,out,Des}$ [°C]	340.359	
$T_{gs,out,Des}$ [°C]	114.097	
$\Delta T_{pp,SR}$ [°C]	15.013	
	Plant's Performances	
$P_{el,max}$ [MW]	2.134	2.128
C_{max}	0.996	0.993
$E_{th,gs}$ [MWh]	191.268	190.927
$E_{th,loss}$ [MWh]	1.000	0.733
$E_{th,ORC}$ [MWh]	190.268	190.043
$e_{el,ORC}$ [MWh]	36.336	36.287
eta_{TES}	0.995	0.995
eta_{ORC}	0.191	0.191
eta_{tot}	0.190	0.190

With respect to Load History 5, the total storage volume and the stored mass have decreased for both the TES configurations. Although the discharge time is increased for this load history, the discharge phase from 12 p.m. to 5 p.m. does not influence the dimensions of the storage, because it happens without bringing the tanks to the limit of capacity for the two tanks configuration, and without bringing the thermocline to the edges of the tank for the stratified tank configuration. Therefore, being the ORC smaller, also the TES is smaller in size.

For the two tanks configuration, the power trends are reported in Figure 5.39, while the trends of the oil mass flow rates, the fill level of the tanks and the temperatures in the hot and the cold tanks are reported in Figure 5.40.

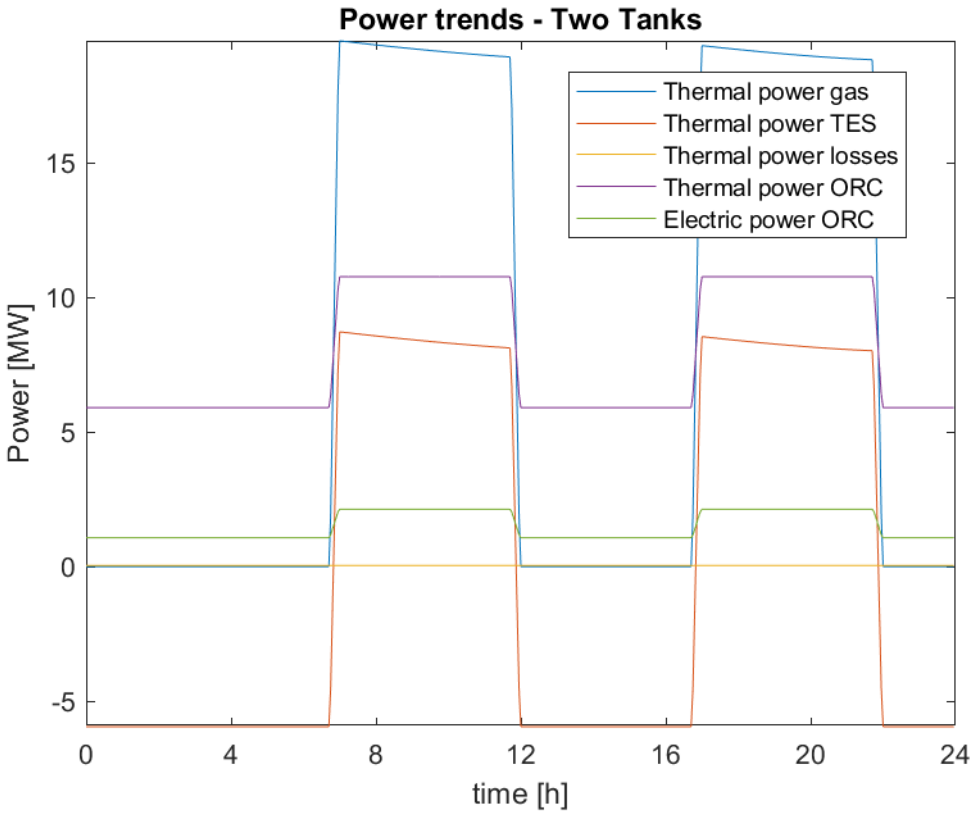

Figure 5.39: Power trends for the two-tanks configuration

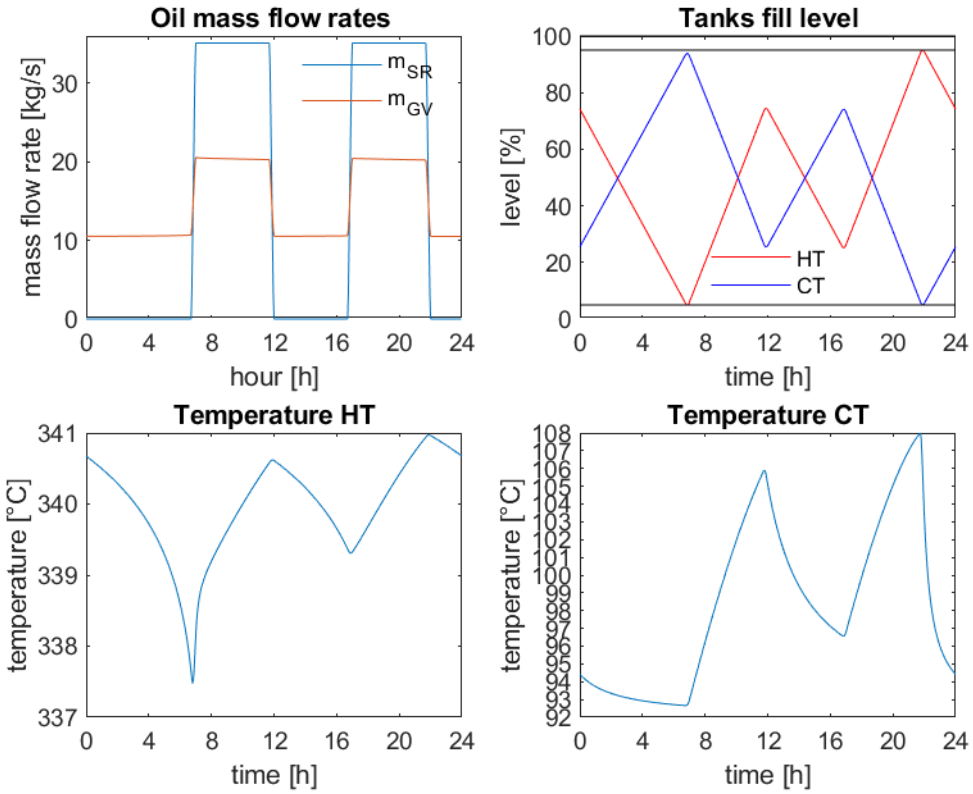

Figure 5.40: Trends of the oil mass flow rates, the fill level of the tanks and the temperatures in the hot and the cold tanks

The TES is in charging phase from 7 a.m. to 12 p.m. and from 5 p.m. to 10 p.m., else is in discharging phase.

As for Load History 5, the temperatures of the oil inside the tanks decrease during discharge and increase during charge.

For the stratified tank configuration, the power trends are reported in Figure 5.41, the trend of the mass flow rates in Figure 5.42 and the temperature trends in the hot and cold side of the tank in Figure 5.43.

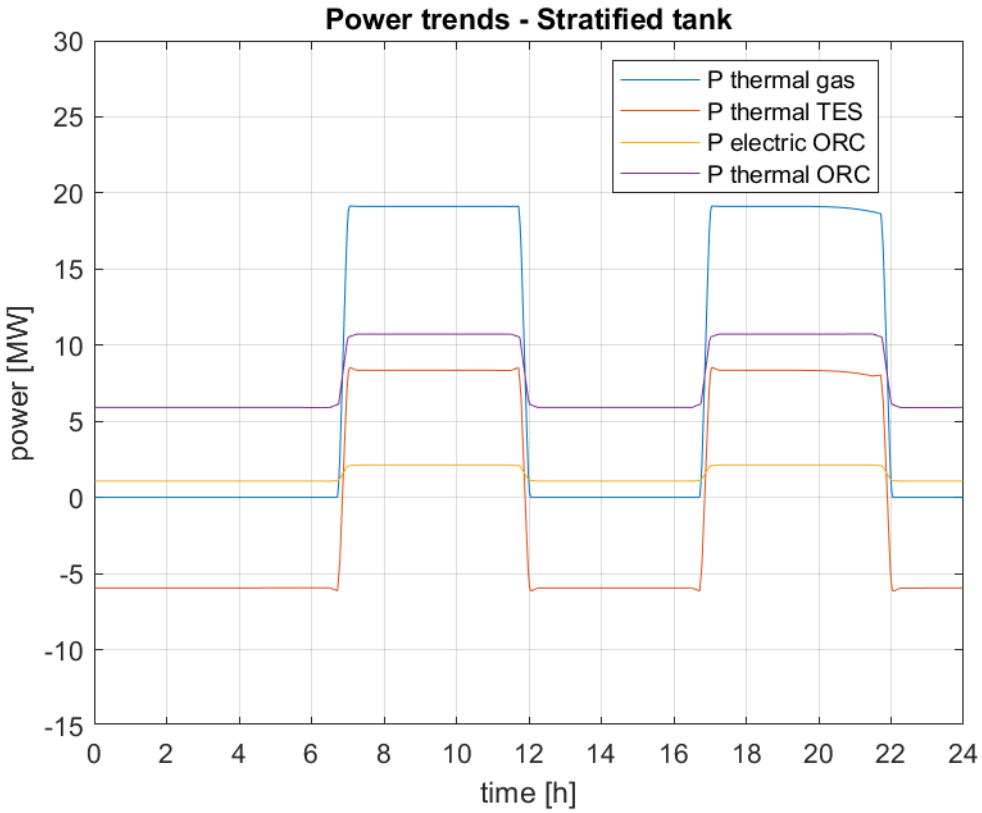

Figure 5.41: Power trends for the stratified tank configuration

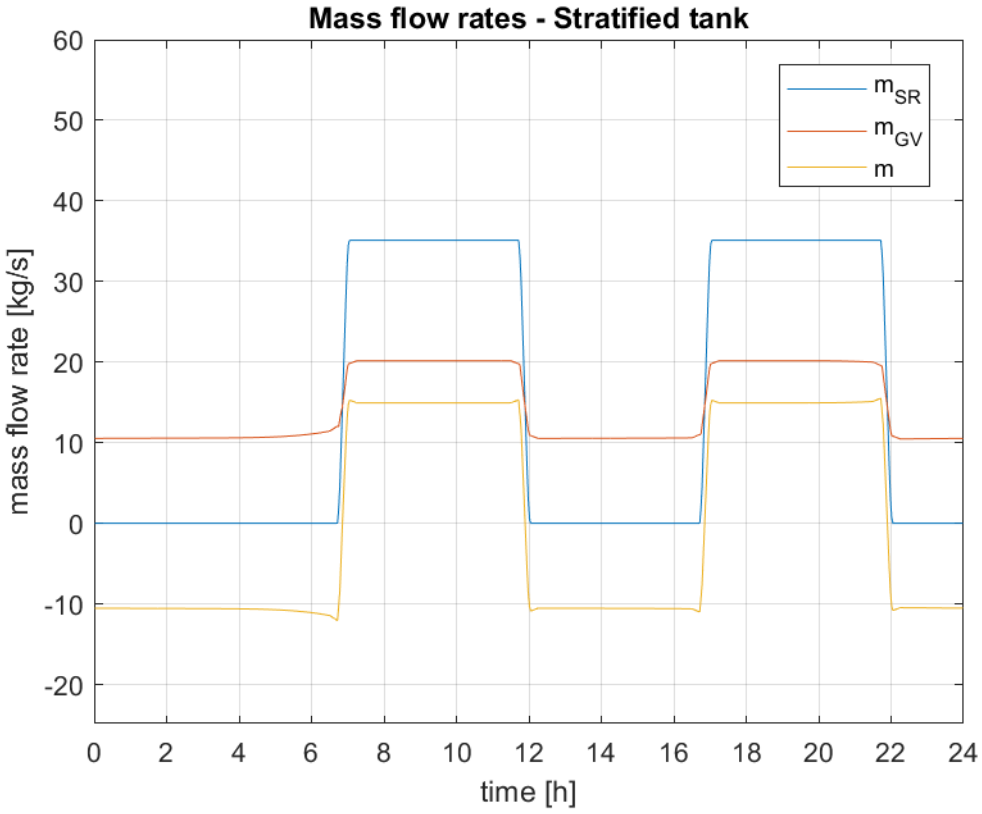

Figure 5.42: Mass flow rate trends for the stratified tank configuration

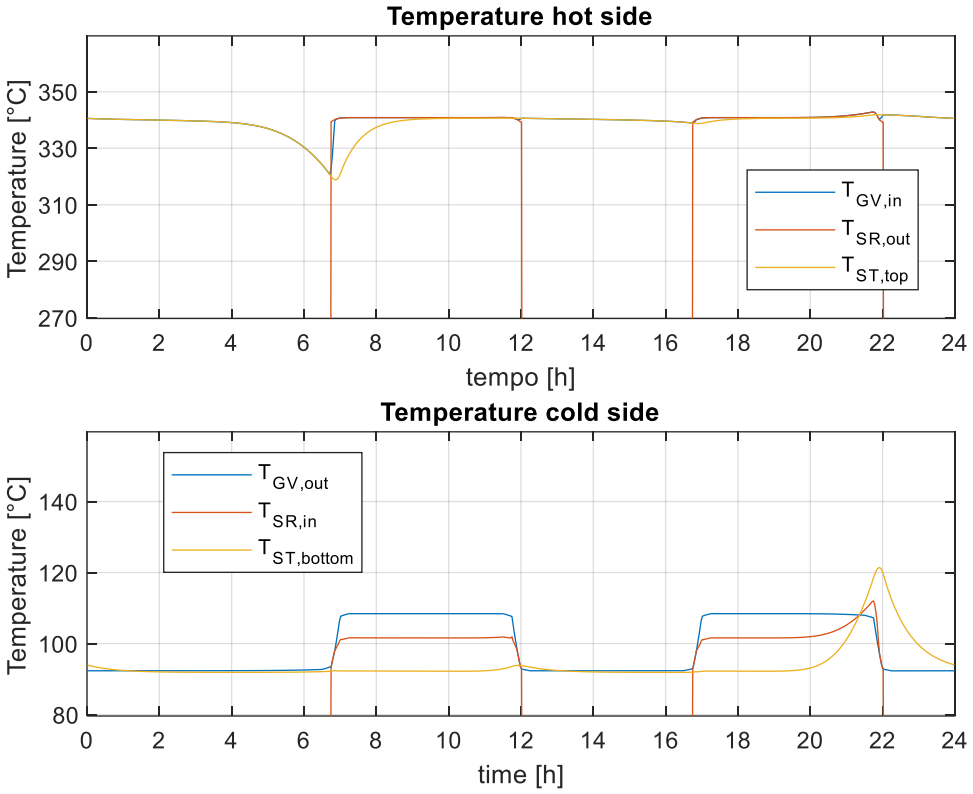

Figure 5.43: Temperature trends on the hot and cold side of the stratified tank

As for the previous load history, when the gas turbine is off, the mass flow rate $\dot{m}_{SR}$ is zero and the recovery heat exchanger doesn't work, therefore the oil temperatures at the inlet and outlet of the recovery heat exchanger $T_{SR,in}$ and $T_{SR,out}$ are not considered because meaningless during this period, because there is no oil that enters or exits the recovery heat exchanger.

6 Economic Analysis

A preliminary economic analysis is performed with the aim of evaluating which of the considered configurations can be more profitable.

For the estimation of the ORC costs, two different methods have been considered and compared.

The first method is based on (23).

In a nutshell, the purchase cost equation for the electric generator and for heat exchangers with an area ranging from 80 m^2 to 4000 m^2 is given by eq. 6.1

$$C_p^0 = C_B \left(\frac{N}{Q_B}\right)^M \qquad 6.1$$

where C_p^0 is the purchased equipment cost, C_B is the base cost of the equipment, M is a constant peculiar to each device, N is the capacity of the size parameter of the equipment, while Q_B is a coefficient.

For the pump, the electric motor of the pump and the heat exchangers with an area less than 80 m^2 eq. 6.2 is used:

$$\log_{10} C_P^0 = K_1 + K_2 \log_{10} N + K_3 (\log_{10} N)^2 \qquad 6.2$$

where N is the capacity or the size parameter of the equipment, and K_1, K_2 and K_3 are correction factors which depend on each piece of equipment.

The bare module cost general equation for different devices can be written as eq. 6.3

$$\mathrm{C_{BM}} = C_P^0 \, F_{BM} \qquad 6.3$$

where F_{BM} is the bare module correction factor.

For the heat exchangers in an area ranging from 80 m^2 to 4000 m^2 F_{BM} is given by eq. 6.4

$$\mathrm{F_{BM}} = F_M \, F_P \, F_T \qquad 6.4$$

where F_M is the material correction factor, F_P is the pressure correction factor, and F_T is the temperature correction factor.

For the remaining devices, F_{BM} is computed as eq. 6.5

$$\mathrm{F_{BM}} = (B_1 + B_2 \, F_M \, F_P) \qquad 6.5$$

where the pressure correction factor F_P can be computed as eq. 6.6

$$F_P = 10^{C_1 + C_2 \log_{10} p + C_3 (\log_{10} p)^2} \qquad 6.6$$

C_1, C_2, and C_3 are correction factors peculiar to each device. For the electrical motor of the pump and the electric generator F_{BM} is directly given.

The purchase cost equation of the multistage expander is given by eq. 6.7

$$C_{Exp} = C_0 \left(\frac{n}{n_0}\right)^{0.5} \left(\frac{SP_{LS}}{SP_0}\right)^{1.1} \quad 6.7$$

where n is the number of stages, SP_{LS} is the last stage size parameter, $C_0 = 1230\ k€$, $n_0 = 2$, and $SP_0 = 0.18\ m$.

To calculate the "new purchase cost" for the different devices, the chemical engineering plant cost index (CEPCI) is used. The new bare module cost of each equipment is given by eq. 6.8

$$C_{BM_{new}} = C_{BM_{ref}} \frac{CEPCI_{new}}{CEPCI_{ref}} \quad 6.8$$

where $CEPCI_{new} = 801.4$ (January 2023) and $CEPCI_{ref} = 394.3$ (2001).

The total cost of the cycle, C_{BM_T}, is given by the sum of the bare module cost of each component C_{BM_i}, eq. 6.9

$$C_{BM_T} = \sum_{1}^{n} C_{BM_i} \quad 6.9$$

The total cost of the plant, C_{ORC}, is then determined by multiplying the total cycle cost by 1.4, eq. 6.10

$$C_{ORC} = 1.4\ C_{BM_T} \quad 6.10$$

For the computation of the area of the heat exchangers, eq. 6.11 is used:

$$A = \frac{Q}{U\ \Delta T_{ml}} \quad 6.11$$

where Q is the exchanged heat, U is the overall heat transfer coefficient and ΔT_{ml} is the mean logarithmic temperature. The overall heat transfer coefficient of each heat exchanger has been chosen according to Table 6.1

Table 6.1: Overall heat transfer coefficients used for the estimation of the heat exchangers area

U_{cond}	300 $Wm^{-2}K^{-1}$
U_{eco}	400 $Wm^{-2}K^{-1}$
U_{evap}	700 $Wm^{-2}K^{-1}$
U_{surr}	300 $Wm^{-2}K^{-1}$
U_{rec}	300 $Wm^{-2}K^{-1}$
U_{SR}	300 $Wm^{-2}K^{-1}$

The coefficient used for performing the economic analysis of each device are listed in Table 6.2 and Table 6.3

Table 6.2: Coefficients used for the economic analysis

Component	**N**	**K_1** **K_2** **K_3**	**C_1** **C_2** **C_3**	**B_1** **B_2**	**F_M**	**F_{BM}**
Heat exchangers	A [m^2]	4.3247 -0.3030 0.1634	0.03881 -0.11272 0.08183	1.63 1.66	1	-
Pump	P[kW]	3.3892 0.0536 0.1538	-0.3935 0.3957 -0.00226	1.89 1.35	1.575	-
Pump electrical motor	P[kW]	2.4604 1.4191 -0.1798	-	-	-	1.5

Table 6.3: Coefficients used for the economic analysis

Component	**N**	**C_B**	**Q_B**	**M**	**F_M**	**F_p**	**F_T**	**F_{BM}**
Heat exchangers	A [m^2]	32800	80	0.68	1	1.5	1.6	-
Electric generator	P[kW]	1850000	11800	0.94	-	-	-	1.5

The second method used for the cost estimation of the ORC plant is based on equations 6.2, 6.3, 6.5, 6.6, 6.8, 6.9, with the use of new coefficients listed in Table 6.4 (24). The cost of the pump electric motor is included in the cost of the pump. For the electric generator, eq. 6.12 (25) has been used:

$$C_{gen} = 2 \cdot 10^5 \cdot \left(\frac{W_{gen}}{500}\right)^{0.67} \qquad 6.12$$

In this case, the 40% increase in the total cycle cost (eq. 6.10) is not considered.

Table 6.4: Coefficients used for the cost estimation of the ORC

Component	**N**	**K_1** **K_2** **K_3**	**C_1** **C_2** **C_3**	**B_1** **B_2**	**F_M**	**F_{BM}**
Heat exchangers	A [m^2]	4.3247 -0.3030 0.1634	0.03881 -0.11272 0.08183	1.63 1.66	1.35	-
Turbine	P[kW]	2.7051 1.4398 -0.1776	-	-	-	6.2
Pump	P[kW]	3.8696 0.3161 0.1220	-0.245382 0.259016 -0.01363	1.89 1.35	2.35	-

A comparison between the two methods is done in Table 6.5, considering the ORC of Load History 1.

Table 6.5: Comparison between the two methods used for the cost estimation of the ORC plant

Load History 1	**Method 1**	**Method 2**
Condenser	1,530,171.90 €	1,160,626.43 €
Evaporator	1,041,589.34 €	1,348,672.95 €
Recuperator	175,389.03 €	341,733.72 €
Recovery Heat Exchanger	972,136.69 €	696,808.90 €
Turbine	2,912,425.59 €	5,058,122.30 €
Pump	480,105.10 €	2,638,820.78 €
Generator	2,321,776.37 €	1,795,383.18 €
ORC total	13,207,031.62 €	13,040,168.26 €

As can be seen, the distribution of costs among the different components is very different for the two methods. In particular, the second method presents a considerable overestimation on the price of the turbine and the pump. Especially for the pump, the price assumes values way far from the current market values.

These differences lead to the thought that the methods for estimating prices are not entirely reliable.

However, the cost of the overall cycle is similar for the two methods, which therefore arrive at the same result even though the price distribution is different.

Knowing that in the industrial world the distribution of costs is a prerogative of the company, which takes into account various criteria that cannot be considered through equation because may vary from case to case, the most important data resulting from the cost estimation is the overall cost of the cycle, that is similar for the two methods and close to an acceptable market value.

For the following considerations, the cost of the ORC resulting from the first method will be used.

The cost of the TES has been estimated considering a price of the diathermic oil Therminol 66 of 5 €/l, and the cost of the storage tanks using eq. 6.13 (26)

$$C_{tank} = 167.19 \cdot 1.1756 \cdot V_{tank} \qquad 6.13$$

where V_{tank} is the volume of the tank.

The total cost of the TES is given by the sum of the cost of the diathermic oil and of the storage tanks, eq. 6.14

$$C_{TES} = C_{oil} + C_{tank} \qquad 6.14$$

For the estimation of the gas turbine cost, a price of 900 €/kW is considered, therefore the total cost is given by eq. 6.15

$$C_{gt} = 900 \cdot P_{tg} \qquad 6.15$$

where P_{tg} is the nominal power of the gas turbine in kW.

The total cost of the site is given by the sum of the costs of the gas turbine, the TES, and the ORC, eq. 6.16

$$C_{site} = C_{gt} + C_{TES} + C_{ORC} \qquad 6.16$$

The results for the six different load histories considered, both for the two tanks and for the stratified tank configuration, are shown in Table 6.6, Table 6.7, and Table 6.8.

Table 6.6: Cost of the overall system and its main components for Load History 1 and Load History 2

	Load History 1		Load History 2	
	TT	**ST**	**TT**	**ST**
ORC	13,207,031.62 €		14,415,878.84 €	
TES	2,463,447.92 €	2,843,564.33 €	1,808,136.10 €	2,261,073.04 €
Gas Turbine	10,125,000.00 €		10,125,000.00 €	
Plant tot	25,795,479.54 €	26,175,595.94 €	26,349,014.94 €	26,801,951.88 €

Table 6.7: Cost of the overall system and its main components for Load History 3 and Load History 4

	Load History 3		Load History 4	
	TT	**ST**	**TT**	**ST**
ORC	11,422,493.19 €		10,357,393.75 €	
TES	1,292,804.74 €	1,616,382.17 €	853,008.54 €	1,148,705.62 €
Gas Turbine	10,125,000.00 €		10,125,000.00 €	
Plant tot	22,840,297.94 €	23,163,875.37 €	21,335,402.28 €	21,631,099.37 €

Table 6.8: Cost of the overall system and its main components for Load History 5 and Load History 6

	Load History 5		Load History 6	
	TT	**ST**	**TT**	**ST**
ORC	10,064,252.36 €		8,387,811.39 €	
TES	2,718,149.51 €	3,921,995.87 €	2,031,316.93 €	3,321,470.65 €
Gas Turbine	10,125,000.00 €		10,125,000.00 €	
Plant tot	22,907,401.87 €	24,111,248.23 €	20,544,128.31 €	21,834,282.03 €

The gas turbine is the same for all the considered cases, therefore its price does not contribute to the difference in prices between the different configurations.

As expected, an increase in ORC and TES size leads to an increase in the corresponding costs.

Being the cost of the oil more relevant with respect to the cost of the tanks, the stratified tank configuration presents a greater cost with respect to the two tanks configuration for all the considered load histories, because despite it is composed of only one tank instead of two, it stores more diathermic oil.

The annual benefits deriving from the electricity sale, the cash flow CF, can be estimated as eq. 6.17

$$CF = (1 - t_{corp})(S_{annual} - C_{O\&M} - C_{fuel}) \quad 6.17$$

t_{corp} is the corporate tax rate, equal to 24% in Italy, S_{annual} is the annual income from the sale of electricity, $C_{O\&M}$ are the annual operation and maintenance costs estimated through eq. 6.18, and C_{fuel} is the annual cost of the fuel.

$$C_{O\&M} = 0.02 * C_{site} \quad 6.18$$

It has been considered that the plant works for 8000 h/year, to take into account any shutdowns due to maintenance.

The prices of electricity and natural gas are taken from (27).

For this economic analysis, the hourly electricity price has been taken as the average value in year 2022; the trend is shown in Figure 6.1

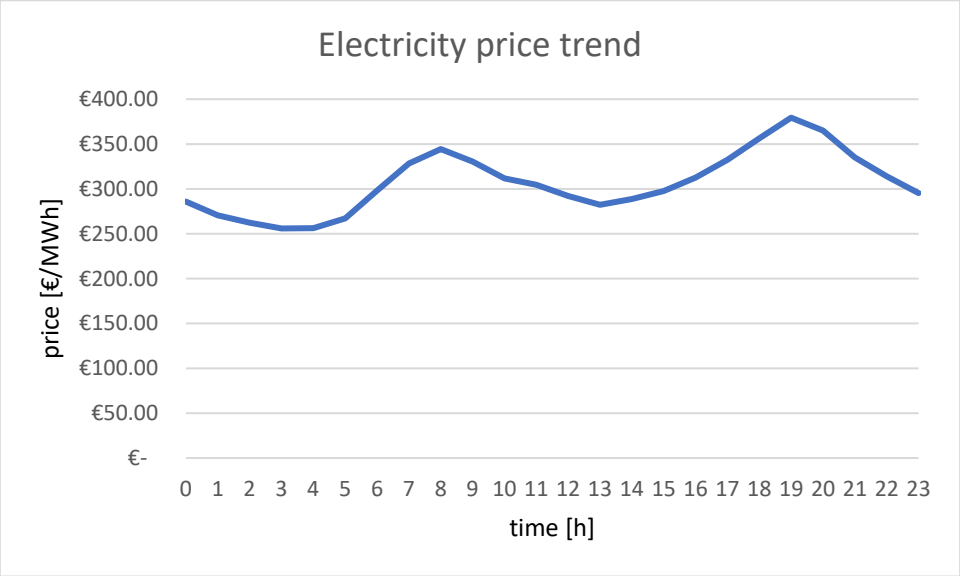

Figure 6.1: Daily trend of electricity prices, taken as average value in 2022

The price of natural gas is also considered as the average price in 2022, 116.94 €/MWh.

The Net Present Value, NPV, is computed as eq. 6.19

$$NPV = CF \cdot RF - C_{site} \quad 6.19$$

where the capital recovery factor RF is given by eq. 6.20

$$RF = \sum_{1}^{n} \frac{1}{(1+i)^n} \quad 6.20$$

i is the annual interest rate, considered equal to 3%, and n is the expected life of the plant, 25 years.

The profitability index is calculated by eq. 6.21

$$IP = \frac{NPV + C_{site}}{C_{site}} \qquad 6.21$$

The Levelized Cost of Energy, defined as the cost associated with each unit of produced electrical energy, is calculated as eq. 6.22

$$LCOE = \frac{C_{site} + C_{O\&M} \cdot RF}{E_{annual} \cdot RF} \qquad 6.22$$

where E_{annual} is the annual production of electricity.

Finally, the simple payback, which is the ratio between the total costs and the annual benefits, can be expressed by eq. 6.23

$$SPB = \frac{C_{site}}{CF} \qquad 6.23$$

The results of the economic analysis are shown in Table 6.9, Table 6.10, and Table 6.11.

Table 6.9: Results of the economic analysis for Load History 1 and Load History 2

	Load History 1		**Load History 2**	
	TT	**ST**	**TT**	**ST**
Annual income [€/year]	36,963,229.97 €	36,947,197.05 €	36,754,848.44 €	36,735,701.04 €
Annual fuel cost [€/year]	33,517,834.39 €	33,517,834.39 €	33,517,834.39 €	33,517,834.39 €
Cash Flow [€/year]	2,226,409.35 €	2,208,446.56 €	2,059,625.65 €	2,038,188.98 €
Net Present Value	12,973,315.24 €	12,280,410.13 €	9,515,550.62 €	8,689,333.83 €
Profitability Index	1.50	1.47	1.36	1.32
LCOE [€/MWh]	16.67	16.92	17.15	17.45
Simple Payback [years]	11.59	11.85	12.79	13.15

Table 6.10: Results of the economic analysis for Load History 3 and Load History 4

	Load History 3		**Load History 4**	
	TT	**ST**	**TT**	**ST**
Annual income [€/year]	31,447,135.41 €	31,446,851.32 €	27,711,440.99 €	27,712,115.07 €
Annual fuel cost [€/year]	28,804,388.93 €	28,804,388.93 €	26,185,808.12 €	26,185,808.12 €
Cash Flow [€/year]	1,661,314.79 €	1,656,180.51 €	835,182.87 €	831,200.57 €
Net Present Value	6,088,421.94 €	5,675,440.39 €	- 6,792,239.68 €	- 7,157,281.11 €
Profitability Index	1.27	1.25	0.68	0.67
LCOE [€/MWh]	17.53	17.78	18.70	18.96
Simple Payback [years]	13.75	13.99	25.55	26.02

Table 6.11: Results of the economic analysis for Load History 5 and Load History 6

	Load History 5		Load History 6	
	TT	**ST**	**TT**	**ST**
Annual income [€/year]	24,068,546.62 €	24,060,501.78 €	16,530,308.70 €	16,520,021.87 €
Annual fuel cost [€/year]	20,948,646.50 €	20,948,646.50 €	13,965,764.33 €	13,965,764.33 €
Cash Flow [€/year]	2,022,931.59 €	1,998,519.04 €	1,636,782.97 €	1,609,354.64 €
Net Present Value	12,318,204.60 €	10,689,258.98 €	7,957,415.26 €	6,189,648.06 €
Profitability Index	1.54	1.44	1.39	1.28
LCOE [€/MWh]	23.68	24.93	32.06	34.09
Simple Payback [years]	11.32	12.06	12.55	13.57

The results regarding Load History 4 present a negative Net Present Value, a Profitability Index less than 1, and a simple payback greater than the expected lifetime of 25 years, therefore it is evident that this solution is not profitable.

Comparing Load History 2 and Load History 4, as well as Load History 1 and Load History 3, which have the same load trends with the difference that for Load History 1 and Load History 2 the gas turbine power output is kept constant while in Load History 3 and 4 the ORC power output is kept constant, it is evident that the more profitable strategy is to keep the gas turbine power output constant and to vary the ORC power output, as in Load History 1 and Load History 2.

In Load History 3 and Load History 4 the gas turbine works in off-design mode at 50% of its load, reducing therefore its energy production and the corresponding profits from the sale. The expenses deriving from the purchase of fuel are also reduced, but the efficiency reduction of the gas turbine in off-design mode leads to the fact that a 50% reduction in power production does not correspond to a 50% reduction in fuel consumption, because more fuel is needed to compensate the decrease in efficiency. This leads to a decrease in the cash flow, and it is more evident for Load History 4 with respect to Load History 3 because in Load History 4 the gas turbine works in off-design for more time. In Load History 1 and Load History 2 this behaviour is not present, because the gas turbine always works at its nominal load and the change in the ORC power output does not influence the fuel consumption.

In Load History 5 and Load History 6, the gas turbine is off for a part of the day. During this period, the fuel consumption is null, and therefore the costs deriving from its purchase, while the ORC still produces energy, earning money from its sale. This positive behaviour is made possible by an increase in the storage investment costs because a larger TES is needed.

As already shown in Table 6.6, Table 6.7, and Table 6.8, the two tanks solution presents less costs with respect to the stratified solution, therefore for all the considered load histories the two tanks configuration present better economic performances.

The most profitable configurations are the ones of Load History 1 and Load History 5.

To see the convenience of the thermal storage integration with respect to the traditional configuration without storage, the economic analysis has also been done for the same plants obtained with the optimisation with TES but considered without the TES integration. In these cases, the power production of the ORC will follow the gas turbine load history, due to the absence of the storage.

The load history considered for the plants obtained for Load History 1 and Load History 3 without TES is the ORC load history of Load History 1, Figure 5.3 (or the gas turbine load history of Load History 3, Figure 5.20); the load history considered for the plants obtained for Load History 2 and Load History 4 without TES is the ORC load history of Load History 2, Figure 5.14 (or the gas turbine load history of Load History 4, Figure 5.26); the load history considered for the plant obtained for Load History 5 without TES is the gas turbine load history of Load History 5, Figure 5.32; the load history considered for the plant obtained for Load History 6 without TES is the gas turbine load history of Load History 6, Figure 5.38.

The results of the economic analysis of the plants without TES are shown in Table 6.12.

Table 6.12: Results of the economic analysis for the plants without TES

	Load History 1 Without TES	Load History 2 Without TES	Load History 3 Without TES	Load History 4 Without TES	Load History 5 Without TES	Load History 6 Without TES
Annual income [€/year]	32,282,208 €	29,364,108 €	30,011,856 €	25,682,391 €	22,901,594 €	15,123,868 €
Annual fuel cost [€/year]	28,804,389 €	26,185,808 €	28,804,389 €	26,185,808 €	20,948,646 €	13,965,764 €
Cash Flow [€/year]	2,288,496 €	2,042,486 €	590,153 €	- 693,929 €	1,177,363 €	598,764 €
Net Present Value	16,517,879 €	11,025,237 €	- 11,271,075 €	- 32,565,884 €	312,346 €	- 8,086,450 €
Profitability Index	1.71	1.45	0.48	-	1.02	0.56
LCOE [€/MWh]	17.55	20.47	17.43	19.53	22.12	32.11
Simple Payback [years]	10.20	12.02	36.51	-	17.15	30.92

Comparing the first two cases without TES integration with the first two with TES integration of Table 6.9 , it can be seen that the introduction of storage does not lead to an improvement in the economic performances, which, however, are positive both in the case with and without storage integration.

A notable improvement can instead be appreciated in the third case, where the introduction of the storage makes profitable an investment that otherwise would not be convenient. In particular, the storage integration allows to increase the production of electricity and therefore the profits deriving from its sale for the same cost of fuel, therefore increasing the cash flow. With an increase in the initial investment cost given by the introduction of the thermal storage, the annual

cash flow can be increased, leading to a positive Net Present Value that otherwise would be negative.

As previously said, the plant obtained for Load History 4 is not profitable, and without thermal storage integration its economic performances are even worse.

In the last two cases, the thermal storage integration improves the economic performances because it allows to earn money from the sale of electricity also when the gas turbine is off, therefore without spending money for the fuel purchase. Also in these cases, the increase in the investment costs due to the integration of the storage system are justified by an increase in the annual cash flow and the Net Present Value.

It is important to remember that this is a preliminary economic analysis based on several assumptions. The costs of the various components have been estimated through correlation that may differ from the real market values, which are difficult to identify and are a prerogative of the manufacturer, depending on many variables. Also, the prices of electricity and natural gas have been taken as average values in 2022; being these prices variables and depending on many factors such as weather conditions and geopolitical events, different values may lead to different results.

7 Conclusions

In this work a procedure for the design of a gas turbine – ORC Combined Power Plant has been developed, with the integration of a thermal energy storage system to increase the flexibility of the plant.

The storage system has been integrated directly storing the diathermic oil present in the oil circuit that recovers the heat from the exhaust gases and feeds the bottoming ORC. Two different solutions for the TES have been considered: a two-tank system and a stratified tank system. Thanks to the storage system, the working conditions of the gas turbine and the ORC can be decoupled.

The procedure starts by defining the gas turbine and its load history during the day, thus defining the characteristics of the thermal source of the bottoming cycle.

The following step consists in the optimization of the design condition of the ORC without TES. Then, the off-design model is used with the ORC without TES for defining some prevision functions that will be needed for the optimisation of the design of the ORC with TES.

After that, the desired ORC load history is defined and the optimisation of the design of the ORC is done. The off-design model is then used again to assess the correctness of the previously used prediction function and to build off-design maps of the plant.

The procedure ends with the sizing of the TES for both the considered configurations and the simulation of the overall plant.

Six load histories have been considered and compared in this work. The first two load histories are characterized by a constant power output of the gas turbine, which always works in design condition, and the ORC that varies its load during the day. In the third and fourth load histories, the ORC has a constant power output, while the gas turbine varies its load. In the last two load histories, both the gas turbine and the ORC varies their load, and the ORC can work even though the gas turbine is off for a period.

The optimisation has shown that the size of the ORC is bigger for the first two load histories, with a nominal power of 4.59 MW and 5.13 MW respectively, and decreases when the gas-turbine varies its load, with a nominal power of 3.48 MW, 3.08 MW, 2.88 MW, 2.14 MW for the other load histories.

Although the ORC size is bigger for the first two load histories, the dimensions of the storages are comparable with the ones of the last two load histories, because in the latter the storage must guarantee the operation of the ORC also when the gas turbine is off, therefore a bigger storage is needed.

For all the load histories, the two tanks configuration occupies a bigger volume with respect to the stratified tank configuration, but the latter needs to store more diathermic oil.

A preliminary economic analysis is then performed, to understand which of the studied configurations are more profitable. Two different methods have been used to estimate the ORC costs, which gave a different distribution of costs among the various components of the cycles, but almost the same cost for the overall plants.

For the estimation of the gas turbine cost, a price of 900 €/kW is considered, while for the TES the price of the tanks is estimated through a correlation and the price of the diathermic oil is set as 5 €/l.

The costs relative to the purchase of natural gas and the revenues deriving from the sale of electricity are estimated considering a natural gas price and a daily trend of the prices of electricity equal to the average values of the prices in 2022.

Cash flow, Net Present Value, Profitability Index, Levelized Cost of Energy, and Simple Payback are calculated for each load history, considering an expected life of the plant of 25 years.

This analysis has shown that the plant obtained for Load History 4 is not profitable, while the most profitable configurations are obtained for Load History 1 and Load History 5.

In general, the two-tanks configuration is shown to be less expensive with respect to the stratified tank configuration.

Comparing the economic performance of the plant with and without the thermal storage integration, for the plants obtained for Load History 1 and Load History 2 the integration of the storage does not lead to an improvement in the profitability, while for the other plants the increase in the investments cost for the integration of the thermal storage is worth, because leads to an increase in the annual cash flow and an increase in the Net Present Value, thus leading to an improvement in the economic performances of those plants.

8 References

1. *Innovations for organic Rankine cycle power systems: Current trends and future perspectives.* **Christoph Wieland, Christopher Schifflechner, Konstantinos Braimakis, Florian Kaufmann, Fabian Dawo, Sotirios Karellas, Giorgio Besagni, Christos N. Markides.** 2023, Applied Thermal Engineering.

2. *Thermodynamic performance limits of the organic Rankine cycle: Working fluid parameterization based on corresponding states modeling.* **Fufang Yang, Fubin Yang, Qingfu Chu, Qiang Liu, Zhen Yang, Yuanyuan Duan.** 2020, Energy Conversion and Management.

3. *Optimization of CCGT power plant and performance analysis using MATLAB/Simulink with actual operational data.* **Naimul Hasan, Jitendra Nath Rai, Bharat Bhushan Arora.** 2014.

4. **Max Schoenfisch, Amrita Dasgupta.** https://www.iea.org/reports/grid-scale-storage. *iea.org.* [Online] 09 2022.

5. **T. Hino, A. Lejeune.** Pumped Storage Hydropower Developments. *Comprehensive Renewable Energy.* 2012.

6. *Pumped Thermal Electricity Storage: A technology overview.* **Anna Stoppato, Alberto Benato.** Padova : s.n., 2018, Thermal Science and Engineering Progress.

7. **Cabeza, L. F., et al.** Introduction to thermal energy storage (TES) systems. *Advances in Thermal Energy Storage Systems.* 2015.

8. *Thermo-economic assessment of flexible nuclear power plants in future low-carbon electricity systems: Role of thermal energy storage.* **Al Kindi Abdullah, Marko Aunedi, Antonio Pantaleo, Goran Strbac, Christos Markides.** 2022, Energy Conversion and Management.

9. *Study of combined heat and power plant integration with thermal energy.* **Chengxu Chen, Zhihua Ge, Youjun Zhang.** 2022, Applied Thermal Engineering .

10. *Improving the load flexibility of coal-fired power plants by the integration of a thermal energy storage.* **M. Richter, M. Bieber, G. K.** 2019, Applied Energy.

11. *Flexible nuclear plants with thermal energy storage and secondary power.* **Panagiotis Romanos, Abdullah A. Al Kindi, Antonio M. Pantaleo, Christos N. Markides.** 2022, e-Prime - Advances in Electrical Engineering, Electronics and.

12. *Parametric multi-objective optimization of an Organic Rankine Cycle with thermal energy storage for distributed generation.* **Elio Antonio Bufi, Sergio Camporeale, Francesco Fornarelli,**

Bernardo Fortunato, Antonio Marco Pantaleo, Arianna Sorrentino, Marco Torresi. 2017, Energy Procedia.

13. *Combined-cycle gas turbine power plant integration with cascaded latent.* **Decai Li, Yukun Hu, Dacheng Li, Jihong Wang.** 2019, Energy Conversion and Management.

14. *Organic Rankine cycle-based waste heat recovery system combined with thermal energy storage for emission-free power generation on ships during harbor stays.* **Enrico Baldasso, Thomas Jérome Achille Gilormini, Maria E. Mondejar, Jesper Graa Andreasen, Lejf K. Larsen, Jianhua Fan, Fredrik Haglind.** 2020, Journal of Cleaner Production.

15. *Performance comparison of two-tank direct and thermocline thermal energy storage systems for 1 MWe class concentrating solar power plants.* **Daniele Cocco, Fabio Serra.** Cagliari : s.n., 2015, Energy.

16. *Optimal design and operation of an Organic Rankine Cycle (ORC) system driven by solar energy with sensible thermal energy storage.* **Haoshui Yu, Henrik Helland, Xingji Yu, Truls Gundersen, Gürkan Sin.** 2021, Energy Conversion and Management.

17. **Piccoli, Cesare.** *Flessibilizzazione di un impianto combinato di piccola taglia mediante l'utilizzo di stoccaggio termico.* DII, Università di Padova. 2022.

18. *The ORC-PD: A versatile tool for fluid selection and Organic Rankine Cycle unit design.* **A. Pezzuolo, A. Benato, A. Stoppato, A. Mirandola.** 2016, Energy.

19. **Lozza, Giovanni.** *Turbine a gas e cicli combinati.* s.l. : Società Editrice Esculapio, 2015.

20. **Theminol 66 thecnical data sheet. [Online] http://twt.mpei.ac.ru/TTHB/HEDH/HTF-66.PDF.**

21. *Thermodynamic analysis of an organic Rankine cycle for waste heat recovery from gas turbines.* Carlo Carcasci, Riccardo Ferraro, Edoardo Miliotti. 2014, Energy.

22. *Alternative ORC bottoming cycles FOR combined cycle power plants.* R. Chacartegui, D. Sánchez, J. Muñoz, T. Sánchez. 2009, Applied Energy.

23. *The IRC-PD Tool: A Code to Design Steam and Organic Waste Heat Recovery Units.* Youcef Redjeb, Khatima Kaabeche-Djerafi, Anna Stoppato, Alberto Benato. 2021, Energies.

24. Richard Turton, Joseph A. Shaeiwitz, Debangsu Bhattacharyya, Wallace B. Whiting. *Analysis, Syntesys, and Design of Chemical Processes, 5th Edition.* 2018.

25. *Thermo-economic analysis of the pumped thermal energy storage with thermal integration in different application scenarios.* Shuozhuo Hu, Zhen Yang, Jian Li, Yuanyuan Duan. 2021, Energy Conversion and Management.

26. ***Exergoeconomic optimization and working fluid comparison of low-temperature Carnot battery systems for energy storage.*** **Ruoxuan Fan, Huan Xi. 2022, Journal of Energy Storage.**

27. ***Gestore Mercati Energetici.*** **[Online] https://www.mercatoelettrico.org.**